AD-A044 269 ARMY ENGINEER WATERWAYS EXPERIMENT STATION VICKSBURG MISS F/G 1/5
ANALYSIS OF PERMANENT DEFORMATIONS OF FLEXIBLE AIRPORT PAVEMENT--ETC(U)
FEB 77 Y T CHOU DOT-FA73WAI-377
UNCLASSIFIED WES-TR-S-77-8 FAA-RD-77-6 NL

1 OF 2
ADA044269

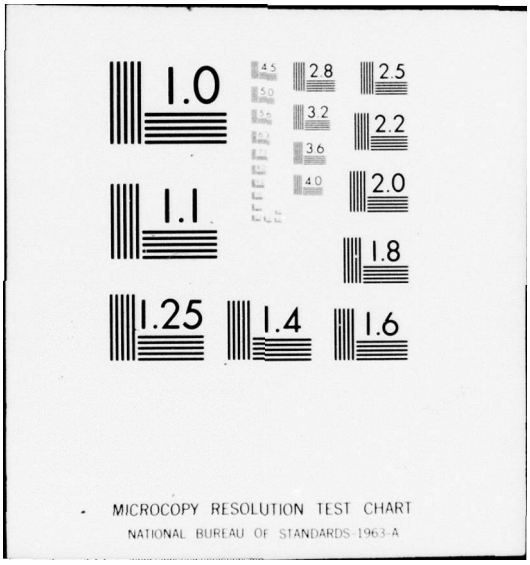
1.0
1.1
1.25
1.4
1.6
1.8
2.0
2.2
2.5
2.8
3.2
3.6
4.0
4.5
5.0
MICROCOPY RESOLUTION TEST CHART
NATIONAL BUREAU OF STANDARDS-1963-A

Report No. FAA-RD-77-6

WES TR S-77-8

12

ADA044269

ANALYSIS OF PERMANENT DEFORMATIONS OF FLEXIBLE AIRPORT PAVEMENTS

Yu T. Chou

U. S. Army Engineer Waterways Experiment Station
Soils and Pavements Laboratory
P. O. Box 631, Vicksburg, Miss. 39180

DDC
RECEIVED
SEP 16 1977
C

FEBRUARY 1977
FINAL REPORT

Document is available to the public through the
National Technical Information Service,
Springfield, Va. 22151

Prepared for

DEPARTMENT OF DEFENSE
DEPARTMENT OF THE ARMY
Office, Chief of Engineers
Washington D. C. 20314

U.S. DEPARTMENT OF TRANSPORTATION
FEDERAL AVIATION ADMINISTRATION
Systems Research & Development Service
Washington, D. C. 20591

DDC FILE COPY

NOTICES

This document is disseminated under the sponsorship of the Department of Transportation in the interest of information exchange. The United States Government assumes no liability for its contents or use thereof.

The United States Government does not endorse products or manufacturers. Trade or manufacturers' names appear herein solely because they are considered essential to the object of this report.

Technical Report Documentation Page

1. Report No.	2. Government Accession No.	3. Recipient's Catalog No.
FAA-RD-77-6		

4. Title and Subtitle	5. Report Date
ANALYSIS OF PERMANENT DEFORMATIONS OF FLEXIBLE AIRPORT PAVEMENTS.	February 1977
	6. Performing Organization Code
	8. Performing Organization Report No.
7. Author(s) Yu T. Chou	WES-TR-S-77-8
9. Performing Organization Name and Address U. S. Army Engineer Waterways Experiment Station Soils and Pavements Laboratory P. O. Box 631 Vicksburg, Miss. 39180	10. Work Unit No. (TRAIS)
	11. Contract or Grant No. DOT-FA73WAI-377
12. Sponsoring Agency Name and Address Federal Aviation Administration Washington, D. C. 20591, and Office, Chief of Engineers, U. S. Army Washington, D. C. 20314	13. Type of Report and Period Covered Final Report.
	14. Sponsoring Agency Code ARD-430

15. Supplementary Notes

115p.

HA762719A7H9

122

16. Abstract

This study was conducted to investigate the deformation characteristics of component materials in a flexible pavement system subject to moving aircraft loadings, and to attempt to develop a prediction model to estimate permanent deformation. A literature survey was first conducted on the deformation characteristics of pavement component materials and the computational techniques to predict the amount of deformation. Series of laboratory repeated load tests measuring permanent strain were performed on subgrade soil and untreated granular materials. The results were used as input to a layered elastic computer program to determine the accumulated permanent deformation that occurred in each layer of the pavement. Pavements used in the analysis were full-scale multiple-wheel heavy gear load test sections constructed and tested at the U. S. Army Engineer Waterways Experiment Station and pavements designed by using the CBR equation.

The literature survey indicated that predicting permanent deformation in the asphaltic concrete layer is not only very costly and time-consuming but also may be incorrect. Different patterns of permanent strain along the asphalt layer were computed by different authoritative agencies. Results of the analysis of this study revealed that permanent deformation in the untreated granular layer cannot be predicted with accuracy. The problem is in the difficulty of estimating stress states in the granular materials under moving aircraft loadings. It was concluded that it is not possible to predict the permanent deformation that occurs in a pavement using the layered elastic computer program; thus, it was recommended that efforts be made to study the basic deformation characteristics of asphaltic concrete and untreated granular soils in a pavement system and later initiate a development program for prediction models when the information becomes available.

The permanent deformation occurring in the subgrade soil of many pavements was computed using the linear layered elastic computer program and laboratory repeated load test data. Results of the analysis indicate that the current concept of the control of subgrade rutting in flexible pavements by the limitation of elastic strain is not strictly correct. When subgrade strain is limited, subgrade rutting may not be limited and may not be controlled.

17. Key Words	18. Distribution Statement
Layered systems Pavement design Permanent deformation	Document is available to the public through the National Technical Information Service, Springfield, Va. 22151.

19. Security Classif. (of this report)	20. Security Classif. (of this page)	21. No. of Pages	22. Price
Unclassified	Unclassified	116	

Form DOT F 1700.7 (8-72) Reproduction of completed page authorized

038100

AB

PREFACE

The study described herein was jointly sponsored by the Federal Aviation Administration as a part of Inter-Agency Agreement No. DOT FA73WAI-377, "New Pavement Design Methodology," and by the Office, Chief of Engineers, U. S. Army, as a part of Military Construction RDTE Project No. 4A762719AT40, "Pavements, Soils, and Foundations," Task 02.

The study was conducted by the U. S. Army Engineer Waterways Experiment Station (WES), Soils and Pavements Laboratory. Dr. Yu T. Chou, under the general supervision of Messrs. James P. Sale, Richard G. Ahlvin, Ronald L. Hutchinson, and Harry H. Ulery, Jr., was in charge of the study and is the author of this report.

COL G. H. Hilt, CE, and COL J. L. Cannon, CE, were Directors of WES during the conduct of this study and the preparation of this report. Mr. F. R. Brown was Technical Director.

ACCESSION for
NTIS White Section
DDC Buff Section
UNANNOUNCED
JUSTIFICATION
BY
DISTRIBUTION/AVAILABILITY CODES
Dist. SPECIAL
A

PRECEDING PAGE BLANK-NOT FILMED

METRIC CONVERSION FACTORS

Approximate Conversions to Metric Measures

Symbol	When You Know	Multiply by	To Find	Symbol
	LENGTH			
in	inches	*2.5	centimeters	cm
ft	feet	30	centimeters	cm
yd	yards	0.9	meters	m
mi	miles	1.6	kilometers	km
	AREA			
in^2	square inches	6.5	square centimeters	cm^2
ft^2	square feet	0.09	square meters	m^2
yd^2	square yards	0.8	square meters	m^2
mi^2	square miles	2.6	square kilometers	km^2
	acres	0.4	hectares	ha
	MASS (weight)			
oz	ounces	28	grams	g
lb	pounds	0.45	kilograms	kg
	short tons (2000 lb)	0.9	tonnes	t
	VOLUME			
tsp	teaspoons	5	milliliters	ml
Tbsp	tablespoons	15	milliliters	ml
fl oz	fluid ounces	30	milliliters	ml
c	cups	0.24	liters	l
pt	pints	0.47	liters	l
qt	quarts	0.96	liters	l
gal	gallons	3.8	liters	l
ft^3	cubic feet	0.03	cubic meters	m^3
yd^3	cubic yards	0.76	cubic meters	m^3
	TEMPERATURE (exact)			
°F	Fahrenheit temperature	5/9 (after subtracting 32)	Celsius temperature	°C

*1 in = 2.54 (exactly). For other exact conversions and more detailed tables, see NBS Misc. Publ. 286, Units of Weights and Measures, Price $2.25, SD Catalog No. C13.10:286.

Approximate Conversions from Metric Measures

Symbol	When You Know	Multiply by	To Find	Symbol
	LENGTH			
mm	millimeters	0.04	inches	in
cm	centimeters	0.4	inches	in
m	meters	3.3	feet	ft
m	meters	1.1	yards	yd
km	kilometers	0.6	miles	mi
	AREA			
cm^2	square centimeters	0.16	square inches	in^2
m^2	square meters	1.2	square yards	yd^2
km^2	square kilometers	0.4	square miles	mi^2
ha	hectares (10,000 m^2)	2.5	acres	
	MASS (weight)			
g	grams	0.035	ounces	oz
kg	kilograms	2.2	pounds	lb
t	tonnes (1000 kg)	1.1	short tons	
	VOLUME			
ml	milliliters	0.03	fluid ounces	fl oz
l	liters	2.1	pints	pt
l	liters	1.06	quarts	qt
l	liters	0.26	gallons	gal
m^3	cubic meters	35	cubic feet	ft^3
m^3	cubic meters	1.3	cubic yards	yd^3
	TEMPERATURE (exact)			
°C	Celsius temperature	9/5 (then add 32)	Fahrenheit temperature	°F

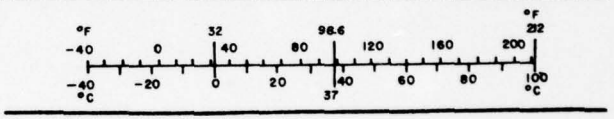

TABLE OF CONTENTS

	Page
PREFACE	1
CONVERSION FACTORS	3
INTRODUCTION	7
BACKGROUND	7
PURPOSE AND SCOPE	9
LITERATURE REVIEW	12
ASPHALTIC CONCRETE (AC)	12
UNTREATED GRANULAR MATERIALS	33
FINE-GRAINED SOILS	48
LABORATORY REPEATED LOAD TESTS	52
SOURCE AND DESCRIPTION OF MATERIAL	52
SPECIMEN PREPARATION, TESTING EQUIPMENT, AND PROCEDURES	52
TEST RESULTS	54
COMPUTATIONS OF PERMANENT DEFORMATION	72
DESIGN IMPLICATIONS OF COMPUTED RESULTS	104
CONCLUSIONS AND RECOMMENDATIONS	109
CONCLUSIONS	109
RECOMMENDATIONS	110
LIST OF NOMENCLATURE	111
REFERENCES	112

PRECEDING PAGE BLANK-NOT FILMED

INTRODUCTION

BACKGROUND

In the rational design of flexible pavements, consideration of permanent deformation (or distortion) constitutes an important factor in the overall design system. Excessive amounts of pavement rutting adversely affect riding quality, and rutting can also cause the pavement to crack and thus result in the loss of pavement serviceability.

Permanent deformation in a pavement is a manifestation of two different mechanisms: densification (volume decrease) and shear deformation (plastic flow with no volume change). Monismith[1] has summarized the various forms of permanent deformation resulting from both traffic- and nontraffic-associated causes, and these are listed in Table 1.

Excessive deformation resulting from densification can be minimized by proper compaction requirements. Control of plastic flow is actually one of the basic distress modes upon which all pavement structural designs are based. In designs of pavement systems to minimize permanent deformation, it is general practice to place a sufficient thickness with adequate strength of each component layer to keep the stresses in the subgrade to a low level relative to the strength of the soil (as in the CBR design procedure).

Since the advent of high-speed computers, two approaches have been advocated using the layered elastic method or others to solve the problems of design to minimize permanent deformation. One of the approaches involves limiting the vertical compressive strain at the subgrade surface to some tolerable amount associated with a specific number of load repetitions (as in the Shell procedure[2]). By controlling the characteristics of the material in the pavement section through materials design and proper construction procedures (unit weight or relative compaction requirements) and by ensuring that materials of adequate stiffness and sufficient thickness are used so that the strain level is not exceeded, permanent deformation can be limited to a value equal to or less than the prescribed amount. The major advantage of the

PRECEDING PAGE BLANK-NOT FILMED

Table 1

Examples of the Permanent Deformation Mode of Distress for Asphalt Pavements (after Monismith[1])

General Cause	Specific Causative Factor	Example of Distress
Traffic-associated	Single or comparatively few excessive loads	Plastic flow (shear deformation)
	Long-term (or static) load	Creep (time-dependent) deformation
	Repetitive traffic loading (generally, large numbers of repetitions)	Rutting (resulting from accumulation of small permanent deformations associated with passage of wheel loads)
Nontraffic-associated	Expansive subgrade soil*	Swell or shrinkage
	Compressible material underlying pavement structure	Consolidation settlement
	Frost-susceptible material	Heave (particularly differential amounts)

* Soils in this category exhibit high shrinkage as well as swell characteristics.

approach is the fact that it is currently a workable tool for the pavement design, and several agencies have introduced procedures based upon it. A summary of existing criteria taken from Reference 3 is shown in Table 2. It should be pointed out that pavements designed based on this procedure will have sufficient thickness to protect the subgrade soil from shear failure but not to insure that permanent deformation in the upper pavement layers will not occur.

The other approach involves prediction of the actual amount of deformation which might occur in the pavement system using material characterization data developed from laboratory tests. In the new, improved pavement design procedure[4] prepared for the Office, Chief of Engineers, U. S. Army, and the Federal Aviation Administration (FAA), two primary distress modes, fracture and distortion, are considered. The consideration of fatigue cracking did not fall within the purview of this study. Rather, the prediction of accumulated permanent deformations in pavement systems under aircraft loadings was studied and the results presented.

PURPOSE AND SCOPE

The purpose of this study was to examine the rutting characteristics of pavement component materials and to develop a prediction model to accurately estimate the amount of rutting occurring in each component layer of a pavement system under traffic loadings.

A literature survey was first conducted on the rutting characteristics of pavement component materials and the computational techniques used to predict the amount of rutting. A series of laboratory repeated load tests measuring permanent strains was performed on subgrade soil and untreated granular materials. The results were used in conjunction with a layered elastic computer program to determine the accumulated permanent deformation occurring in each layer of the pavement induced by aircraft loadings. Pavements analyzed were full-scale, multiple-wheel heavy gear load test sections constructed and tested at the U. S. Army Engineer Waterways Experiment Station (WES) and typical pavements as designed using the Corps of Engineers CBR equation.

Table 2

Limiting Subgrade Strain Criteria (After Yoder and Witczak[3])

	Original Shell Oil Co.	Revised Shell Oil Co.	Asphalt Institute	Kentucky Highway
Strain parameter*	ε_{vs}	ε_{vs}	ε_{vs}	ε_{vs}
Year introduced	1962-1965	1970-1972	1971-1973	1971-1973
Type pavement	Highway	Airfield	Airfield	Highway
Allowable strain				
$N_j = 10$	--	--	--	--
10^2	--	--	2548	--
10^3	2700	4500	1904	790
10^4	1680	2700	1646	639
10^5	1050	1700	1508	502
10^6	650	1030	1423	364
10^7	420	650	--	227
10^8	260	400	--	89
∞	--	--	1060	--
Effective E_1, ksi	140 (thin AC) 200 (thick AC)	150 --	100 --	480 (33 percent AC) 300 (100 percent AC)

* ε_{vs} is maximum compressive subgrade strain, 10^{-6} in./in.

Design implications based on the results of computations were analyzed, and recommendations for the design of flexible pavements to minimize permanent deformations were determined.

LITERATURE REVIEW

In recent years, much research effort has been devoted to the study of permanent deformation in flexible pavements. Experience indicates that under normal pavement conditions deformation within asphaltic materials occurs only during warm weather. Under cold weather conditions, little deformation occurs in either the asphalt material or the subgrade, due mainly to the very stiff condition of the former. In some cases, the subgrade soil may be frozen in the winter and provide firm support for the overlying asphaltic concrete (AC) layer and thus reduce pavement deformation. While rutting and fatigue are two separate modes of distress, rutting can contribute to fatigue failure of a pavement due to tensile strains in the surfacing which result from bending caused by rutting in the base and subgrade.

In this chapter, reviews are presented for AC, untreated granular materials, and fine-grained soils. A literature review was not conducted on stabilized soils because it is the general consensus that stabilized soils with sufficient amounts of agent experience insignificant amounts of permanent deformation under traffic loadings.

ASPHALTIC CONCRETE (AC)

INTRODUCTION

Hofstra and Klomp[5] investigated permanent deformation of AC using a laboratory test track. The pavement structure was simplified by utilizing full-depth AC construction with 2.0-in.,* 3.9-in., 5.6-in., and 7.9-in. layers of various asphalt mixes laid directly on subgrade with a CBR of 18. The mixes had high asphalt contents to induce greater rutting than would normally occur in practice, and a strong subgrade was used to minimize deformation in that material.

Experiments to investigate the effect of temperature indicated that for a 2-in. layer of AC, rutting was partly due to deformation of the subgrade but for the 3.9- and 5.6-in. layers rutting was due entirely

---

* A table of factors for converting units of measurement is presented on page 3.

to deformation in the AC. It was found that deformation was due to plastic flow of the material and not to densification. A range of temperatures from 20 to 60° C was investigated, during which the AC modulus decreased by a factor of approximately 60 but the permanent deformation increased by a factor of 250 to 350.

A series of tests was carried out to investigate the mix variables of asphalt type, asphalt content, and aggregate type. It was found that stiffer asphalts produced mixes less susceptible to permanent deformation, and the same effect was noted for mixes with low asphalt contents or higher percentage of coarse aggregates. It was also found that rut depth per wheel pass decreased with an increasing number of wheel passes. It appeared that the mix built up a resistance to flow during the process of deforming under repeated loading. This was probably due to the asphalt being expelled from between aggregate particles producing greater interlocking, which would explain why angular aggregate produces better performing mixes than rounded aggregates.

Studies of the distribution of permanent deformation with depth in the AC layers showed that deformation was almost uniformly distributed through the entire depth. Calculations of vertical strain distribution with depth using the computer program, BISTRO, and assuming a constant asphalt stiffness modulus showed a reasonably uniform strain distribution. However, in a 7.9-in. layer, the calculated strain was much higher at the top of the layer than at the bottom, whereas measured permanent deformation was only slightly higher. The strains and deformations were not in agreement with observations of Heukelom and Klomp.[6] This could be partly explained by the fact that vertical strains measured near the bottom of the layer were much larger than the values calculated at that position, possibly due to the constant modulus assumed for the whole layer.

McLean[7] describes a methodology to permit estimation of permanent deformation in pavement structures from laboratory triaxial repeated load and creep tests. His analysis concentrated primarily on techniques to estimate the distortion characteristics of AC and the use of these data together with both linear elastic and linear viscoelastic theory

to predict rutting in asphalt-bound layers of pavement structures. This approach when used to study the influence of a number of parameters on pavement response resulted in the following observations:

a. Subgrade stiffness appeared to have little influence on the accumulation of permanent deformation in the asphalt-bound layer--at least for the range in stiffnesses examined.

b. AC stiffness exerted a significant influence on rutting in the asphalt-bound layer.

c. Like the measurements of Hofstra and Klomp,[5] the calculation procedure indicated that rut depth in the asphalt layer was independent of layer thickness for the range examined.

Morris[8] developed a mathematical model from the laboratory experimental results to predict the rut depth of the full-depth sections at the Brampton Test Road in Canada. The computed results match very well with the measurements. However, Morris found that the majority of the deformations occurred in the lower portion of asphalt layer where tensile stresses exist. The conclusions of Morris's study were different from those of Hofstra and Klomp[5] and McLean.[7] The details of these works will be explained in the later sections.

METHODS TO PREVENT PERMANENT DEFORMATION OF AC

The following discussion is taken from Monismith's[9] study of available methods to prevent excessive deformation in the AC layers of a pavement.

Standing and Uniformly Moving Traffic. Two of the methods in widespread use (presented in Corps of Engineers Technical Manual TM 5-824-2[10] and California Division of Highways Materials Manual, Test Method 304[11]) have the capability to produce reasonably performing mixtures so long as the actual service conditions correspond to those for which the basic criteria were developed. For conditions beyond the realm of current procedures, the triaxial compression test has the potential to provide parameters which, when used with analyses of systems representative of pavement structures, can provide useful design guides. A number of investigators, as will be seen subsequently, make use of bearing capacity relationships for materials whose strength characteristics can be represented by an equation of the form

$$\tau = c + \sigma \tan \phi \tag{1}$$

where

τ = shear strength

c = cohesion

σ = normal stress

ϕ = angle of internal friction

By performing triaxial compression tests at temperatures and rates of loading associated with specific field conditions, the parameters c and ϕ can be ascertained for design estimates. The analysis of Nijboer[12] can be helpful to properly define the parameters c and ϕ for design purposes

$$\eta_{mass} \frac{d\varepsilon_1}{dt} = \frac{2 \cos \phi}{3 - \sin \phi} \left[\frac{\sigma_1 - \sigma_3}{2 \cos \phi} - \left(\frac{\sigma_1 + \sigma_3}{2} \tan \phi \right) - \tau_e \right] \tag{2}$$

where

η_{mass} = viscosity of mass

$\frac{d\varepsilon_1}{dt}$ = rate of application of axial strain

σ_1, σ_3 = major and minor principal stresses, respectively

τ_e = initial cohesion when $\frac{d\varepsilon_1}{dt} = 0$

and

$$c = \tau_e + \eta_{mass} \frac{d\varepsilon_1}{dt} \tag{3}$$

For standing loads, the value of c corresponds to τ_e.

Equations 2 and 3 are used to solve for ϕ and c, respectively. Data indicate that ϕ is relatively unaffected by rate of loading, and both Nijboer[12] and Smith[13] have recommended a minimum desirable value of 25 deg. To develop ϕ values equal to or greater than this, the aggregate should be rough-textured, angular, and well-graded.

The investigation of Nijboer can be of assistance in providing mixtures with specific values of c necessary to satisfy particular loading conditions. He has shown that c increases with an increase in asphalt viscosity; is dependent on the fineness of mineral filler

(minus 0.00029-in. fraction); increases with an increase in the amount of filler; increases up to a point with an increase in the amount of asphalt; increases with an increase in the rate of loading; increases with increase in mix density; and is dependent on the proportion of coarse aggregate (>0.004 in.) in the mix. More specifically, Nijboer has shown that

$$c \simeq \frac{V}{0.9}\left(\frac{FB}{0.5}\right)^{4.2}\left(\frac{D}{20}\right)^{-0.36} \tag{4}$$

where

V = void factor $[1 - (\text{air void content})^{2/3}]$, when the air void content = 0.03 and $V = 0.9$

FB = filler-bitumen factor; i.e., $\dfrac{\text{volume filler}}{\text{volume filler + volume bitumen}}$

D = equivalent particle size of filler (0.000004 in.)

The triaxial compression tests appear quite useful since they provide friction ϕ and cohesion c factors which, as suggested by Nijboer,[12] can be used in a solution of the Prandtl equation for a continuous strip loading:

$$q_{ult} = c \cdot F(\phi) \tag{5}$$

where

q_{ult} = bearing capacity, psi or kg/cm^2

$F(\phi)$ = function dependent on ϕ ; e.g., for $\phi = 25$ deg, $F(\phi) = 20.7$

When q_{ult} is made equal to a specific contact pressure, c and ϕ are related as shown in Figure 1. In this figure, a mixture with a value of c and ϕ lying on or to the right of the curve would be adequate for vehicles equipped with 100-psi tires.

Saal[15] has suggested modification of this relationship recognizing that the bearing capacity for a circular area is larger than that for a continuous strip. The corresponding values for c and ϕ according to this relationship are also shown in Figure 1, which is recommended with c and ϕ derived from triaxial compression tests at slow rates of loading and high temperatures.

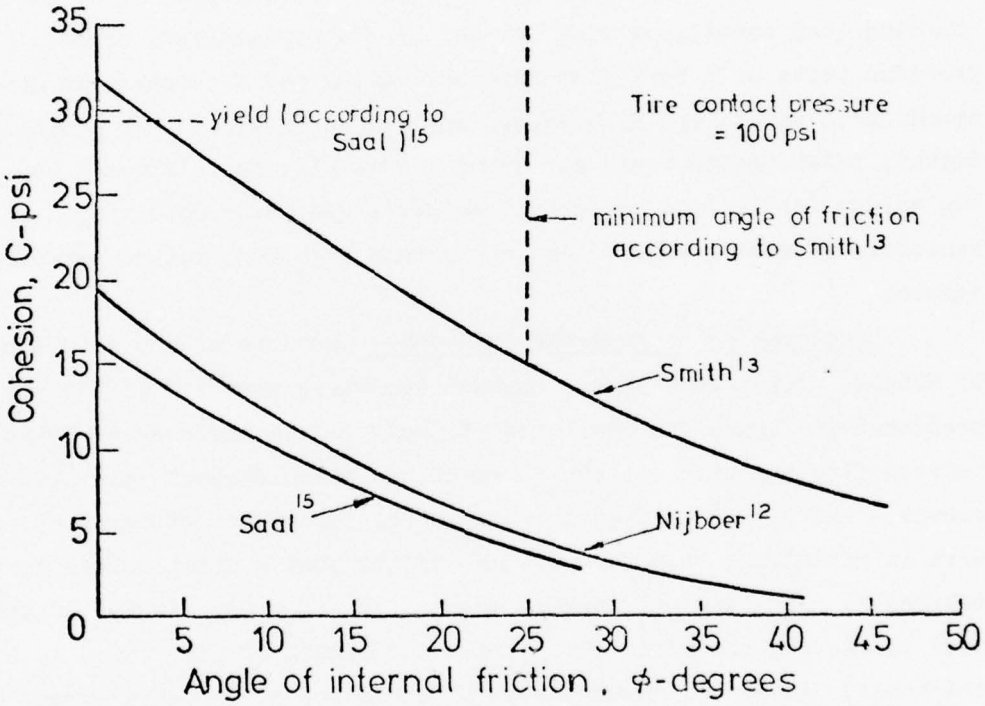

Figure 1. Relationship between cohesion and angle of internal friction to prevent plastic flow or overstress at a particular point in an asphalt mixture (after McLeod[14])

Smith[13] has presented a relationship between c and ϕ and bearing capacity for a circular area based on a yield criterion rather than a plastic flow condition as in the above formulations. For the same contact pressure, larger values of c and ϕ are required than in the previous case, as seen in Figure 1. Smith also suggests a minimum angle of friction of 25 deg to minimize the development of instability from repeated loading.

The relationships suggested by Saal[15] would appear reasonable for standing load conditions with c and ϕ determined from triaxial compression tests at a very slow rate of loading and a temperature corresponding to an average high value expected in service. For moving traffic, Smith's relationship would appear most suitable; in this case, however, the values for c and ϕ should be developed under conditions representative of moving traffic and an average high temperature expected in service.

Decelerating or Accelerating Loads. Results of one such analysis by McLeod[14] for a load with a contact (or tire) pressure of 100 psi are presented in Figure 2. The terms P and Q are measures of friction between tire and pavement and pavement and base, respectively. The curves A and B in this figure indicate the importance of pavement thickness in minimizing this form of instability when a frictionless contact between AC surfacing and base is assumed ($P - Q = 1$). As the AC thickness increases, the ratio ℓ/t (ratio of length of tire tread to AC thickness) decreases, resulting in lower values of c at a given ϕ to prevent instability.

When $P - Q = 0$ (full friction between pavement and base--a more practical situation in well-designed and constructed pavements) and the thickness of the AC is in the range of 4 to 6 in. (curve C), the more critical conditions are defined by the curve suggested by Smith[13] as shown in Figure 2.

Nijboer[16] and Saal[15] have considered shoving by decelerating traffic to be the accumulation of permanent parts of successive viscoelastic deformations and these permanent deformations to occur above a

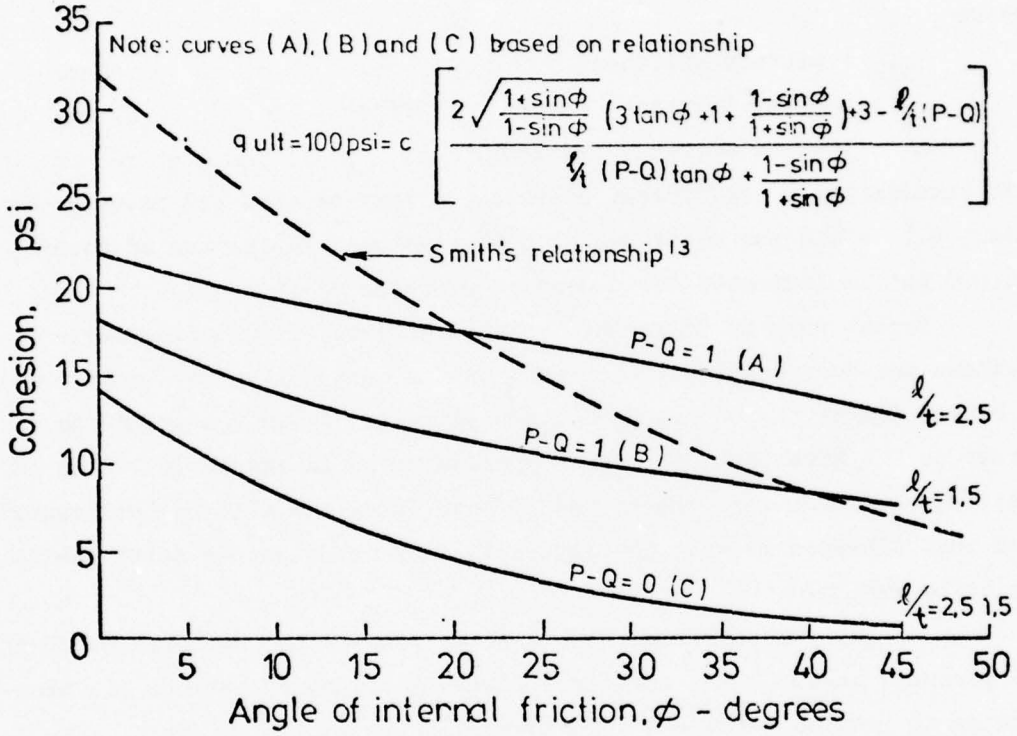

Figure 2. Stability curves for asphalt mixtures subjected to braking stresses (after McLeod[14])

shear strain of 1 percent for time and temperature conditions critical for shoving (0.33 sec and 122° F for their experience).

Using the relationship

$$S_{min} = 3\tau \frac{1}{\gamma} \tag{6}$$

where

S_{min} = minimum stiffness
τ = shear (braking) stress at surface
γ = shear strain (1 percent)

and considering a coefficient of friction between tire and pavement of about 0.5, a minimum stiffness at this time and temperature of about 15,000 psi is indicated for a contact pressure of 100 psi.

Recent work by Valkering[17] on the effects of multiple-wheel systems and horizontal surface loads on pavement structures could provide a better framework for design against shoving. Attention should be drawn to the fact that, at high temperatures in pavements with thin AC layers, the shear stresses at the AC/base interface will be the highest, and that adhesion between the layers is very important if serviceability is to be retained.

For gap-graded mixes, with a stone content in the range of 30 to 50 percent, Marais[18] has suggested limiting values of various mix properties to prevent permanent deformation.

Recent developments by Shell for the solution of stresses and deformations in layered elastic systems due to horizontal forces applied to the pavement surface (BISAR[17]) may provide the framework for a procedure to examine the influence of braking or accelerating stresses on distortion using a procedure similar to that suggested by Heukelom and Klomp[19] for vertical loading.

METHOD TO PREDICT PERMANENT DEFORMATIONS OF AC

The methods presented in the previous section are limited in that they do not give an indication of the actual amount of rutting which may

occur under repetitive traffic loading. Unfortunately, no method presently exists whereby such estimates can be made. Promising procedures include the use of linear viscoelastic theory[20-22] and the use of linear elastic theory suggested by Heukelom and Klomp,[6] Barksdale,[23] and Romain.[24] In the layered elastic procedure, the stresses and strains are computed in the pavement structure and from these values permanent deformations in each material are predicted from constitutive relationships determined by laboratory repeated load triaxial tests on the materials.

Elastic theory together with creep data from simple laboratory tests may also be used to estimate permanent deformation. This approach has been pursued by Shell investigators[25-27] to estimate the rutting occurring in asphaltic layers.

In the Heukelom and Klomp procedure, the vertical strain distribution along a vertical axis is estimated within the asphalt-bound layers utilizing layered elastic theory. Permanent deformation can then be determined by means of the equation

$$\delta_p = \int_0^h f(\varepsilon_v)\, dz \qquad (7)$$

where

δ_p = permanent deformation

$f(\varepsilon_v)$ = function relating the permanent strain ε_p to total strain ε_v ; i.e., $\varepsilon_p = f(\varepsilon_v)$

Such a technique appears useful at this time to assess, at least, the effects of changes in tire pressure and/or gear configuration (and load) on asphalt-bound layers. In addition, it may be possible to establish limiting values for ε_p by comparing computed strains for particular field sections for which well-documented field measurements are available. Like fatigue characteristics, however, it is highly probable that any such criteria established for permanent deformation will be dependent on mixture stiffness (and thus on temperature).

In this review, investigations to determine permanent deformation at the University of Nottingham,[28,29] University of California at Berkeley,[7] University of Waterloo,[8,30] and at the Esso Laboratories in France[31] are discussed.

University of Nottingham.[28] Repeated load triaxial tests were carried out by Snaith[28] on a dense bitumen macadam. The effects of six major variables were investigated: (a) vertical stress, (b) confining stress, (c) temperature, (d) frequency of the vertical stress pulse, (e) rest periods, and (f) asphalt content.

In confined tests, some samples developed longitudinal cracks during the test, and all unconfined samples showed a volume increase. The cracking was caused by the cyclic variation of tensile hoop strain at the surface of the sample, and would contribute to volume increase and sample failure. In confined tests, volume increase did not occur and cracking was observed. This result is comparable to in situ conditions in which restraint is offered by the large mass of material. Hofstra and Klomp[5] measured strains of up to 15 percent in situ, whereas strains measured at failure by Snaith were only about 2 percent, supporting the theory that adjacent material in situ prevents the cracking which hastens failure of a test sample.

The effect of confining stress was not thoroughly studied in Snaith's investigation. Problems arose in predicting permanent strains in the AC layers if the extreme points in the layer were considered, since the range covered by Snaith's results only dealt with stresses near the center of the layer. However, he suggested, as an approximation, that the layer could be considered as a whole, and stress conditions at the center taken as a mean, since Hofstra and Klomp[5] found that the permanent strains were reasonably constant with depth. Snaith found that, when considering a pavement with a 7.9-in. layer (such as that tested by Hofstra and Klomp) that was divided into three sublayers, he could determine the permanent strain in the two top sublayers and obtain good agreement with measurements made in them. The computer program BISTRO was used in the elastic analysis to calculate the stresses and the center of each sublayer, using appropriate values of stiffness and Poisson's ratio.

The following conclusions were drawn from Snaith's work on repeated loading of dense bitumen macadam:

a. An increase in temperature caused a significant increase in strain.

b. An increase in vertical stress caused an increase in strain.

c. An increase in confining stress caused a decrease in strain.

d. The level of static confining stress which gave the same strain as the dynamic confining stress was approximately equal to the mean level of that stress.

e. Realistic changes in the relative lengths of vertical and confining stress pulses did not affect the strain.

f. The rate of strain appeared to be time-dependent at frequencies above 1 Hz.

g. Rest periods between vertical stress pulses had a negligible effect on strain.

h. An optimum asphalt content of 4 percent existed for maximum resistance to strain between 10 and 30° C. At 40° C better resistance was achieved with a 3 percent asphalt content.

i. The results obtained from laboratory tests when applied to the pavement design problem produced reasonable values of rut depth.

Conclusion h indicates the relative importance of aggregate interlock and asphalt viscosity in resisting permanent strain. The former is paramount at high temperatures. It should be pointed out in conclusion h that asphalt content of 3 or 4 percent is optimum only with respect to rutting, but may not be optimum with respect to other considerations, such as fatigue and stability.

So far, when calculations of permanent deformations have been made, one combination of the principal stresses has been used at the center of each layer, whereas, in situ, this combination will change at a particular point each time a vehicle passes. It remains to be seen whether the adoption of a standard wheel load can accurately represent the wide variation of random applications of wheel loads. A limited test program is under way at Nottingham,[32] using Snaith's equipment suitably modified, to investigate this. In particular, the effects of temperature change and vertical stress change during a test are being investigated.

University of California at Berkeley.[7] Repeated load triaxial tests were carried out on AC specimens by McLean. An attempt was made to cover the whole range of stresses to be encountered in situ by

adopting three types of tests to reproduce conditions at the top, center, and bottom of an AC layer. These were triaxial extension (cycling lateral stress only), unconfined compression (cycling vertical stress only), and triaxial tension (cycling vertical stress in tension and lateral stress in compression).

The permanent deformation, strain, and stress states of a 0.79-in. layer of material such as that used by Hofstra and Klomp[5] were investigated by applying the theoretical model derived from the experimental results and using Barksdale's approach.[23] Good agreement with Hofstra and Klomp's results was noted. In particular, the same form of rut depth versus load applications curve was obtained. Figure 3 shows the distribution of elastic stresses and strains and permanent strains with depth for a particular condition. The similarity between the distributions of permanent strain, stress difference, and elastic strain could be significant. Unlike the observed results of Hofstra and Klomp, the distribution of permanent strain was not uniform, possibly due to the simplifications adopted by McLean with regard to loading time.

The following conclusions were drawn from the investigations:

a. The subgrade stiffness appears to have little influence on the accumulation of permanent deformation in the AC layer, at least for the range of stiffness examined.

b. Asphalt concrete stiffness exerts a significant influence on rutting in the AC layer.

c. Like the measurements of Hofstra and Klomp, the calculation procedure indicated that rut depth in the AC layer was reasonably independent of layer thickness.

University of Waterloo.[8,30] Research carried out at the University of Waterloo by Morris was based on an approach for the prediction of rut depth using a combination of linear elastic theory and the results of laboratory triaxial testing of AC. Two series of laboratory tests were carried out, compression tests and tension tests. Both involved the application of a cyclic confining stress and this was combined with cyclic axial compressive and tensile stresses, respectively. Both vertical and lateral deformations were measured. For the compression tests, the vertical deformation was of interest for prediction purposes while the lateral deformation was relevant for the tensile tests since

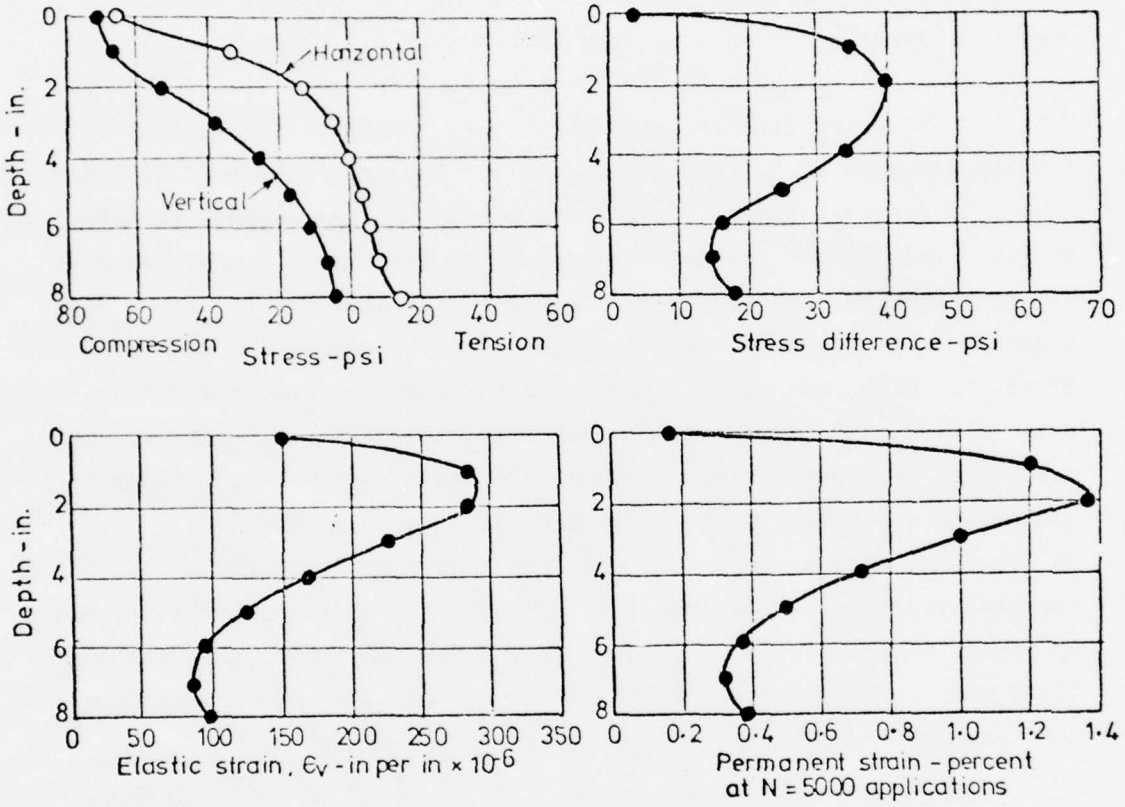

Figure 3. Stress and strain distributions in an 8-in.-thick AC pavement subjected to a 1500-lb wheel load with 70-psi contact pressure (after McLean[7])

it represented the vertical in situ deformation in the lower half of the AC layer.

The results showed remarkably good agreement in view of the many potential sources of error both in the laboratory test technique and in the application of the results to practice. A typical result showing the variation of permanent deformation along the pavement section is shown in Figure 4. It can be seen that nearly all permanent deformation in the AC layer occurred in the lower half of the layer and resulted from the action of tensile lateral stresses, which is in contrast with the observations of Hofstra and Klomp[5] and the predictions of McLean.[7]

In a recent paper, Brown[33] commented that the methods used by Morris[30] and McLean[7] may not be as sound as their good respective predictions for permanent deformation at the surface suggest. Brown suggested a procedure involving the use of stress invariants which are functions of the principal stresses, mean normal stress, and octahedral shear stress, but are independent of the orientation of the axes. Corresponding strain invariants can be determined from the laboratory tests and better estimates of the in situ vertical strain obtained.

Using this approach, some of the inherent disadvantages of the triaxial test can be overcome. In particular, the tension zone stresses in an asphaltic layer can be reproduced more accurately under the conditions when large permanent deformations are likely. Lower temperatures and thin layers, however, do still present a problem.

RELATIONSHIP BETWEEN RUTTING AND CREEP TESTING

The use of creep tests on asphaltic materials together with elastic layer theory to represent the response of the pavement structure to load is an alternative approach proposed recently by Shell investigators[25-27] to estimate the amount of rutting occurring in the AC layers of the pavement. Three phases may be distinguished in the work carried out by Shell, i.e.:[31]

a. A study of the creep properties of asphalt mixes.[25]

b. A correlation of rutting and creep tests on asphalt mixes.[26]

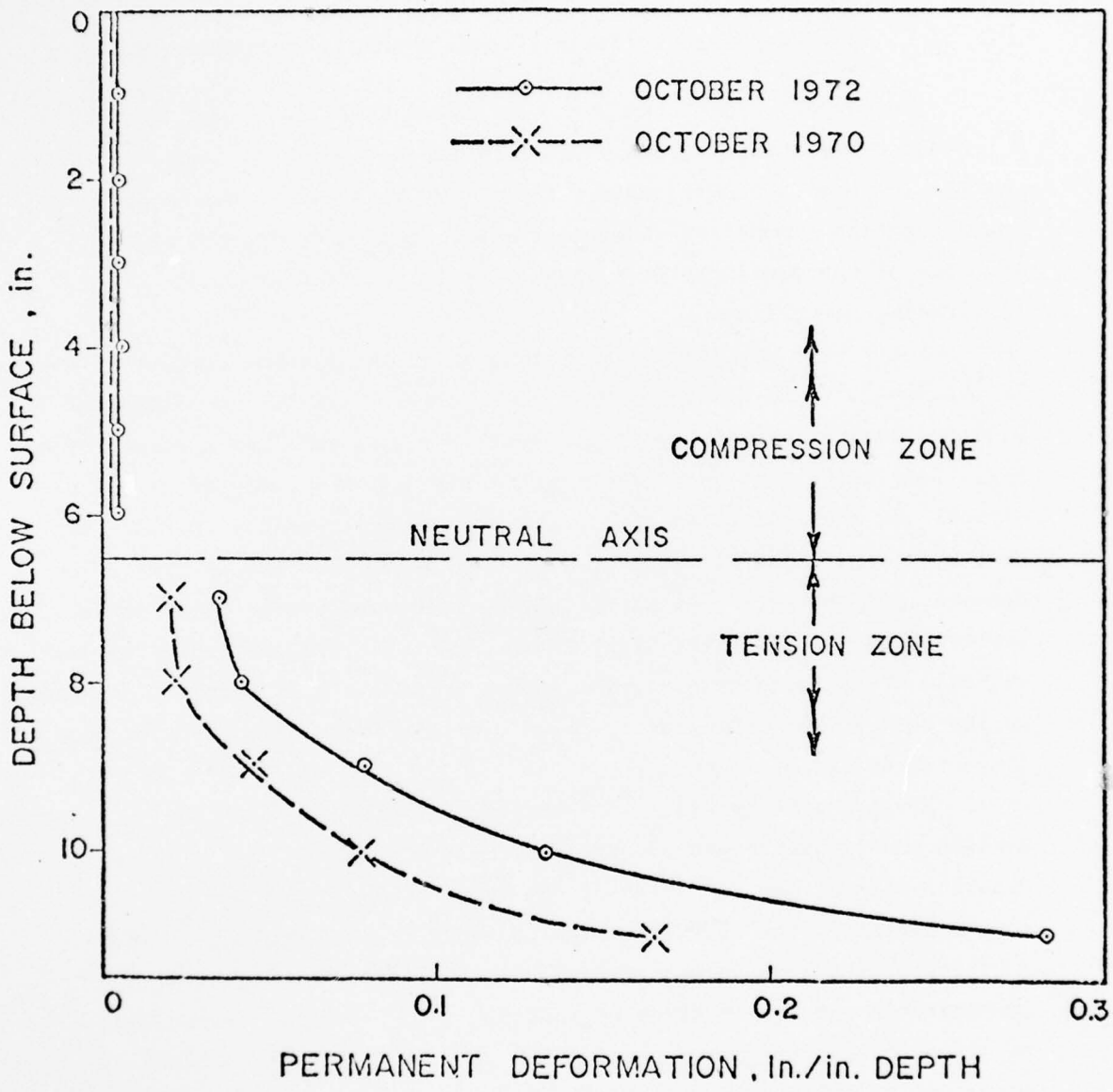

Figure 4. Variation of permanent deformation rate in an 11-1/2-in. AC pavement (after Morris[8])

c. The systematic discrepancies observed in the second phase were studied with regard to the main points of difference between the creep and rutting tests, i.e., unconfined-confined and static-dynamic.[27] A design procedure was then proposed for estimating, from the creep behavior of a mix in the laboratory, the performance of the actual pavement based on the "predetermined criteria of the pavement deformation and desired service life."

The overall aim of the work, as stated by Hills,[25] was to provide a procedure whereby rut depth could be predicted when the asphaltic mix and the in-service conditions are known. To this end, creep tests were carried out in a modified version of a soil consolidation apparatus. The ends of the specimens were lubricated by powdered graphite thus eliminating barrelling.

Tests were carried out in a controlled temperature room at either 10, 20, or 30° C on specimens that were usually 0.79 in. in height and 2.36 in. square in cross section. Specimens were cut from a slab of the mix. Some tests were carried out on cylindrical specimens of Marshall dimensions, the load being applied in the axial direction. Failure of test specimens was defined as the point at which the rate of strain increased, and the experimental data given were confined to those parts of the creep curves where the strains were less than the critical "failure" values. Creep tests were carried out on a range of mix compositions and, in the case of one composition, for a series of specimens that had been compacted by various methods.

Earlier work by Shell[34,35] had shown that for short times of loading and low temperatures, the stiffness of the mix S_{mix} was a function only of the stiffness of the bitumen S_{bit} and the volume concentration of the aggregate when the void content did not exceed 3 percent. The results reported by Hills[25] indicate that, at higher temperatures and longer times of loading, S_{mix} becomes insensitive to variations in the corresponding low values of S_{bit} and tends to level out to a limiting value. Furthermore, in addition to the effect of the volume concentration of aggregate, the gradation and shape of the aggregate play a role and the state and method of compaction exert a strong influence on the behavior. Other results indicate that:

a. In the case of two mixes with the same aggregate grading but with different asphalt contents and compacted in the same way, the mix with the lower asphalt content has a higher value of S_{mix} at any particular value of S_{bit}.

b. The effect of substituting crushed for rounded aggregate is to produce, at low values of S_{bit}, higher values of S_{mix}.

c. Void content of the mix cannot be used in itself for specifying the state of compaction.

Hills suggested that creep curves indicate a continuous change in the internal structure of a mix during the course of a test, and theoretical models for the deformation were developed to take this into account.

A study of the correlation between the creep and rutting properties of asphalt mixes in laboratory tests is described by Hills, Brien, and Van de Loo.[26] There were two types of rutting tests in both of which a wheel was rolled on the material in a single-wheel path. In the one, rutting tests were carried out on an indoor circular test track. A wheel ran at a constant speed in a circular path on a track which was 27.6 in. wide and consisted of an AC layer laid on sand compacted to give a uniform CBR of 10. The average tire contact pressure was 72.5 psi. In the other test, a solid rubber-tired wheel passed back and forth over an 11.8- by 11.8- by 2-in. AC slab which lay on a rigid steel base. In all tests, tire contact pressure was 117.5 psi.

To enable comparison between the results of the creep and the rutting tests, it was necessary to express the results of both in the same units, i.e., in terms of S_{mix} and S_{bit}. For the purpose of evaluating S_{mix} for the rutting tests, use was made of the BISTRO computer program to take into account the differences in geometry between these tests and the creep tests together with effects due to modular ratio between the AC layer and the supporting medium. The effect of repeated loading was accounted for by a summation procedure in which it was assumed that only the viscous component of the stiffness modulus of the AC contributed to permanent deformation. The results of creep and rutting tests were then compared directly by plotting the stiffness modulus of the mix S_{mix} against that of the bitumen S_{bit} for the creep tests and against the viscous part of the bitumen modulus $\left(S_{bit}\right)_{visc}$ for the rutting tests.

It was concluded that, when plotted in this way, there was good agreement between the creep and rutting curves for a variety of asphalt mixes and test conditions and that the internal deformation mechanisms in the mixes were the same for both rutting and creep. It was further concluded that the analytical procedures used for the two types of test were satisfactory. It was thus considered reasonable to make use of the creep test in predicting the deformation that would occur under prescribed conditions in a rutting test in which the loaded wheel runs in a single-wheel path.

The calculated and observed rut depths for 10 mixes tested in the tracking machine and the laboratory test track were compared. It was found that for both kinds of rutting test and a wide range of mix types, rut depths can be predicted from the results of creep tests within a factor of about 2 for rut depths ranging from approximately 0.04 to 0.4 in.

The results showed that the observed deviations were systematic, and the measured deformations were generally higher than those calculated. It was thus decided to investigate[27] the main differences that exist between the two test methods; i.e., an unconfined, static test (creep) and a confined, dynamic test (rutting experiments).

In determining S_{mix} for the rutting tests, use was made of a correction factor of 2 derived from an analysis using the BISTRO computer program. To establish if this assumption of elastic behavior was in fact an oversimplification, parking tests were carried out with a static wheel on the test track pavement. The parking tests were carried out for 24 hr at ambient temperature and the contact stress was taken to be equal to that in the rutting test, i.e., 72.5 psi. A comparison of the measured rutting and parking deformations at equal values of $\left(S_{bit}\right)_{visc}$ indicated that the parking deformations showed the same systematic deviations from the rutting values as those calculated from the creep test. The fact that the systematic deviations in the parking test were almost a factor of 3 as opposed to a factor of 2 for the creep tests suggests that the use of an "elastic" correction was a better approximation than a procedure in which the geometry was simulated in a continuous parking or indentation test. It was thus concluded that

the systematic difference between the two types of test did not result from the use of the "elastic" correction factor or from the fact that the one was confined and the other was not, but rather from the fact that the one was static and the other dynamic.

The assessment of the "static-dynamic" contribution to the observed deviation was made by carrying out unconfined creep tests, with continuous and repeated loading. The measured total and permanent deformations, or the stiffness of the mix derived from them ($S_{mix} = \sigma/e_{mix}$), were in all cases compared at equal values of S_{bit} and $\left(S_{bit}\right)_{visc}$, respectively.

It was concluded that, with regard to permanent deformation, the dynamic stiffness modulus of an asphalt mix is always lower than the static one, compared at equal values of S_{bit} and $\left(S_{bit}\right)_{visc}$.

It was found that even in the most simple laboratory rutting experiment (constant speed, constant load, single-wheel path, controlled temperature) it was not possible to predict rut depth with a higher accuracy than a factor of 2. The accurate prediction of rut depths on the actual road was thus considered to be extremely difficult and it was concluded that the main purpose of laboratory test methods must be limited to the ranking of materials rather than the prediction of rut depths.

Some creep testing was also undertaken by Snaith[28] in association with his repeated load tests. The object was to see if a relatively simple test could be used to predict the permanent deformation under the more complex repeated load situation. Similar ranges of vertical stress and temperatures to those used in the repeated load tests were investigated. It was intended to determine the level of static stress which gives the same creep curve as a particular dynamic stress. This has been done in Figure 5 where the strains after 100 and 500 sec have been plotted against the applied stresses. It was found that at low stresses the static and dynamic results are similar. However, at the higher stress levels, a static stress of about 65 percent of the dynamic value would be required to produce the same strain at a particular time.

In the creep tests, the mechanism of deformation was not complicated by the cracking noted for the dynamic tests. Shorter lives would,

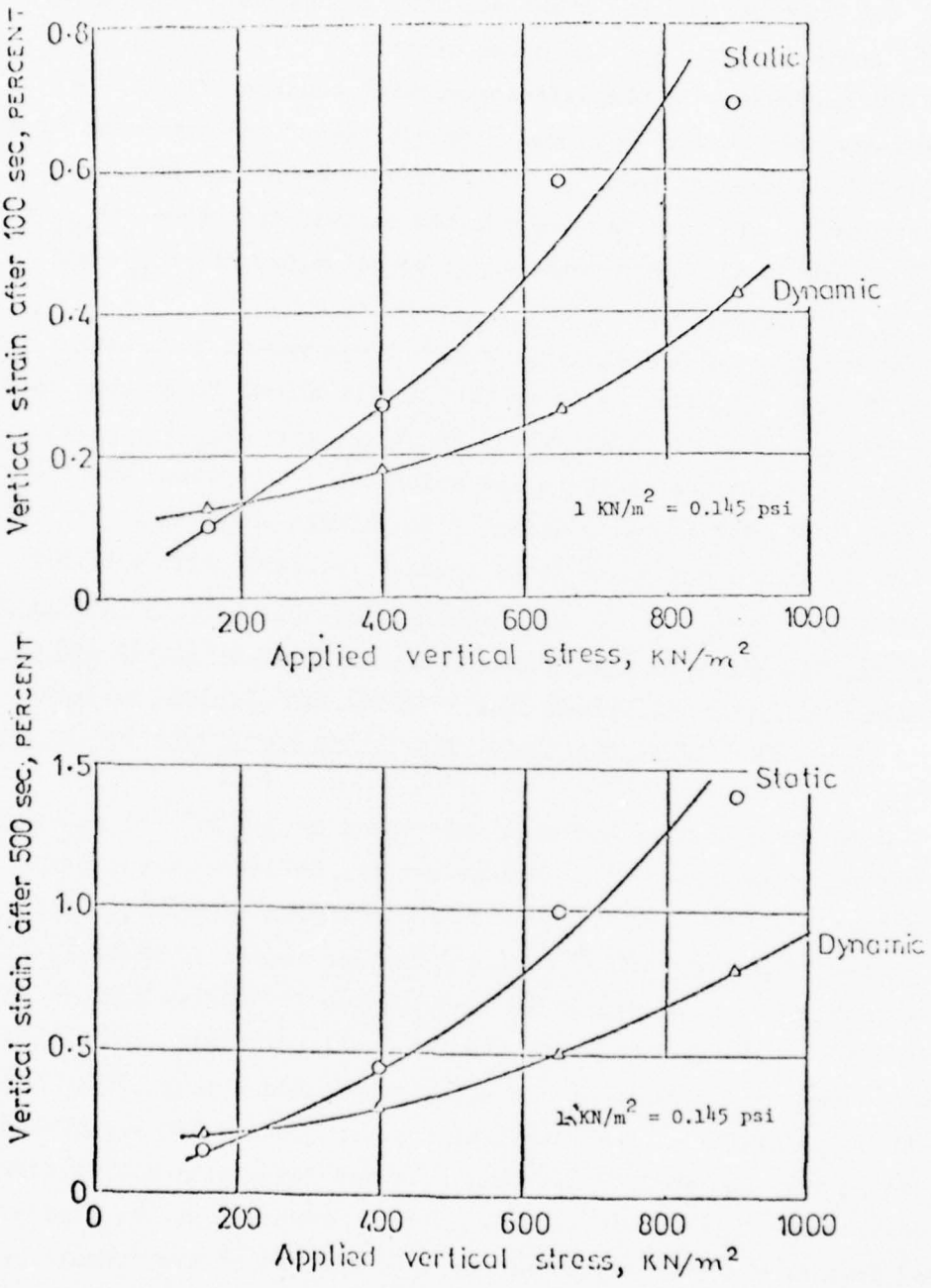

Figure 5. Comparison of results from dynamic tests and creep tests at 20° C

therefore, be expected in the dynamic case under comparable conditions. The fact that the creep stress necessary to produce strains similar to those in a dynamic test is 65 percent of the dynamic stress rather than 50 percent supports this.

Lateral deformations were not measured in the creep tests, so no measure of volume change was obtained. Hills, Brien, and Van de Loo[26] have, however, reported volume decreases in similar creep tests. This suggests a different mode of failure from that occurring in the dynamic case where dilation takes place.

UNTREATED GRANULAR MATERIALS

No effort has been made to investigate the characteristics of deformation of pavement materials and to predict rut depths of a pavement using rational methods until very recently. Research in this area conducted by Barksdale,[23] Allen,[36] Kalcheff,[37] Brown,[38] and Barrett[39] is presented below.

GEORGIA INSTITUTE OF TECHNOLOGY

Barksdale[23] was first to investigate the plastic deformation of a variety of granular materials tested in the repeated triaxial cell and developed a method for estimating the rut depth in flexible pavement. Table 3 summarizes the 10 different kinds of base materials Barksdale tested in the repeated load triaxial cell. The specimens were tested to an average of 100,000 load repetitions at constant confining pressures of 3.5 and 10 psi. The tests were performed using deviator stresses varying from approximately 1 to 6 times the confining pressure.

The relationship for a granite gneiss (Base 6) between the axial plastic strain occurring in the cylindrical specimens and the number of load applications for varying deviator stresses is shown in Figure 6. The plastic strain accumulates approximately logarithmically with the number of load applications. For very low deviator stresses, the rate of accumulation of plastic strain tends to decrease as the number of load applications increases. As the deviator stress increases, a critical value is reached beyond which the rate of strain development

Table 3

Summary of Material Characteristics of Bases Tested in the Repeated Load Triaxial Apparatus (after Barksdale[23])

Base	Description	Grain-Size Distribution Percent Passing					Maximum Density			Soil Characteristics		
		1 in.	3/4 in.	No. 10	No. 60	No. 200	Test Method*	γ_d pcf	w_{opt} percent	Liquid Limit LL	Plasticity Index PI	Classification**
1	Orange-tan, slightly clayey, silty sand	100	100	100	63	40	GHD-7	115.4	13.0	22	6	A4(1); SM-ML
2	40% silty fine sand and 60% No. 467 crushed granite gneiss	99	85	42	25	13	GHD-49	138	4.2	SIC†	N.P.	A-2-4(0); SM
3	40% silty sand and 60% No. 467 crushed biotite gneiss	100	72	39	23	11	T-180C	138	7.5	SIC	N.P.	A-2-4(0); SM
4	17% silty sand and 83% crushed biotite granite gneiss	95	60	30	13	8	GHD-49 T-180C	143 141.6	4.6 5.9			A-2-4(0); SM
5	21% sandy silt and 79% crushed biotite granite gneiss	97	78	28	28	14.8	GHD-49 T-180C	140 140	6.0 6.3	35	15	A-6(5); ML
6	Crushed prophyritic granite gneiss - 3% fines Source 1	100	60	25	9	3	GHD-49 T-180C	136 137.4	3.7 6.5			
7	Crushed porphyritic granite gneiss - 11.25% fines Source A	100	90	45	27	11.25	GHD-49 T-180C	135 135	5.7 6.0			
8	Crushed biotite granite gneiss - 3% fines Source B	100	60	25	9	3	T-180C	137.4	6.5			
9	Crushed biotite granite gneiss - 11.25% fines Source B	100	90	45	27	11.25	T-180C	135	6.0			
10	Crushed biotite granite gneiss - 22% fines Source B	100	90	45	27	22	T-180C	132.9	6.1			

* Maximum density obtained by the State Highway Department of Georgia's test methods GHD-7 and GHD-49, corresponding approximately to AASHO designations T-99 and T-180, respectively.

** The AASHO Classification System is given first and the Unified Soil Classification System second.

† Soil slid in cup of Atterberg limit device.

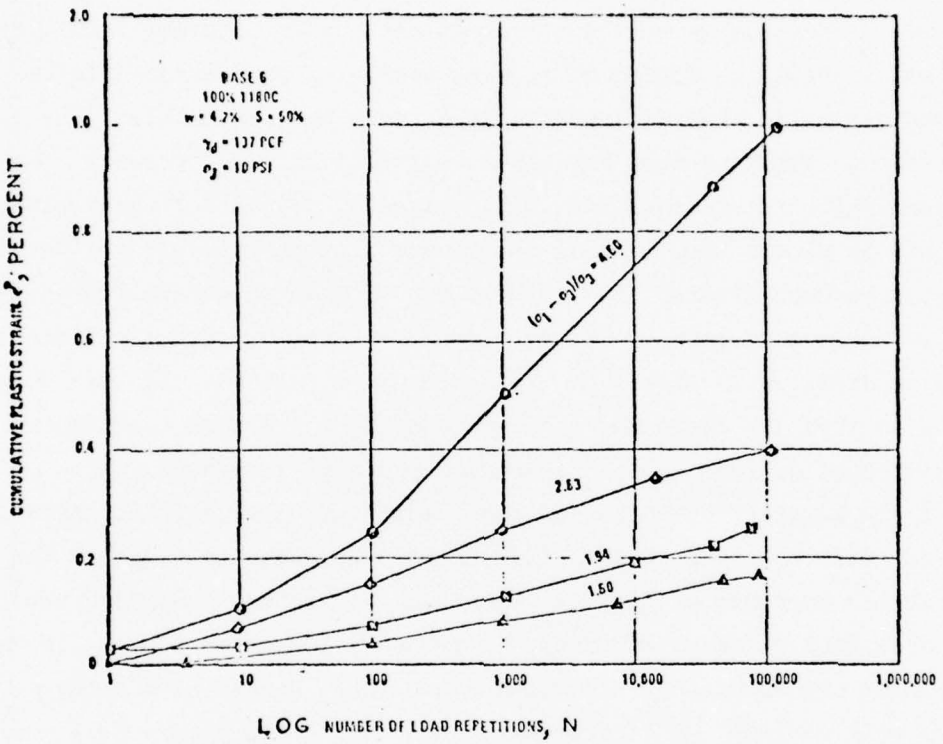

Figure 6. Influence of number of load repetitions and deviator stress ratio on plastic strain in a porphyrite granite gneiss, 3 percent fines (after Barksdale[23])

tends to increase with increasing numbers of load repetitions. Furthermore, after a relatively large number of load repetitions, the specimen may undergo an unexpected increase in the rate of plastic strain accumulation.

To study rutting in pavement systems in a rational manner, plastic stress-strain curves can be plotted, such as shown in Figure 7. These curves are analogous to the stress-strain curves obtained from a series of static tests performed at varying confining pressures. Similar plots were also obtained for the other nine base materials. The plastic stress-strain curves exhibit a typical nonlinear response. At a given confining pressure for small values of deviator stress, plastic strain is almost proportional to the deviator stress. As the deviator stress becomes greater, the development of plastic strain increases at an increasing rate until the plastic strains become very large as the apparent yield stress of the material is reached. Elastic strain is also strongly dependent upon the confining pressure, undergoing a significant decrease as the confining pressure increases.

A summary comparison of the plastic stress-strain characteristics of the base course materials investigated is given in Figure 8 for a confining pressure of 10 psi. Although the average confining pressure in a typical pavement structure is probably less than 10 psi, the comparisons are shown for this value since these stress-strain curves were more well defined. All materials compared in this figure were compacted to 100 percent of AASHO T-180 density or its equivalent except the silty sand which was compacted to 100 percent of AASHO T-99 density.

The base materials exhibiting by far the largest plastic strains were Base 1, a fine silty sand base, and Base 2 which was a 40-60 soil aggregate base. For deviator stress ratios greater than 2.5, the measured plastic strains in the silty sand were larger than those in the 40-60 soil aggregate. Base 3, which was another 40-60 soil aggregate base, exhibited approximately one-half the plastic strain occurring in the first 40-60 soil aggregate base due apparently to slight differences in the soil properties. For deviator stress ratios greater

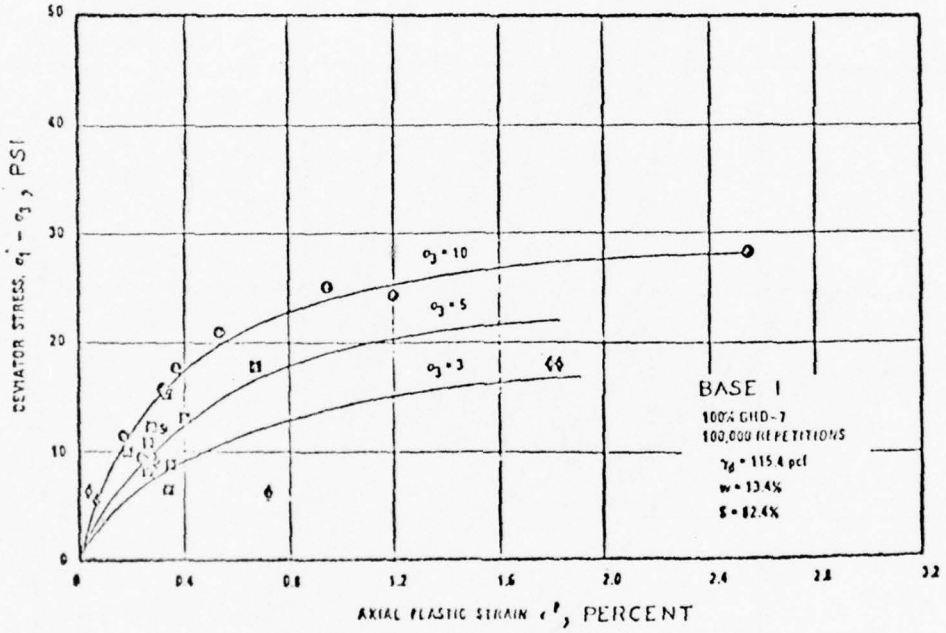

Figure 7. Influence of deviator stress and confining pressure on plastic strain after 100,000 repetitions in a fine silty sand (after Barksdale[23])

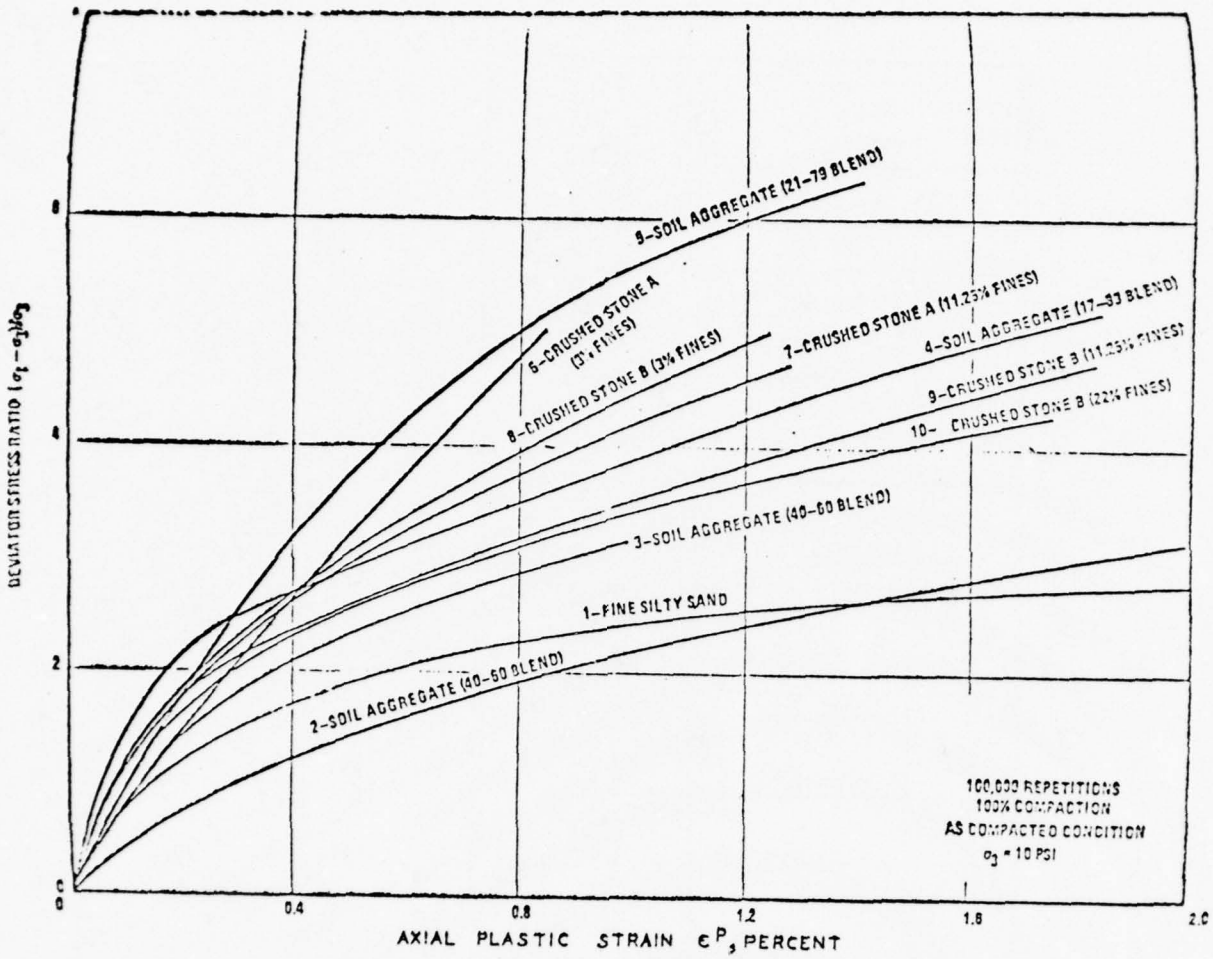

Figure 8. Summary of plastic stress-strain characteristics at 100,000 load repetitions and a confining pressure of 10 psi (after Barksdale[23])

than 2.5, the average plastic strains in this soil aggregate base were, however, still almost twice those occurring in Bases 4 and 5 which had only approximately 20 percent soil. Figure 8 shows that both soil aggregate bases tested having nominally 20-80 blends had significantly better plastic strain characteristics than did the two 40-60 bases. The plastic strain characteristics of the graded soil aggregate bases tested in the as-compacted condition were thus found to vary from very poor to quite good depending apparently on the soil characteristics, the percent of soil used in the base, and the degree of saturation.

For deviator stress ratios greater than about 2.5, the 17-83 soil aggregate (Base 4) exhibited significantly more plastic strain than did the best performing crushed stone (Base 6) which had 3 percent fines. For deviator stress ratios less than 5, the plastic strains occurring in the 21-79 blend soil aggregate (Base 5) were on the average about 20 percent less than those occurring in the best crushed stone; at greater stress ratios, however, apparently the trend was reversed for 21-79 blend and best crushed stone.

The curves shown in Figure 8 for the crushed stone bases indicate that the plastic strains occurring in the biotite granite gneiss (Bases 8 and 9) are greater than those in a porphyritic granite gneiss (Bases 6 and 7) for the same specified gradations. The significant influence of an increase in percent fines and deviator stress on the plastic strains occurring in a crushed biotite granite gneiss is illustrated in Figure 9. The plastic strains increased significantly as the percent fines increased, with greater differences occurring at the larger deviator stress levels.

A limited number of repeated load triaxial tests were performed on specimens at 90, 95, and 105 percent of maximum density. The results indicated that for all of the materials studied an average of 185 percent increase in plastic strain occurs if the base is compacted at 95 instead of 100 percent of maximum density. For an increase from 100 to 105 percent of maximum density, the corresponding average reduction in plastic strain was only about 10 percent. Barksdale remarked that more extensive testing may show the effect to be somewhat greater.

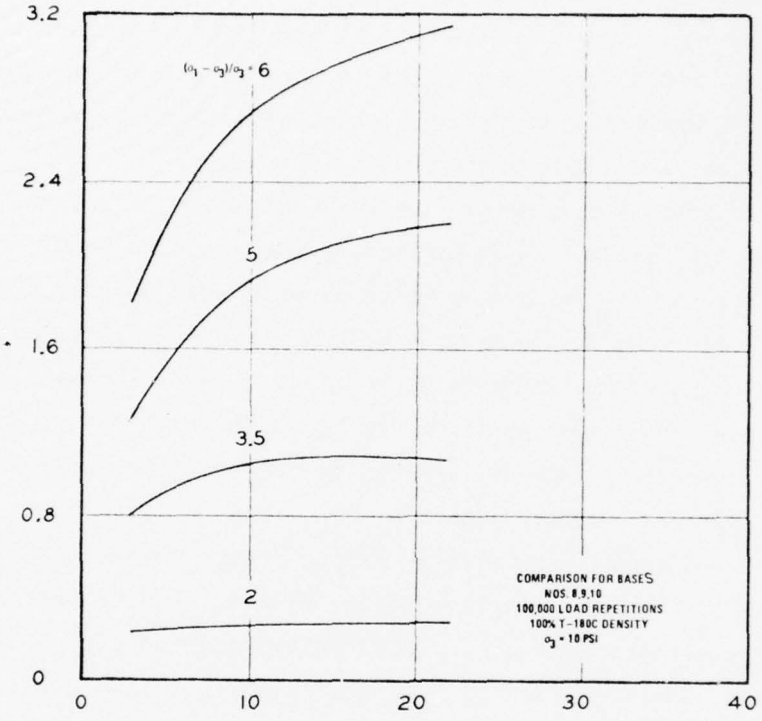

Figure 9. Influence of fines and deviator stress ratio on plastic strain in a crushed granite gneiss base after 100,000 load repetitions (after Barksdale[23])

The experimental results also indicate that for all of the materials tested an average increase in plastic strain of 68 percent occurs when the test is performed on specimens that are soaked, as compared with the results obtained from tests performed on specimens in the as-compacted condition. It should be remembered that the "soaked" specimens had a high degree of saturation but may not have been completely saturated. These specimens were tested in a manner which permitted a free flow of water into and out of the specimen so that a significant buildup of pore pressure was not likely to have occurred during application of the 100,000 load repetitions. Therefore, if a significant buildup of pore pressure should occur in the field in any of these materials due to poor drainage conditions, the laboratory test results would probably underpredict the effects that soaking of the base would have on the actual amount of rutting. Materials having the lower permeabilities such as the silty sand and graded aggregate bases would be more susceptible to such a pore pressure buildup in the field.

In summary, the plastic strains of granular materials increase with increasing deviator stress; decrease with increasing confining pressures; and increase significantly with increasing fines, with greater differences occurring at the larger deviator stress levels. Laboratory tests also revealed that the plastic strains increased drastically if the base is compacted at 95 instead of 100 percent of maximum density. The failure of plastic deformation could be more serious than predicted in the laboratory if a significant buildup of pore pressures should occur in the field due to poor drainage conditions.

In order for the rutting characteristics of base materials to be easily compared, Barksdale[23] proposed the concept of a rut index. This is defined as the sum of the plastic strains in the center of the top and bottom halves of the base, multiplied by 10^4. This requires that values of deviator and confining stresses be selected for a typical pavement, and the plastic strains obtained at a particular number of load repetitions. Barksdale presents rut indices at 10^5 load repetitions for the materials tested. These give a numerical comparison representative of the curves shown in Figure 8, and are given in Table 4.

Table 4

Summary of Elastic and Plastic Base Characteristics
Evaluated From Repeated Load Triaxial Tests

Base	Base Description	Sample Condition	Plastic Strain, 10^2 percent, of Cited Deviator Stress Ratio of 100,000 Repetitions*			Rutting Characteristics	
			2.5	3.5	6.0**	Rut Index at 100,000 Repetitions	Rut Potential at 1,000,000 Repetitions
1	Silty fine sand	100% GHD-7	114	00	00	Very Large	----
		soaked					
2	Soil aggregate 40-60 blend	100% GHD-49	128	270	780	1050	1130
		soaked	128	270	---	(Extrapolated)	
3	Soil aggregate 40-60 blend	100% T-180C	58	120	285	405	467
		soaked	90	190	---		
4	Soil aggregate 17-83 blend	100% GHD-49	30	82	250	332	372
		soaked	36	---	---		
5	Soil aggregate 21-79 blend	100% GHD-49	30	44	120	164	202
		soaked	40	64	---		
6	Crushed porphyrite granite gneiss - Source A 3% fines	100% T-180C	38	56	120	176	254
		95% T-180C	50	76	170		
		soaked	70	114	---		
7	Crushed porphyritic granite gneiss - Source A 11.25% fines	100% T-180C	38	72	226	298	360
		95% T-180C	126	large	---		
		soaked	170	large	---		
8	Crushed biotite granite gneiss - Source B 3% fines	100% T-180C	36	78	100	258	292
9	Crushed biotite granite gneiss - Source B 11.25% fines	100% T-180C	46	105	280	385	630
10	Crushed biotite granite gneiss - Source B 22% fines	101.4% T-180C	46	105	314	419	5520

* σ_3 = 10 psi.

** These values were in most instances extrapolated from laboratory test data.

It is desirable to be able to predict rutting at higher numbers of load repetitions, i.e., 10^6 or more, but, to test specimens to this extent would be time-consuming and expensive in practice. It is thought acceptable to extrapolate through one decade on a plastic strain versus log number of repetitions plot and then use the results to construct plastic stress-strain curves from which the rut potential can be estimated. Rut potentials at 10^6 load repetitions are presented in Table 4.

The rut index and rut potential offer a rapid approximate comparison of rutting characteristics of base materials of the same thicknesses, subject to the same loading and environmental conditions.

UNIVERSITY OF ILLINOIS

Allen[36] conducted a series of laboratory repeated triaxial tests on three different granular materials subjected to both constant and variable confining pressures. Test data indicated that the nonrecoverable deformations associated with the constant confining pressure (CCP) portion of the tests exceeded those associated with the variable confining pressure (VCP) portion for every specimen. Table 5 shows the total plastic axial strain accumulated by each specimen during the entire test series. It also shows the percentage of the total plastic strain accrued during the CCP and VCP portions of each test series. From Table 5 it can be seen that the CCP portion of each test series produced results from 2 percent to 56 percent greater plastic axial strains than the VCP portion test. Finn[40] has shown that, on the basis of the Mohr-Coulomb yield criteria for soils, plastic strain is accompanied by volume change. From this viewpoint, the greater volume change observed during the CCP test is compatible with the greater resultant plastic strains.

NATIONAL CRUSHED
STONE ASSOCIATION

An extensive laboratory repeated triaxial test was conducted by the National Crushed Stone Association (NCSA) to study the characteristics of plastic deformation of graded aggregates. Kalcheff[37] reported

Table 5

Percentage Total Axial Strain Accumulated
During VCP and CCP Tests

Specimen	Total Plastic Axial Strain ε_p in./in.	Percent ε_p During VCP Test	Percent ε_p During CCP Test
HD-1	0.0036	49	51
MD-1	0.0149	22	78
LD-1	0.0191	48	52
HD-2	0.0158	42	58
MD-2	0.0173	43	57
LD-2	0.0204	43	57
HD-3	0.0063	49	51
MD-3	0.0152	46	54
LD-3	0.0193	43	57

that the plastic strains are greatly dependent on the degree of consolidation for the same gradation, the amount and type of fines in the gradation, the stress sequence and magnitude, and for some types of fines the moisture content. The procedure is extremely useful for optimizing materials combinations or for the relative ranking of different materials at the same stress conditions. The NCSA investigations show that graded aggregates can be proportioned for minimum plastic deformations to provide a base that improves its resistance to rutting with time and one which will not crack or lose stability with age. Figure 10 is an illustration of how density affects the plastic strains. The load magnitude for this material was the same.

Kalcheff[37] also illustrated in Figure 11 the effects of different types of fines on the plastic response of two types of aggregates. The gravel mix shown in the figure with either type of dust had the same elastic properties. Kalcheff thus emphasized that all graded aggregates

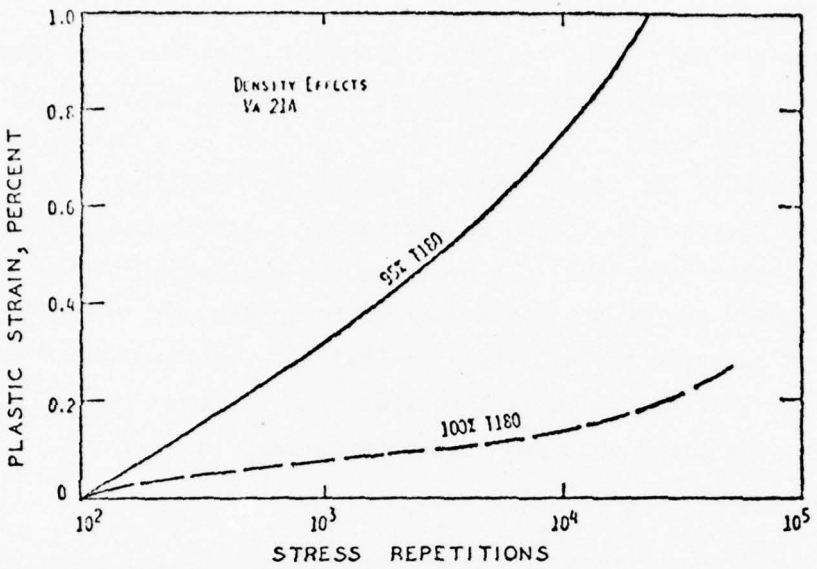

Figure 10. Effect of density on the plastic strain accumulations with load application (after Kalcheff[37])

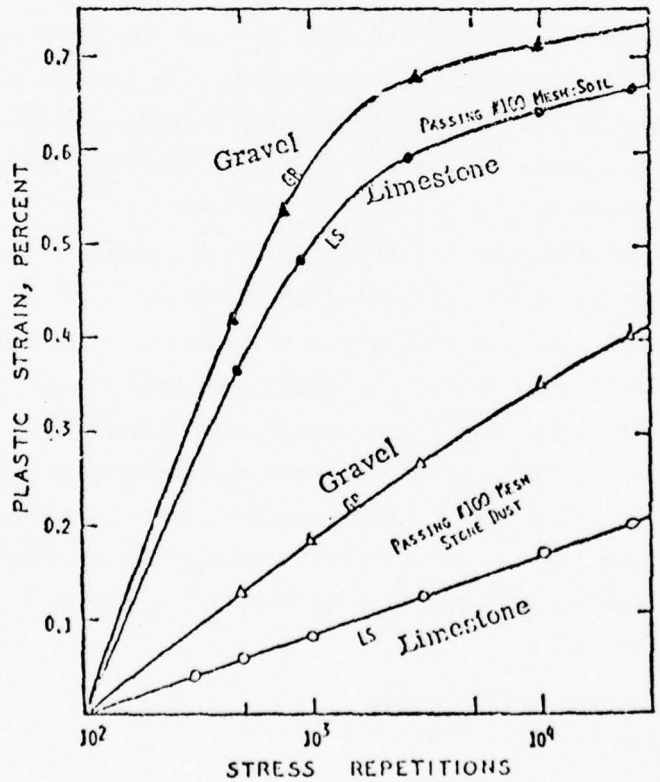

Figure 11. Effect of type of fines on the plastic strains of two graded aggregate bases (after Kalcheff[37])

do not have the same plastic strain responses under the same loading conditions even though their elastic properties and the quantity of fines may be the same.

Similar to the report made by Barksdale,[23] Kalcheff also noted the plastic strain accumulated approximately logarithmically with the number of load repetitions. In practice the magnitude of plastic strain which may occur during the first year would double only after about 10 years of carrying the same type of traffic. Kalcheff promoted the idea of stage construction which will provide time for the majority of plastic strains to take place when good clean stone base is used.

UNIVERSITY OF NOTTINGHAM

Brown[38] conducted a series of laboratory repeated triaxial tests on a crushed granite with a 0.2-in. maximum particle size. Plastic deformations were measured for each specimen. He found that under drained conditions the permanent strain reaches equilibrium values after approximately 10^4 cycles of deviator stress. The permanent strain at equilibrium could be related to the applied stresses by the equation $\varepsilon_p = 0.01\ (q/\sigma_3)$, where q is the effective deviator stress and σ_3 the confining pressure.

In a recent extension of this work at Nottingham[41] researchers investigated the influence of loading sequence and that of applying cyclic cell pressure to the same granular material. The limited study of loading sequence showed that the resilient modulus was unaffected by this but that permanent strain was significantly affected. The permanent strain which built up after successive applications of about 10^5 cycles of gradually increasing level was less than half the value resulting when the highest stress level was applied constantly. This finding is similar to that reported by Monismith, Ogawa, and Freeme[42] for a fine-grained soil.

COMMONWEALTH SCIENTIFIC AND INDUSTRIAL RESEARCH ORGANIZATION, AUSTRALIA

Barrett[39] examined existing data on permanent strain behavior of base course materials in an attempt to define the variables that affect

the recorded material response. He commented that permanent deflection of the pavement surface is due not only to vertical strain in each pavement layer, but deformation also occurs transversely due to the lateral spreading of the pavement materials. The author further commented that the emphasis on characterization through static triaxial tests often ignores the different structural changes that occur under trafficking as well as stress history, reorientation of load axes, and compound loading conditions. The use of repetitive triaxial tests to mirror traffic conditions fails to provide for any difference between the intermediate and minor principal stresses and for the continuous change between the orientation of the structural and loading axes during the trafficking. Experimental results for sands show that reorientation of principal stress axes during cyclic shear tests produced large increases in density. The density increase was related directly to the magnitude of the cyclic shear strain and was virtually independent of the normal pressure. The effect of stress reorientation in granular materials would thus seem to be to produce larger permanent strains than those predicted by cyclic triaxial testing. This would involve an increase in densification with a resulting increase in stiffness of the material and perhaps lead to stress-induced anisotropy.

Barrett also commented on the inadequacy of characterizing granular base materials as continuum rather than as a dense, graded assembly of oriented particles. He suggested that a particulate approach to internal load distribution should be used to study the deformations of granular base materials under traffic loads. The results of such an analysis would include coupled stresses rather than only satisfying equilibrium conditions at grain-to-grain contacts, and would be distinctly different from those based on a nonlinear stress-dependent continuum as is often used at present.

Barrett concluded that no model has been put forward which would adequately characterize base course material behavior under realistic field conditions.

FINE-GRAINED SOILS

Very little work has been done investigating the permanent deformations of fine-grained subgrade soils. Recently, Monismith, Ogawa, and Freeme[42] conducted a series of repeated load tests on fine-grained soils to ascertain the effects of compaction conditions, stress magnitude, and stress sequence on the accumulation of permanent strain with repeated stress repetitions.

Test results were plotted semilogarithmically with axial, radial, and volumetric strain against the number of stress repetitions. Plots of change in strain per cycle showed that the rate of strain decreases with increasing load repetitions and that permanent strain increased with increasing deviator stress. The results also showed that specimens compacted to near the maximum dry density tended to deform less.

Results of the tests to investigate stress history showed that specimens subjected to small levels of stress before being subjected to greater stress levels deformed less than those without the conditioning stress. A test series in which various combinations of 3, 5, and 10 psi were applied to specimens showed again that when the smaller stresses are applied first the specimen deforms less.

When results were plotted on a log-log basis, straight lines were obtained, as in Figure 12. These log-log plots strongly resemble similar ones plotted by Snaith[28] for bituminous material, and the form of the equation developed to represent them is the same.

In practice, subgrades are generally subjected to lower stress levels than those to which the specimens in the laboratory were subjected. The laboratory values were chosen to obtain measurable strains. Monismith, Ogawa, and Freeme applied the hyperbolic rule to their test results, and found good comparison between predicted and actual curves. Deformations at lower stress levels could then be predicted.

Equations were developed to represent the relationship between applied stress and plastic strain at a particular number of stress repetitions, and these may be used to predict permanent deformation in fine-grained soils.

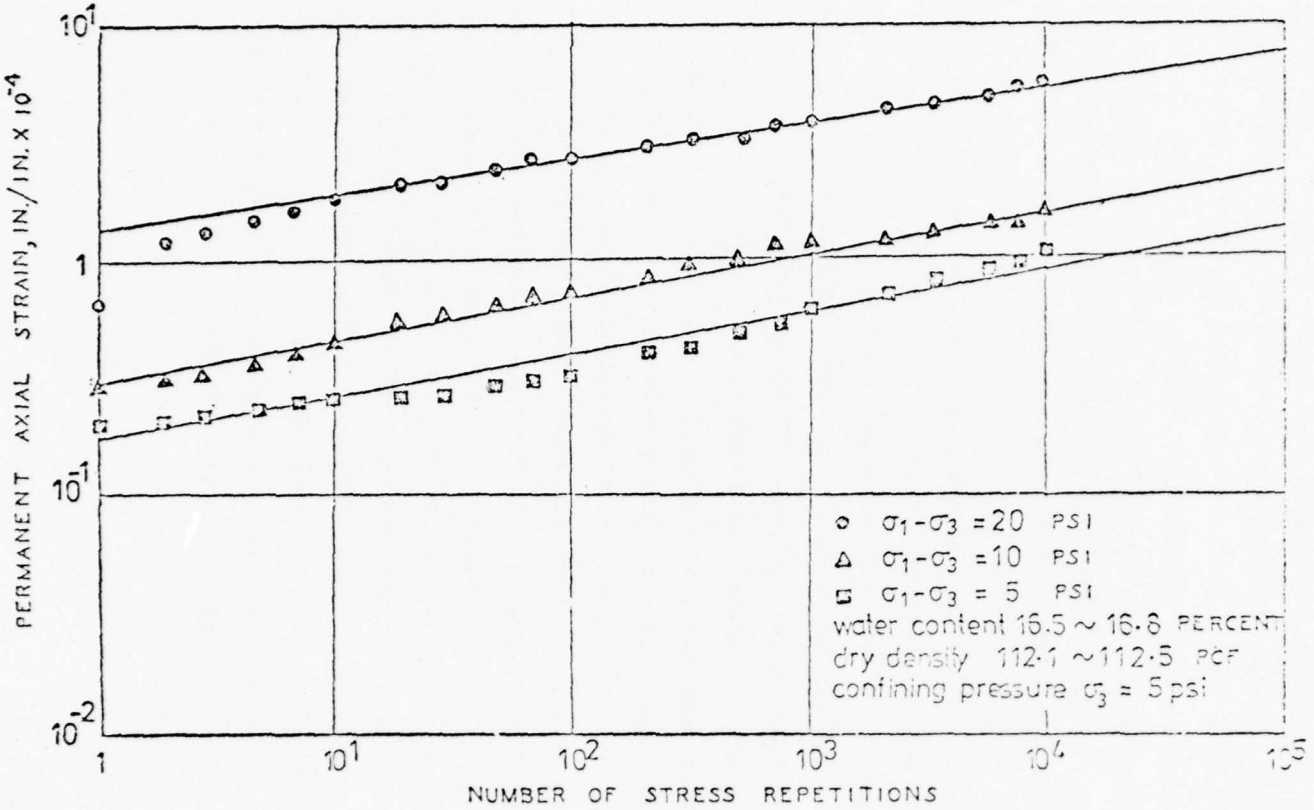

Figure 12. Relationship between permanent axial strain and number of stress repetitions (after Monismith, Ogawa, and Freeme[42])

Monismith, Ogawa, and Freeme[42] also introduced the concept of cumulative loading in this type of material, i.e., of predicting the effect of cumulative loading in the field. There are two methods available to obtain the cumulative permanent strain from results of simple loading tests: a "time hardening" procedure, and a "strain hardening" procedure. These are illustrated in Figure 13, total deformation after N_1 repetitions at σ_1 and N_2 repetitions at σ_2 being $\varepsilon_{p1} + \varepsilon_{p2}$. When these two approaches were used to predict the behavior of specimens tested with a combination of stress levels of 3, 5, and 10 psi, neither gave results that agreed quantitatively, but they were in qualitative agreement. The time hardening procedure provided better agreement when the stress levels were successively increased, while strain hardening gave better results when the loads were successively decreased. These two methods can, therefore, be used as a rough guide to bound the actual response.

Recently, Barker[43] analyzed data of repetitive triaxial tests reported by many agencies and showed that relationships exist between permanent strain and resilient strain in these data. A procedure was presented by which these relationships could be used for predicting the magnitude of rutting that a pavement would develop under traffic. Predictions of rutting were made for full-scale test sections and the predicted rut depths compared with the measured rut depths. The predicted rut depth at low levels of traffic was greater than the measured but at higher levels of traffic the measured rut depth was greater than the predicted rut depth. The difference between measured and computed values was believed to be caused by the inability to compute resilient strains. The procedure is currently under review, and a separate study is being conducted at WES to improve the technique to compute the resilient strain.

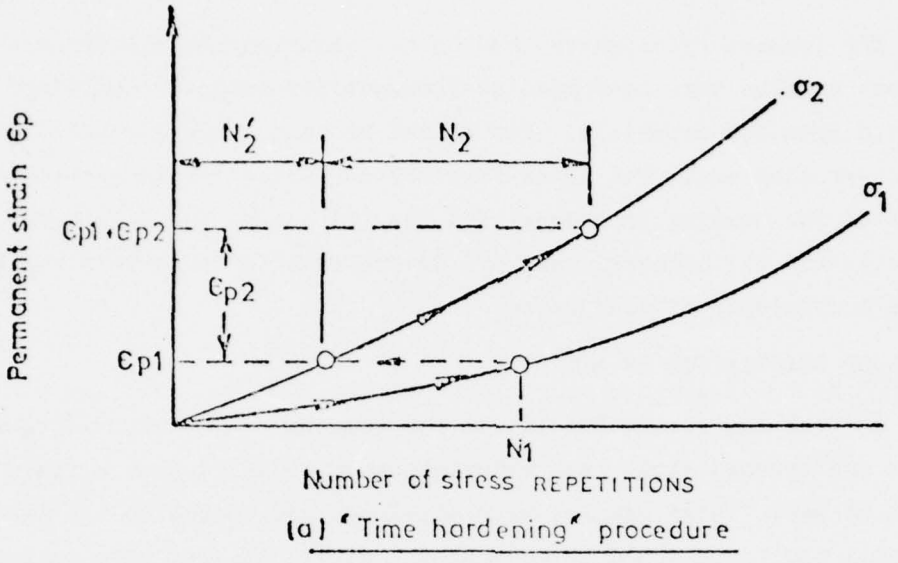

(a) "Time hardening" procedure

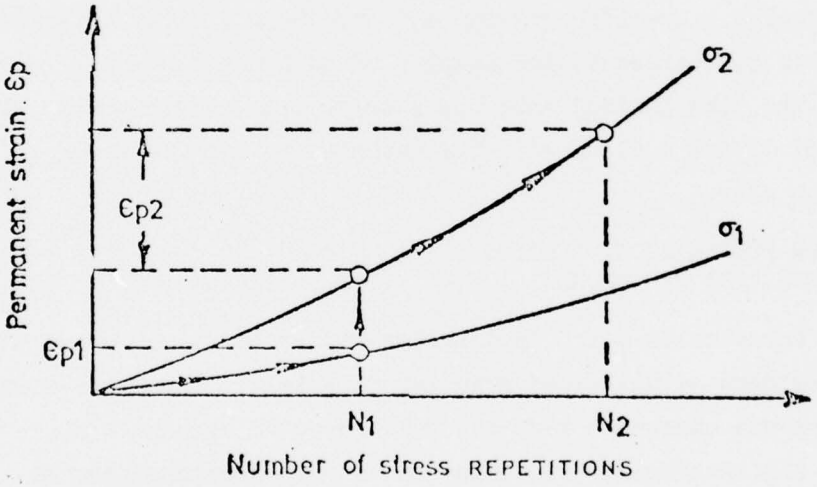

(b) "Strain hardening" procedure

Figure 13. Procedures to predict cumulative loading from the results of simple loading tests (after Monismith, Ogawa, and Freeme[42])

LABORATORY REPEATED LOAD TESTS

The laboratory repeated load tests measuring the elastic and permanent strains were performed on fine-grained subgrade soils and untreated granular materials. Two series of tests were conducted on the fine-grained soil, but tests were not conducted for AC specimens. Details of the testing procedures and results can be found in References 44 and 45; however, they are described briefly in this report for the convenience of discussion.

SOURCE AND DESCRIPTION OF MATERIAL

Several representative 100-lb bag samples of the sand and gravel subbase and crushed stone base materials were obtained from a field test section at WES. These samples were air-dried and stored in the laboratory until the tests could be conducted. Sieve analyses were conducted on representative samples of each material to determine the grain-size distribution. Specific gravity and Atterberg limits tests were also conducted on representative samples of each material.

The fine-grained soil was a heavy clay (CH) material which has an LL of 73 and a PI of 48. The material is locally known as Vicksburg buckshot clay.

SPECIMEN PREPARATION, TESTING EQUIPMENT, AND PROCEDURES

Large molds 6 in. in diameter and 15 in. high were used in molding the specimens of untreated granular materials. The large-diameter specimen was chosen so that the full range of aggregate sizes could be used. All specimens were compacted using a drop hammer with a 2.0-in.-diam striking face, a weight of 10 lb, and a fall of 18 in. Specified densities were attained by varying the number of layers per specimen and the number of blows per layer. A triaxial cell similar to most conventional triaxial cells was used for untreated granular soils except that it was made sufficiently large to accommodate the large samples. The repeated axial stress was applied to the specimen through a closed-loop electrohydraulic-actuated piston. Program input was provided by

a function generator connected to the axial load controller. Loading was applied in a haversine stress-time wave form for a 0.2-sec duration at 2-sec intervals. The actual loading applied to the specimen was monitored internally by placing a miniature 5000-lb electronic load cell on top of the specimen cap. Axial strains were measured inside the chamber by an LVDT arrangement calibrated to the nearest 0.0001 in. LVDT clamps were mounted 3.4 in. on either side of the specimen midheight and strain was measured by monitoring the relative movement between these two clamps. The radial strains were measured by LVDT's mounted on the LVDT ring clamps so as to measure twice the actual radial movement.

Two series of laboratory repeated load tests were conducted on fine-grained soil specimens prepared at several water contents to obtain different CBR values. The batched materials were sealed in a container and allowed to cure for several days. Several 2.8-in.-diam by 6.0-in.-high specimens were compacted from each batch using CE 12 compaction effort. Each specimen was compacted and sealed in a rubber membrane at least 48 hr before it was tested. This was done to insure that the water content was uniform throughout the specimen. One CBR specimen was prepared from each batch using the CE 12 compaction effort so that laboratory CBR tests could be conducted. A conventional triaxial cell was used for testing, and the repeated axial stress was applied pneumatically. Loading was applied in a trapezoid stress-time wave form for a 0.2-sec duration at 2-sec intervals. The loading was monitored by placing a miniature electronic load cell on top of the specimen cap. Axial strains were measured over the central 4 in. of the specimen by an LVDT arrangement. LVDT ring clamps were placed approximately 1 in. from each end of the specimen and strain was measured by monitoring the relative movement between these two clamps. Radial strains were not measured. Frictionless end platens, incorporating a layer of Teflon between the end platens and the specimen, were used to minimize end restraint effects. A membrane was placed on each specimen to minimize the loss of moisture during testing. No confining pressure was used in the first series of tests, but a constant confining pressure of 2 psi

was used in the second series of tests. The details of the equipment can be found in References 44 and 45.

Prior to the repeated load tests, an unconfined compression test was conducted on the fine-grained soil to determine its compressive strength. The applied repeated load stress equal to or less than 70 percent of the unconfined compressive strength was used in conducting the repeated load tests. Higher stress near the failure strength of the soil was not used in the tests.

TEST RESULTS

During the laboratory repeated load tests, both elastic (resilient) and plastic (permanent) strains were measured. Analyses were made on these measured values. The details can be found in References 43, 44, and 45. In this section, only the permanent strain data are presented and analyzed.

Figures 14 and 15 show the accumulated plastic strains for crushed limestone base and gravelly sand subbase materials. The specimens were prepared in a uniform condition, but small variations in density were observed. Two expressions of stress ratios were used in the analysis. One is the ratio of deviator stress to confining stress $(\sigma_1 - \sigma_3)/\sigma_3$, and the other is the ratio of octahedral shear stress to octahedral normal stress τ_{oct}/σ_{oct}. It was found that the use of octahedral stresses was more advantageous in this study. They will be discussed later in the report. The expressions for the octahedral shear stress and octahedral normal stress are shown below, respectively.

$$\tau_{oct} = \frac{1}{3}\sqrt{(\sigma_1 - \sigma_2)^2 + (\sigma_2 - \sigma_3)^2 + (\sigma_1 - \sigma_3)^3} \qquad (8)$$

$$\sigma_{oct} = \frac{1}{3}(\sigma_1 + \sigma_2 + \sigma_3) \qquad (9)$$

where σ_1, σ_2, and σ_3 are the major, intermediate, and minor principal stresses, respectively.

Figures 14 and 15 show that the permanent deformation of untreated granular materials increases with increasing load repetitions and stress intensity, but decreases as the confining pressure is increased. The inconsistencies of some data may be due to the variations in density.

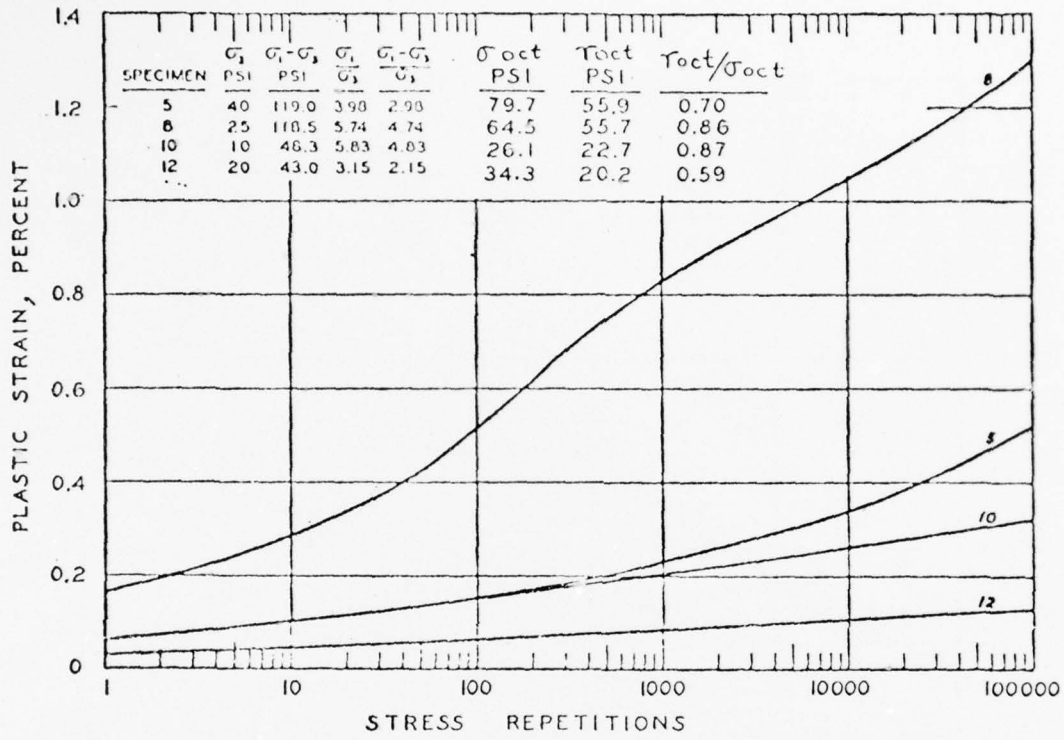

Figure 14. Accumulated plastic strains for crushed limestone specimens

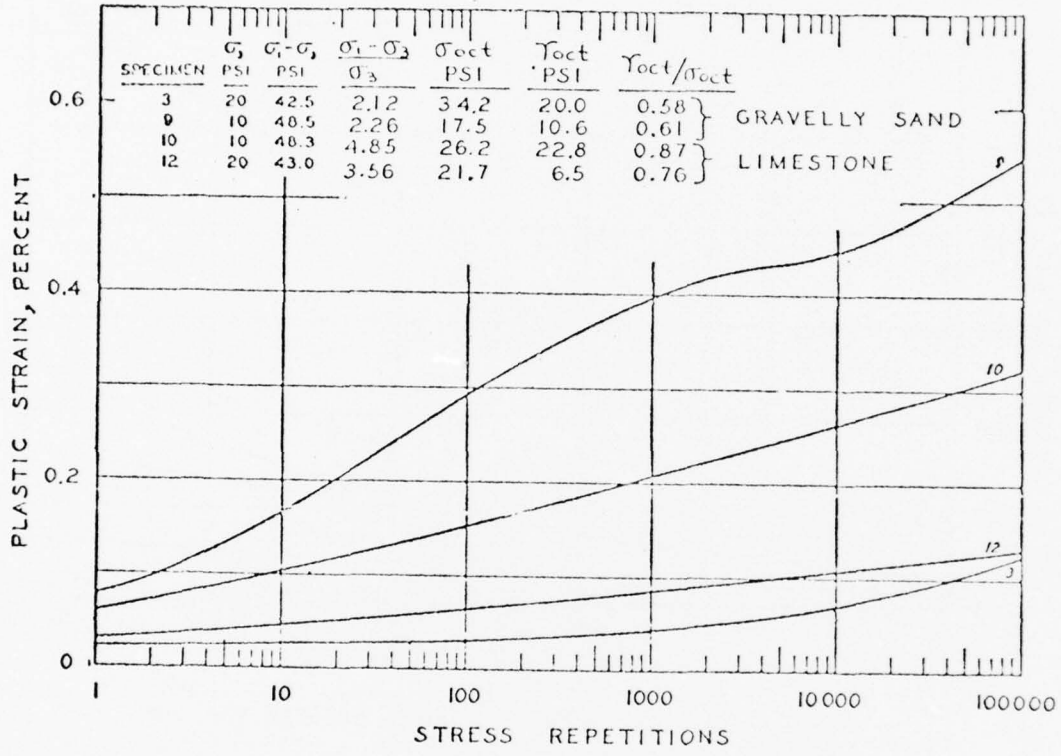

Figure 15. Accumulated plastic strains for gravelly sand and crushed limestone specimens

For instance, Specimens 5 and 8 in Figure 14 had nearly the same stress ratios but had different densities. The accumulated plastic strain for Specimen 8 (137.1-pcf density) was much higher than that for Specimen 5 (141.9-pcf density).

Figures 16a-16d show the permanent deformations of fine-grained soils having four different CBR values in the first series of tests. The CBR values were 2.4, 3.2, 5.4, and 6.3, as shown in Figures 16a, 16b, 16c, and 16d, respectively. The water contents, dry densities, and other information of each specimen tested are listed in Table 6. The repeated load tests were conducted with zero confining pressure, and the tests were carried out only up to 1000 repetitions.

Figures 17a-17e show the permanent deformations of fine-grained soils of three different CBR values in the second series of tests. The CBR values were 3.7, 7.5, and 13.8. The water contents, dry densities, and other information for each specimen tested are listed in Table 7. A constant confining pressure of 2 psi was applied to the specimens during the tests and the tests were carried out to 50,000 repetitions.

Results for both series of tests shown in Figures 16 and 17 indicate that the permanent strain increases with an increase in load repetitions, and increases rapidly with an increase in load intensity. Figure 18 shows the relation between permanent strain and load intensity at four CBR values for the soils of the first series of tests. The load repetition level was extrapolated to 5000. It can be seen that as the CBR of the soil increases, the soil's resistance to permanent deformation increases rapidly.

Elastic strains were measured in each soil specimen during the tests. Figure 19a shows the relationships between the elastic and permanent strains measured at 1,000 repetitions for soil specimens from the first series of tests. Figure 19b shows the relationships at 50,000 repetitions from the second series of tests. It can be seen that the permanent strain increases with increasing elastic strains, and at a given elastic strain, the permanent strain increases with decreasing soil strength. Similar relationships are also found for other strain repetitions. The significance of this observation will be discussed later.

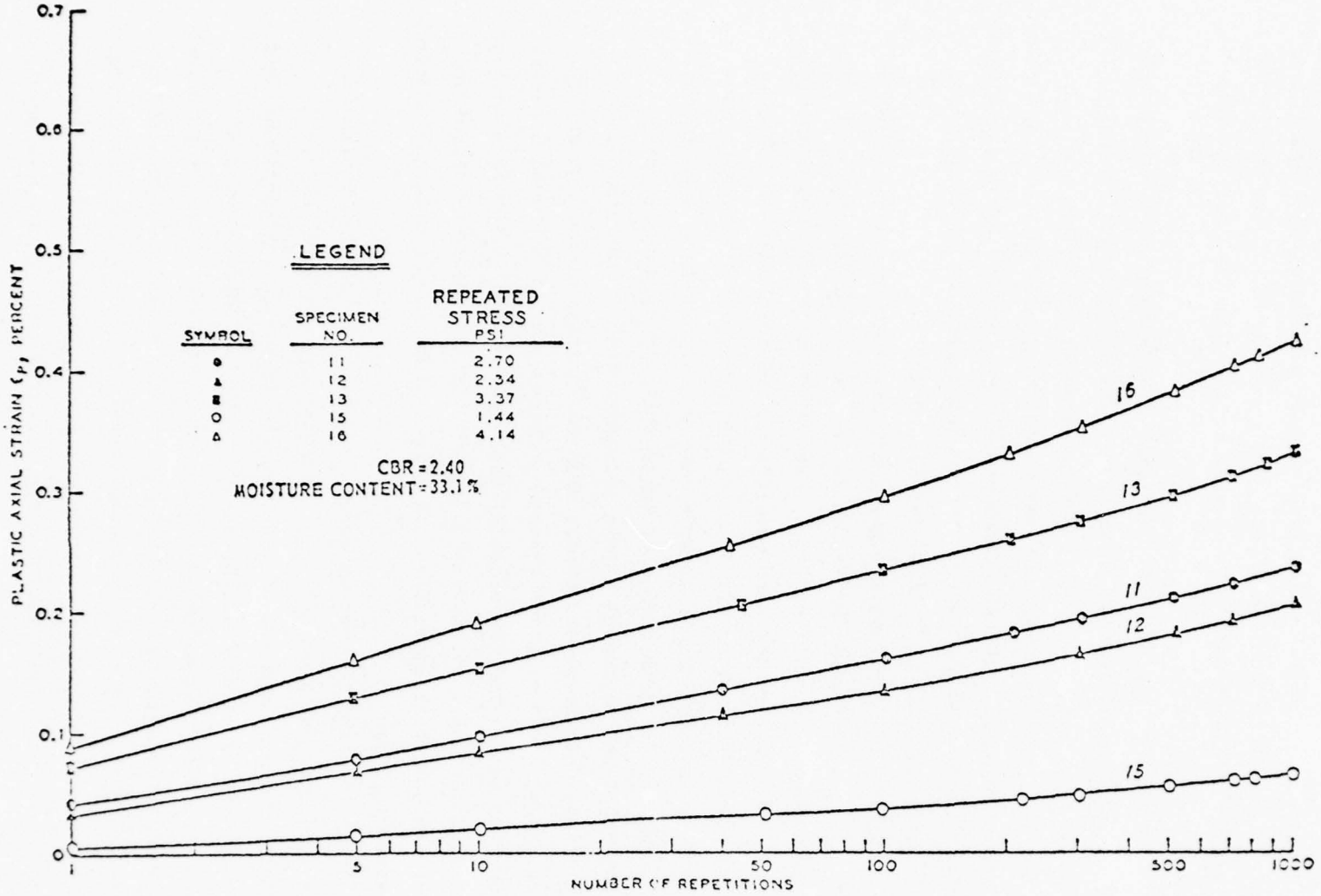

Figure 16a. Accumulated plastic strains for fine-grained soil, CBR = 2.4, first series of tests

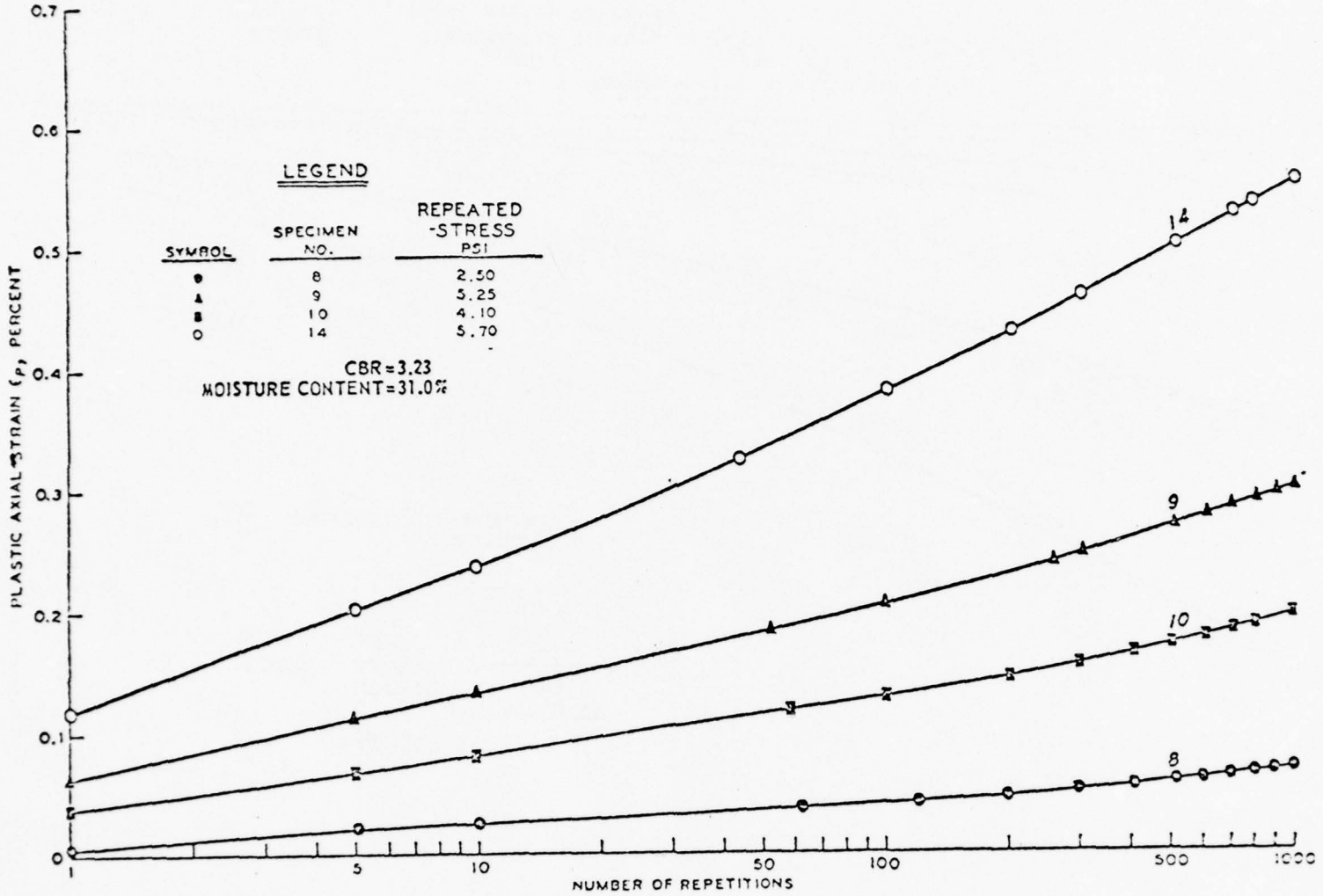

Figure 16b. Accumulated plastic strains for fine-grained soils, CBR = 3.23, first series of tests

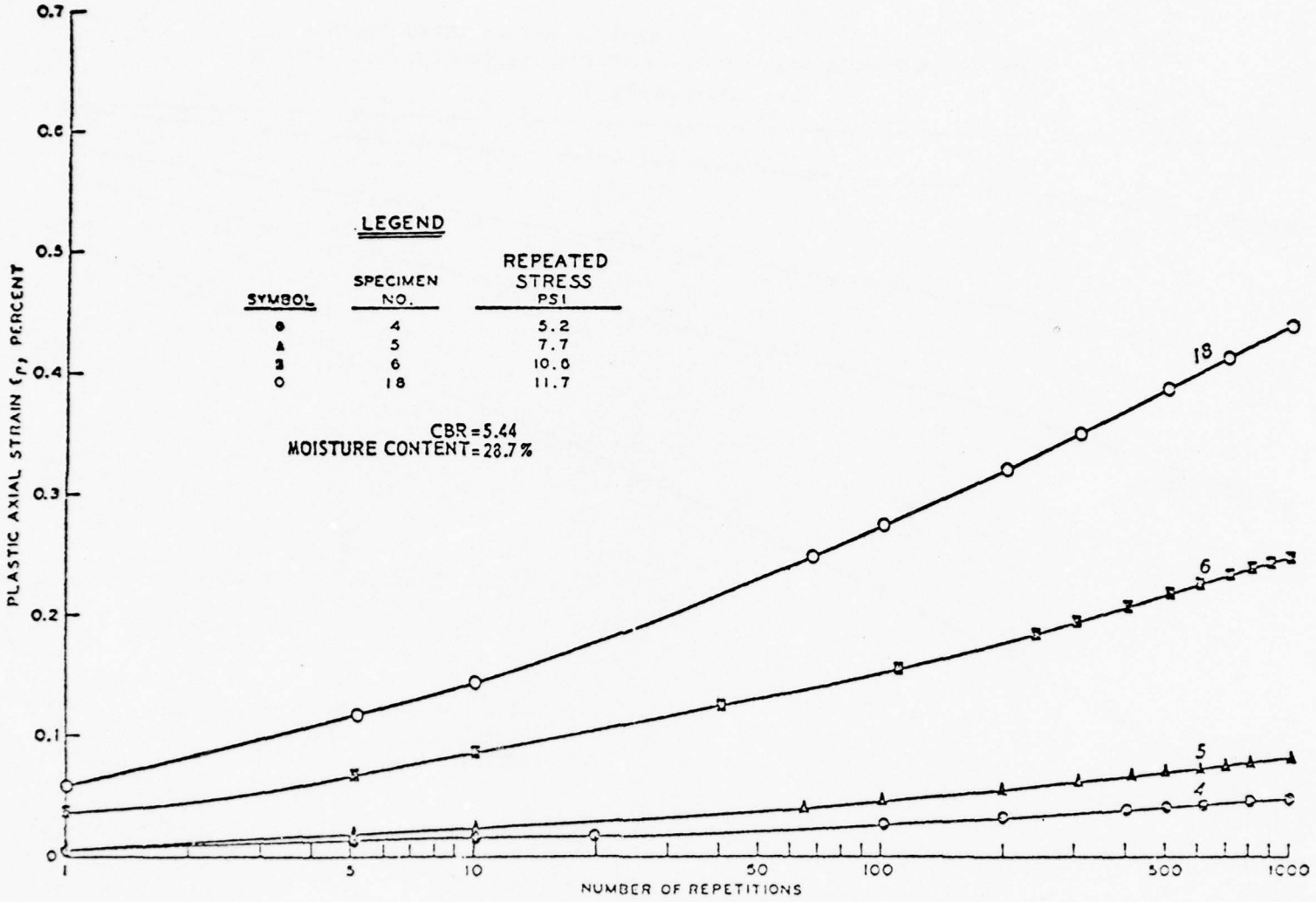

Figure 16c. Accumulated plastic strains for fine-grained soil, CBR = 5.44, first series of tests

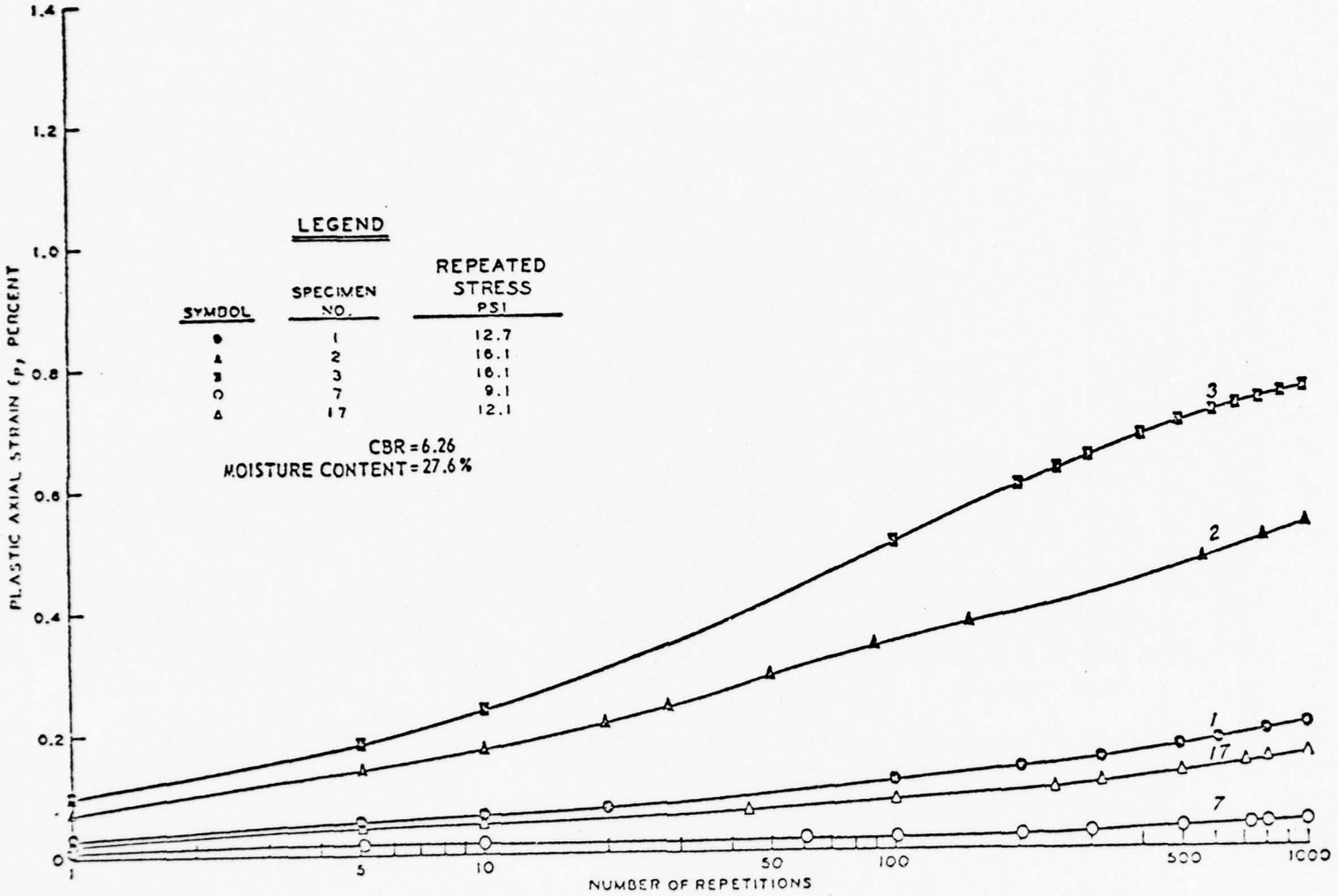

Figure 16d. Accumulated plastic strains for fine-grained soil, CBR = 6.26, first series of tests

Table 6

Specimen Identification and Composition Data
(First Series of Tests)

Specimen No.	Moisture Content percent	Dry Density pcf	Saturation percent	Cycled Stress psi	CBR at 0.1-in. Penetration
			Batch I		
1	27.6	93.0	92.4	12.7	--
2	27.7	92.4	91.1	16.1	--
3	27.9	92.1	91.4	16.1	--
7	27.4	92.1	89.6	9.1	--
17	27.1	93.1	90.8	12.1	--
CBR-I	27.6	94.1	95.0	--	6.26
Average	27.6	92.8	91.7	--	--
			Batch II		
4	28.7	91.6	92.7	5.2	--
5	28.7	91.6	92.7	7.7	--
6	28.8	90.9	91.7	10.6	--
18	28.6	91.9	91.9	11.7	--
CBR-II	28.7	92.9	95.3	--	5.44
Average	28.7	91.8	92.9	--	--
			Batch III		
8	30.9	88.8	93.2	2.50	--
9	31.0	88.9	94.0	5.25	--
10	30.8	89.0	93.4	4.10	--
14	31.2	88.5	93.4	5.70	--
CBR-III	31.1	88.2	92.4	--	3.23
Average	31.0	88.7	93.3	--	--
			Batch IV		
11	33.1	85.8	93.0	2.70	--
12	33.3	85.7	93.0	2.34	--
13	33.3	85.8	93.7	3.37	--
15	33.1	85.9	93.2	1.44	--
16	32.7	86.3	93.0	4.14	--
CBR-IV	33.5	85.8	94.3	--	2.40
Average	33.1	85.9	93.4	--	--

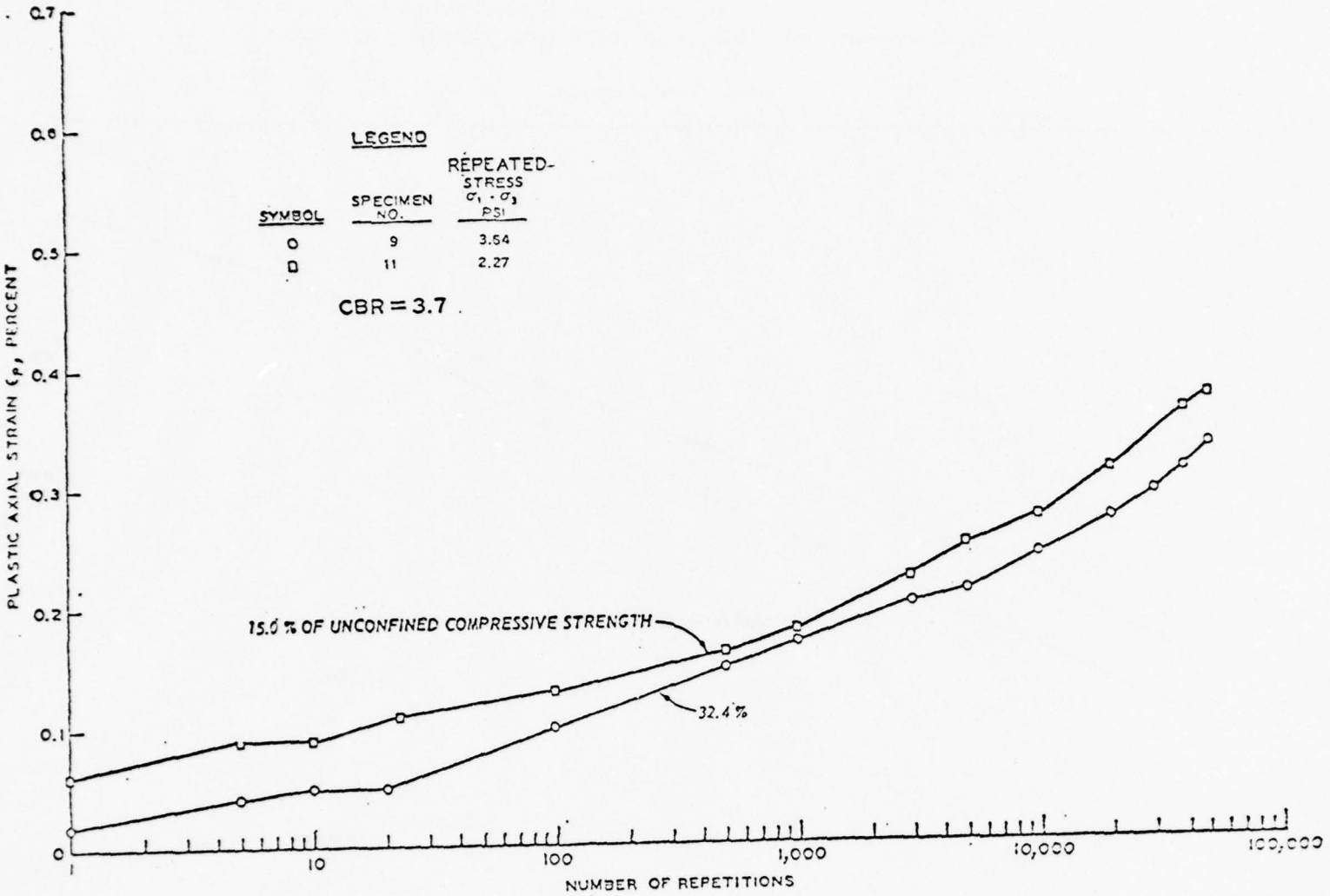

Figure 17a. Accumulated plastic strains for fine-grained soil, CBR = 3.7, second series of tests

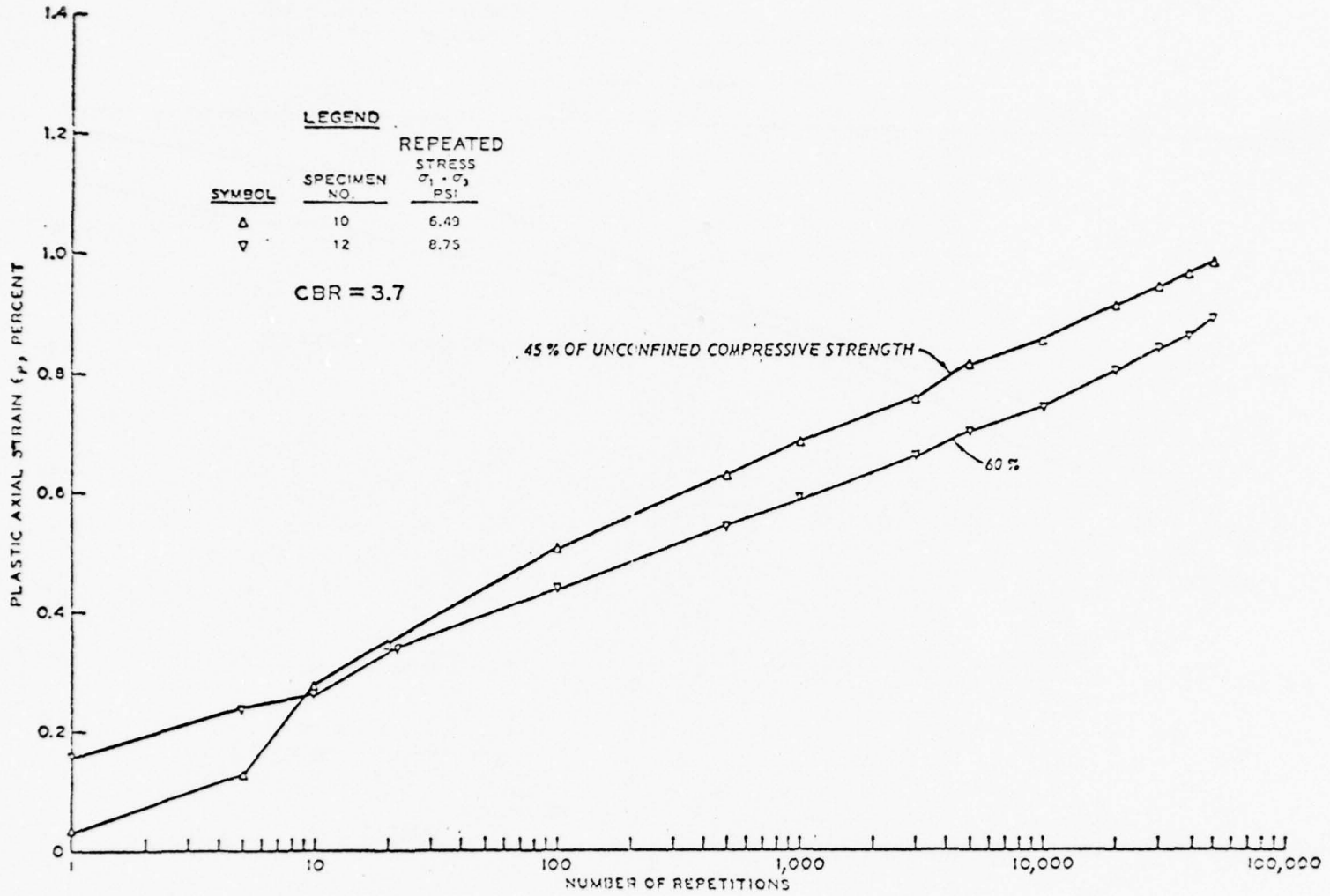

Figure 17b. Accumulated plastic strains for fine-grained soil, CBR = 3.7, second series of tests

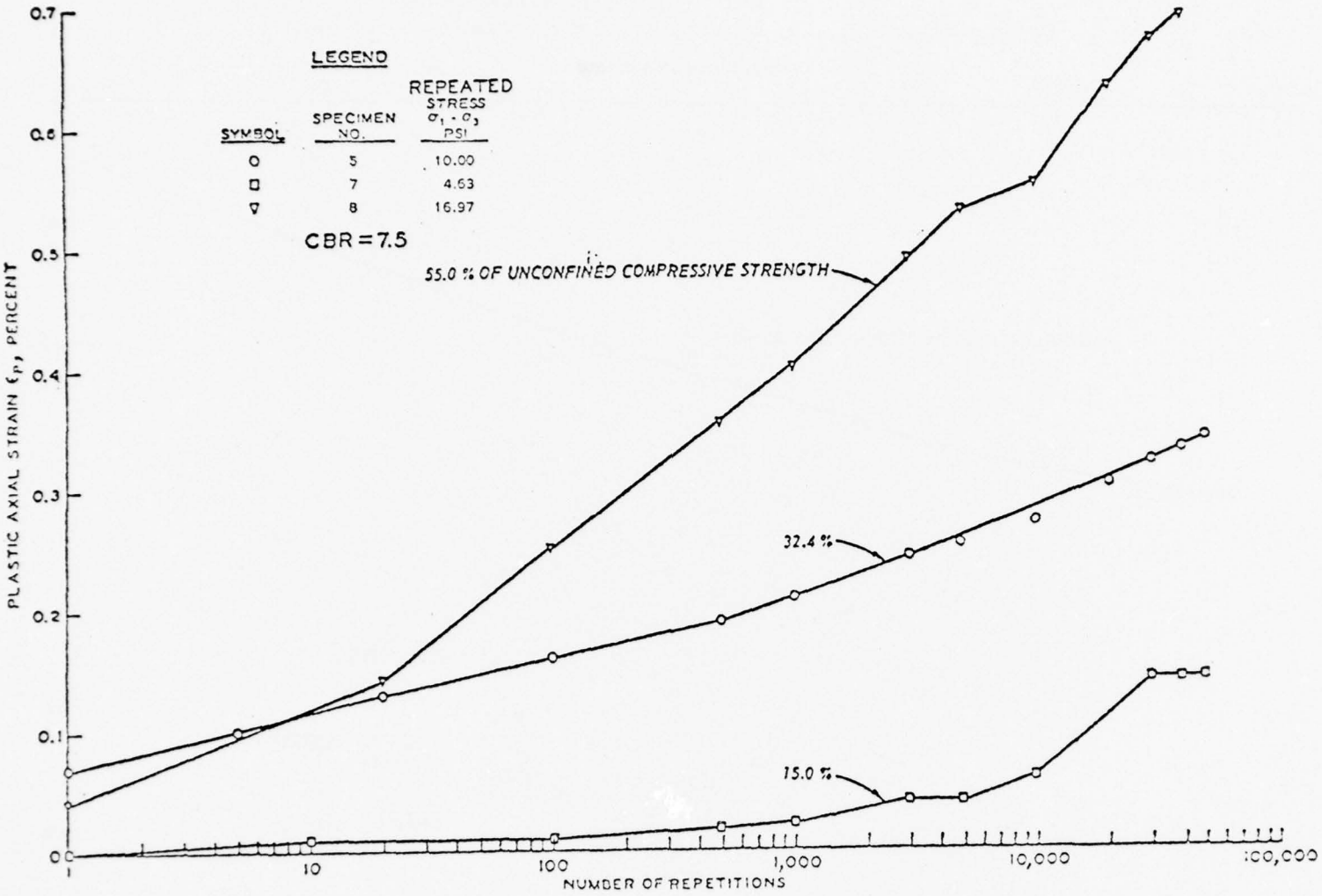

Figure 17c. Accumulated plastic strains for fine-grained soil, CBR = 7.5, second series of tests

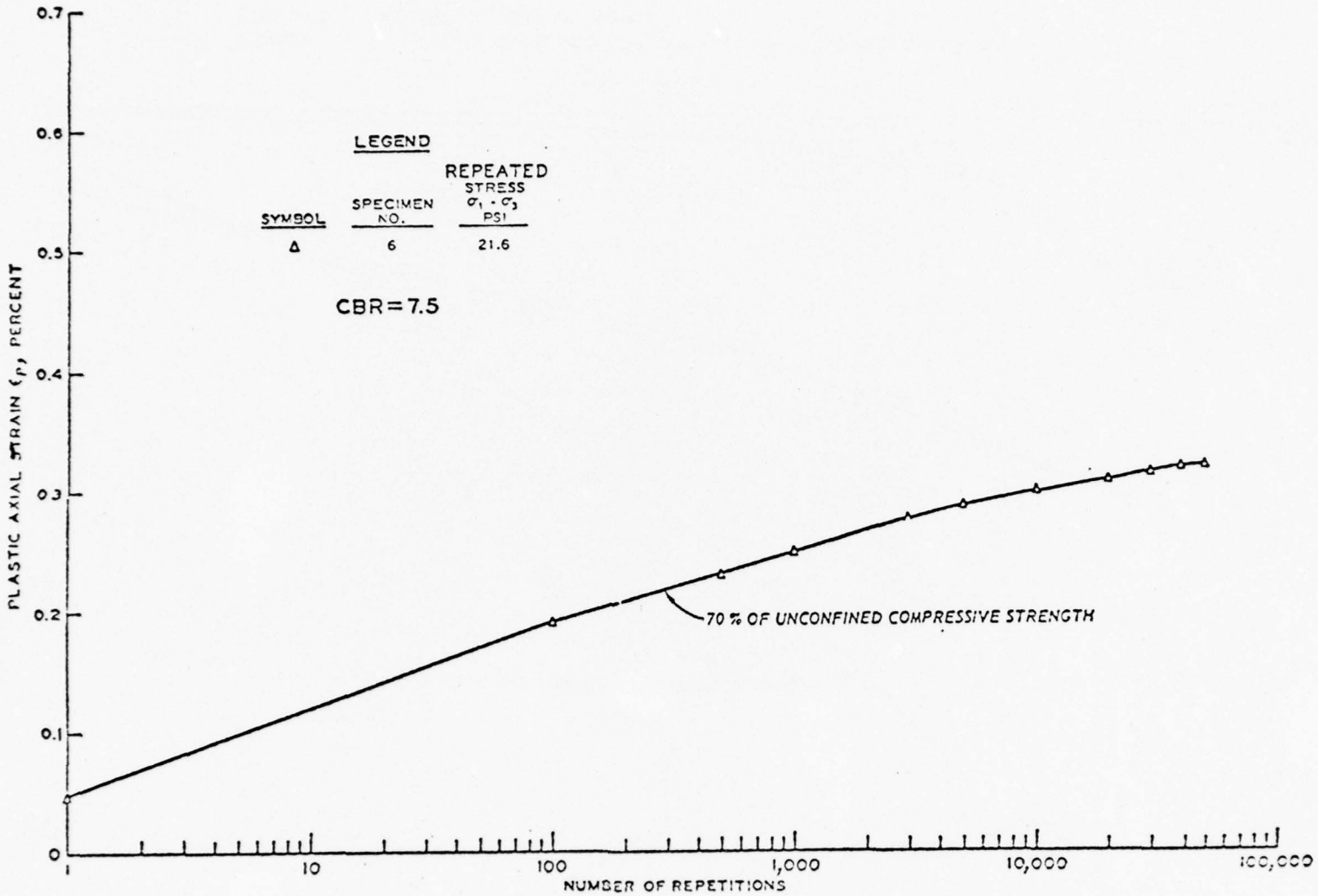

Figure 17d. Accumulated plastic strains for fine-grained soil, CBR = 7.5, second series of tests

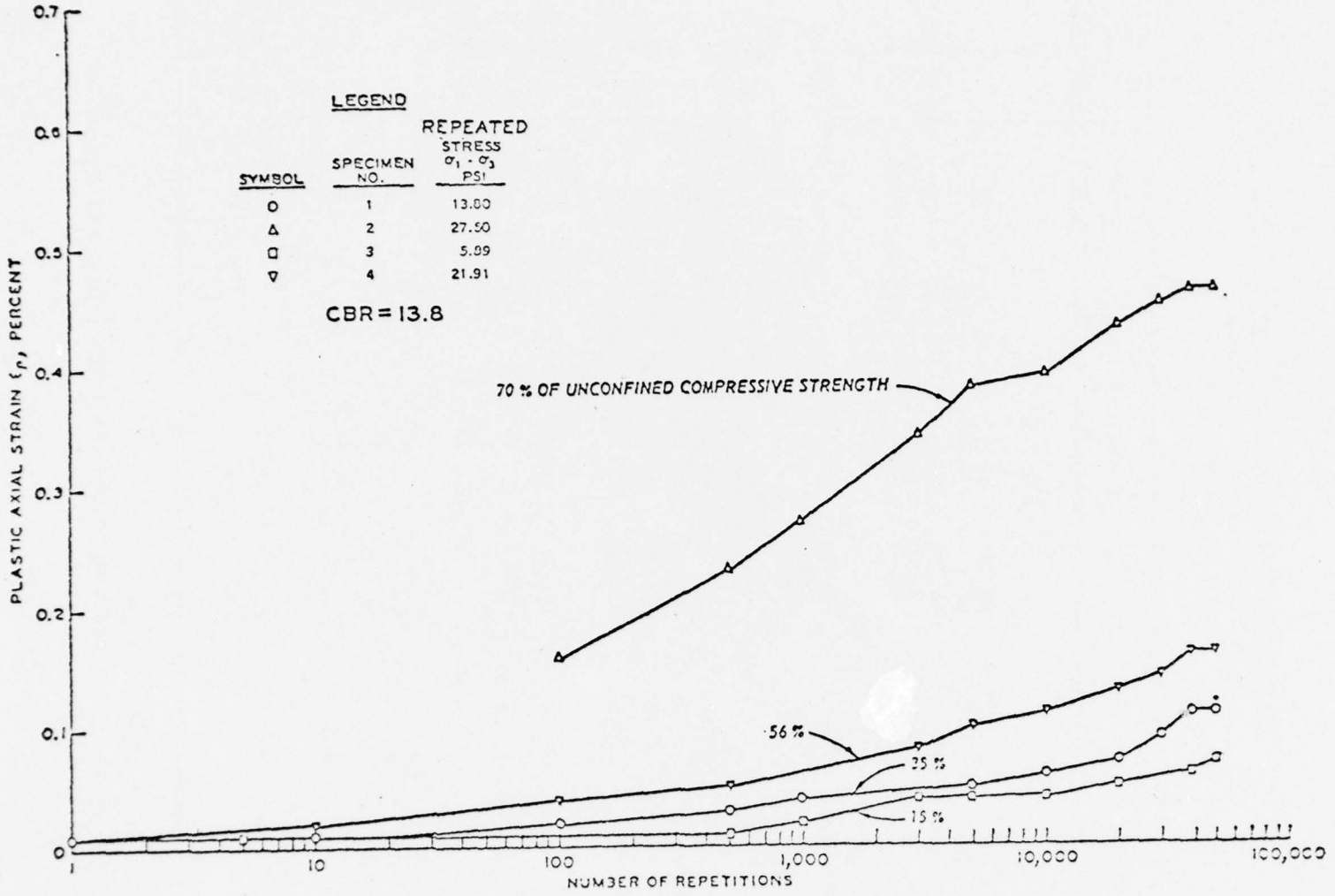

Figure 17e. Accumulated plastic strains for fine-grained soil, CBR = 13.8, second series of tests

Table 7

Specimen Identification and Composition Data
(Second Series of Tests)

Specimen No.	Moisture Content percent	Dry Density pcf	Saturation* percent	Cycled Stress psi	UCS** percent	CBR at 0.1-in. Penetration
			Batch V			
1 19	25.43	96.27	91.90	13.8	35	
2 20	23.24	97.7	86.95	27.5	70	
3 21	24.17	95.95	86.70	5.89	15	UCS = 39.3
4 22	23.19	96.64	86.45	21.91	55.8	
Average of Specimens	24.13	96.64	88.0			13.8
CBR	23.2	98.2				
			Batch VI			
5 23	26.78	94.77	93.26	10.0	32.4	
6 24	26.77	94.89	93.59	21.6	70	
7 25	26.69	95.52	94.16	4.63	15	UCS = 30.9
8 26	26.83	94.96	93.92	16.97	15	
Average of Specimens	26.77	95.04	93.73			7.5
CBR	26.0	95.9				
			Batch VII			
9 27	31.0	89.15	94.38	3.64	25.3	
10 28	30.45	89.97	94.52	6.50	45	
11 29	30.55	89.83	94.53	2.27	15	UCS = 14.4
12 30	29.69	91.15	94.83	8.73	60	
Average of Specimens	30.42	90.03	94.57			3.7
CBR	30.4	90.0				

* Based on G_s = 2.69 est.

** Percent of unconfined compressive strength (UCS) represented by cycled stress.

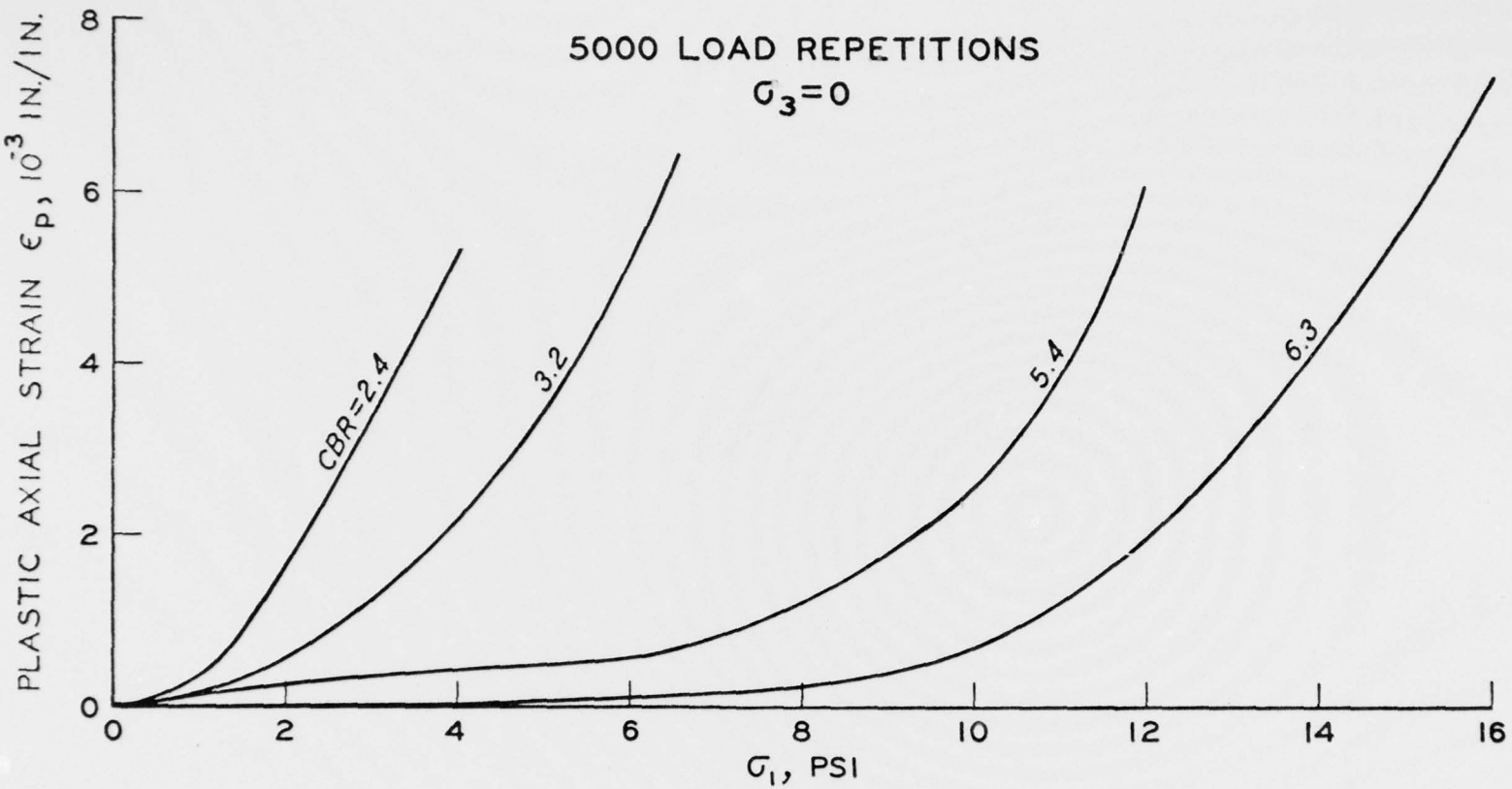

Figure 18. Relationships between plastic strain and stress intensity, first series of tests

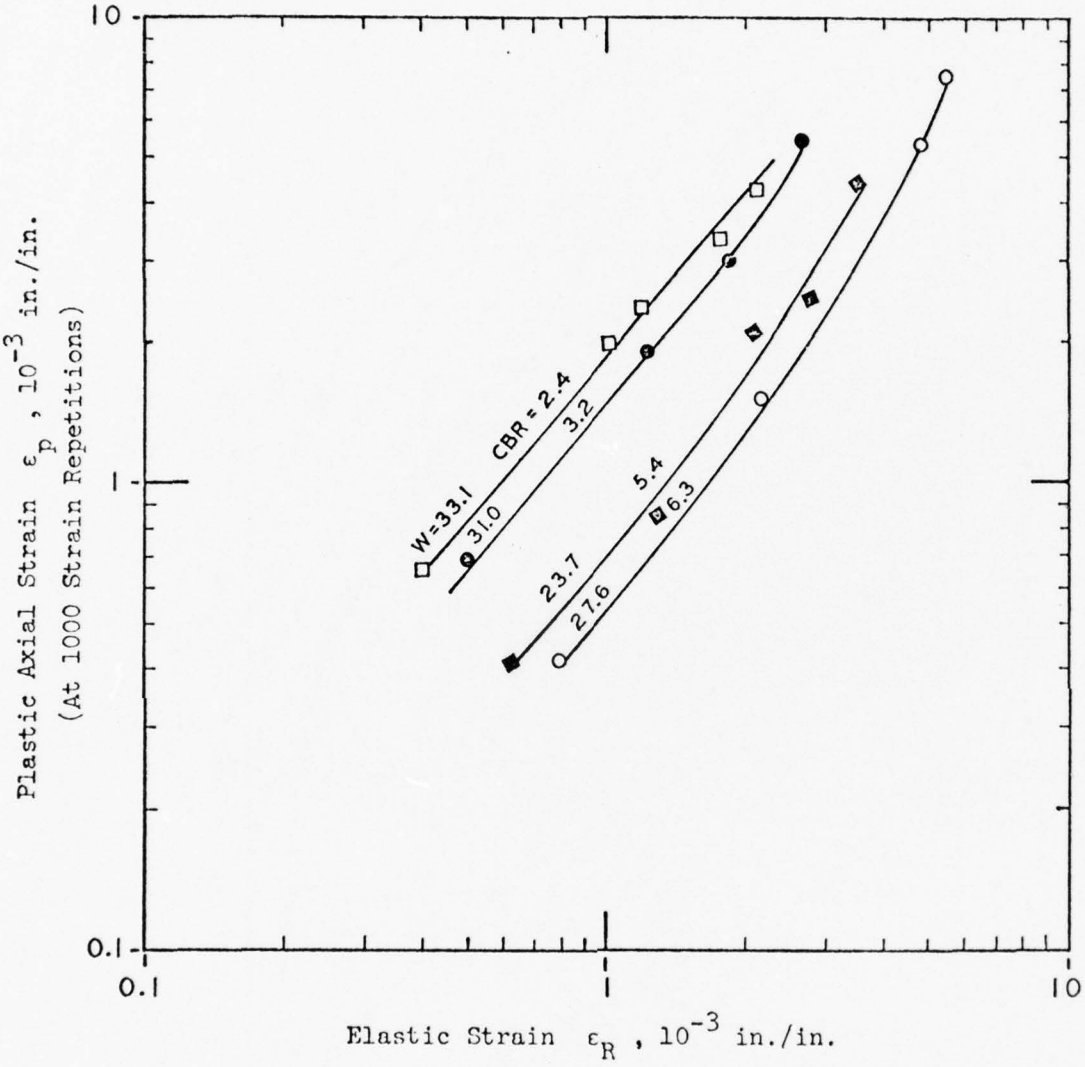

Figure 19a. Relationships between plastic strain and elastic strain for fine-grained soil at 1000 repetitions, first series of tests

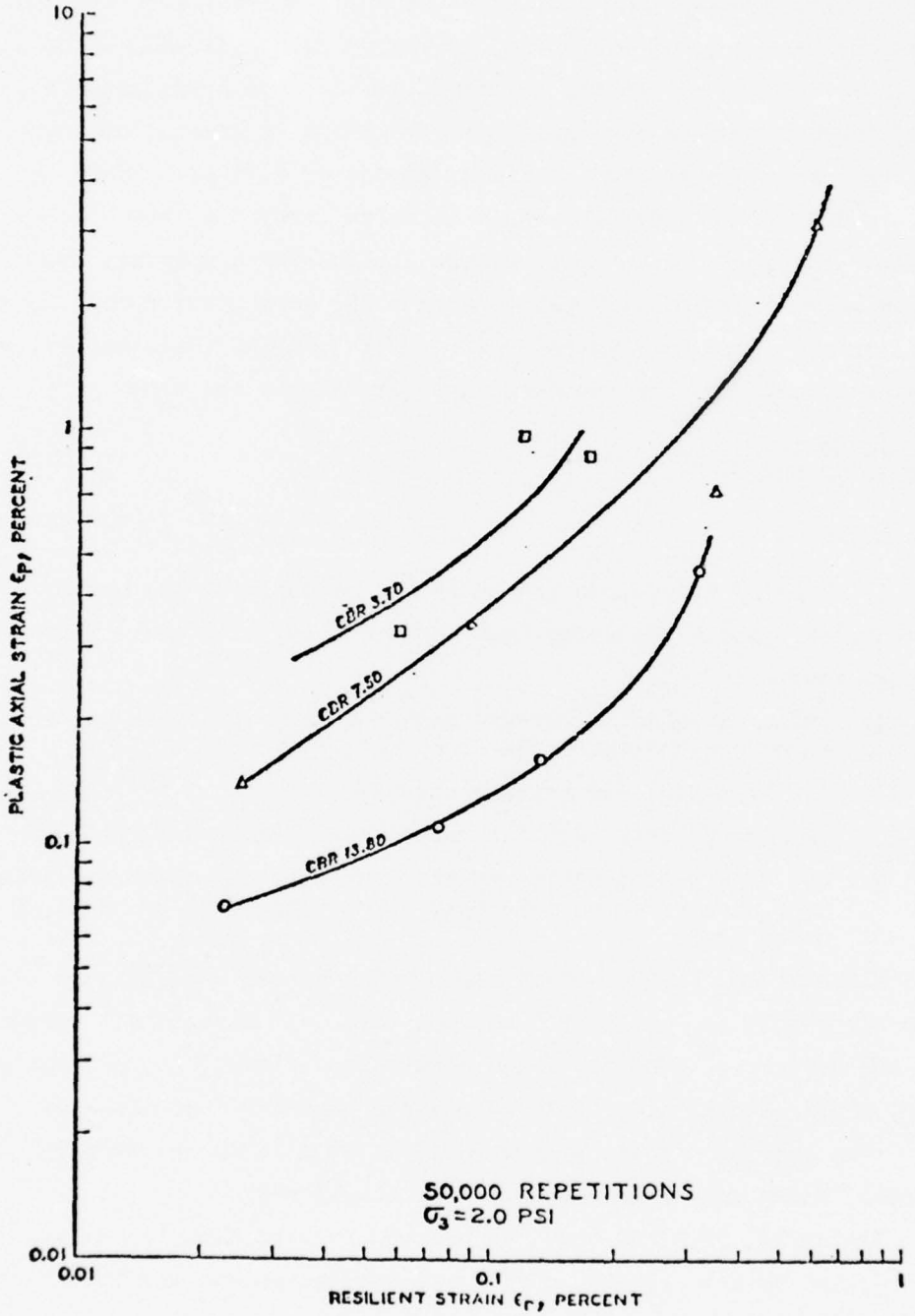

Figure 19b. Relationship between plastic strain and resilient strain for fine-grained soil at 50,000 repetitions second series of tests

Results of the first series of tests (Figure 16) were much more consistent than those of the second series (Figure 17). Figure 17b (CBR = 3.7) indicates that the permanent strains for a specimen subjected to a deviator stress of 6.49 psi (Specimen 10) were greater than those for a specimen subjected to a deviator stress of 8.75 psi. This is obviously due to the wide difference in water content of the specimens. Also shown in Figure 17a, the permanent strains for a specimen subjected to a deviator stress of 2.27 psi (Specimen 11) were greater than those of a specimen subjected to a deviator stress of 3.64 psi (Specimen 9), while the water contents of the two specimens were nearly the same.

COMPUTATIONS OF PERMANENT DEFORMATION

METHODOLOGY

A number of procedures are available to estimate the amount of permanent deformation resulting from repeated traffic loads. They may be categorized as:

a. Use of an elastic layered system to represent the pavement structure and materials characterization by:
   (1) Repeated load triaxial tests.
   (2) Creep tests (not for untreated granular materials).

b. Use of a viscoelastic layered system to represent the pavement structure and materials characterization by means of creep tests.

Since linear layered elastic program has been used by many researchers, such as Monismith,[1] McLean,[7] Morris,[8] Barksdale,[23] Brown, Pell, and Brodrick,[32] Snaith,[28] and Hofstra and Klomp,[5] it was decided that it would be used along with laboratory repeated load tests in this study. The layered elastic program used in this study is described in Reference 46 and only linear behavior is considered.

Monismith[1] proposed that, to use the layered elastic analysis, relationships between plastic strain and applied stress must be available for each of the pavement component materials; i.e.,

$$\varepsilon^p = f(\sigma_{ij}) \tag{10}$$

where

ε^p = plastic or permanent strain

σ_{ij} = stress state

For a particular layer, it is then possible to estimate the permanent deformation occurring in that layer. This is done by computing the permanent strain at a number of points within the layer, the number being sufficient to reasonably define the strain variation with depth. Permanent deformation is then determined by summing the products of the average permanent strains and the corresponding difference in depths between the locations at which the strains were determined (Figure 20), i.e.,

$$\delta_i^p(x, y) = \sum_{i=1}^{n} \left(\varepsilon_i^p \Delta Z_i\right) \tag{11}$$

where

$\delta_i^p(x, y)$ = permanent deformation in the i^{th} position at point (x, y) in the horizontal plane

ε_i^p = average permanent strain at depth $\left(Z_i + \frac{\Delta Z_i}{2}\right)$

ΔZ_i = difference in depth (or the thickness of the layer)

Total permanent deformation may be estimated by summing the contributions from each layer.

With the knowledge of plastic strain at various numbers of load repetitions, the development of permanent deformation with traffic can thus be estimated. In this study, ΔZ_i was taken as 6 to 8 in. in the granular layer, and was a variable in the subgrade. The thickness of the layers used in the computations ΔZ_i, measuring down from the subgrade surface, were 10, 10, 10, 20, 20, 20, 50, 50, 100, 100, 100, and 200 in. The stress intensities became very small below that depth. For single-wheel loads, the permanent strains were computed at points along

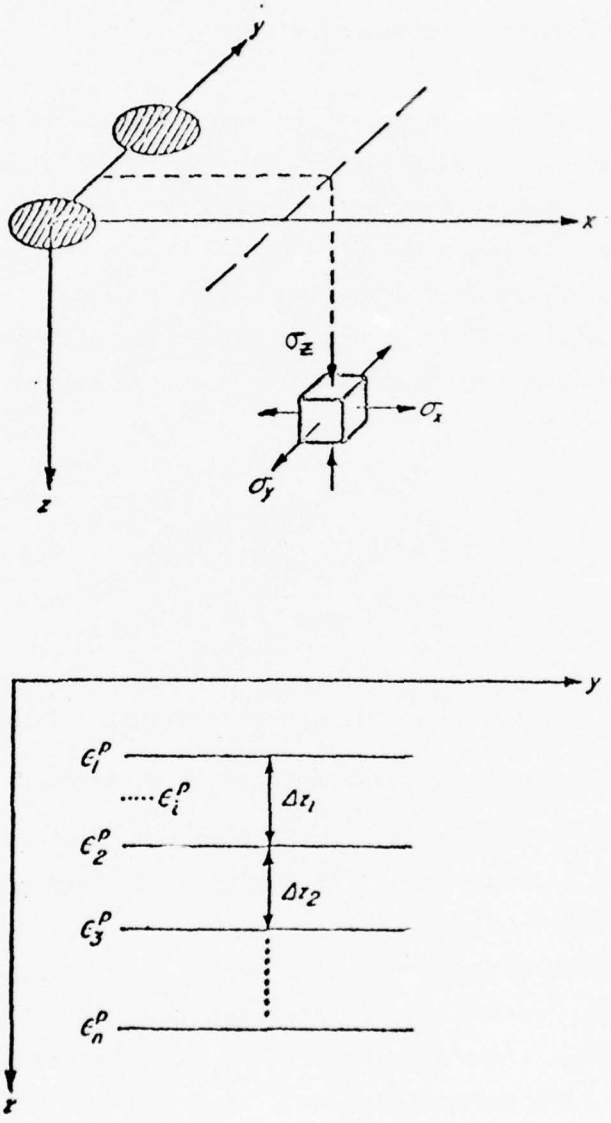

Figure 20. Schematic representation of pavement system used to estimate permanent deformation (after Monismith[1])

the load axis. For multiple-wheel loads, the permanent strains were computed at points along the vertical axis at the centroid of the Boeing 747 twin-tandem assembly and at points along the vertical axis under one of the inner wheels in the second row of the C-5A 12-wheel assembly, where the computed values are generally the maximum. The gear configurations for a C-5A 12-wheel gear assembly and a Boeing 747 twin-tandem gear assembly are shown in Figure 21. To compute the stress states using the layered elastic computer program, the selections of modulus values for AC, unbound granular materials, and subgrade soils are explained below.

ASPHALTIC CONCRETE (AC)

Because of the thermo-viscoelastic nature of asphaltic materials, the most important factors influencing the stress-strain relationships are temperature and rate of loading. The resilient moduli of asphaltic materials should be evaluated in the laboratory at different temperatures and at different rates of loading. However, such data for the actual asphaltic mixtures were not available during the preparation of this report; therefore, resilient moduli of asphaltic mixtures developed by The Asphalt Institute were used.[47] For each test pavement, a mean temperature versus depth relation for the entire traffic period was determined and was used in the computations. For pavements designed by the CBR equation, moduli of 140,000, 150,000, and 160,000 psi were selected for AC layers having thicknesses of 2, 3, and 4 in., respectively. In the computations, Poisson's ratio of 0.4 was used for all asphaltic mixtures.

UNTREATED GRANULAR MATERIALS

The modulus ratios of the untreated granular layer to the subgrade used by The Asphalt Institute[48] were adopted in this study. The ratios were used by The Asphalt Institute in the development of subgrade failure criterion of the full-depth AC airfield pavements based in part on the analysis of Corps of Engineers field test data. The ratios used were 2.9, 2.3, and 1.8 for CBR's of 3, 5, and 10, respectively. The values were selected from a theoretical study of the stress dependence of the

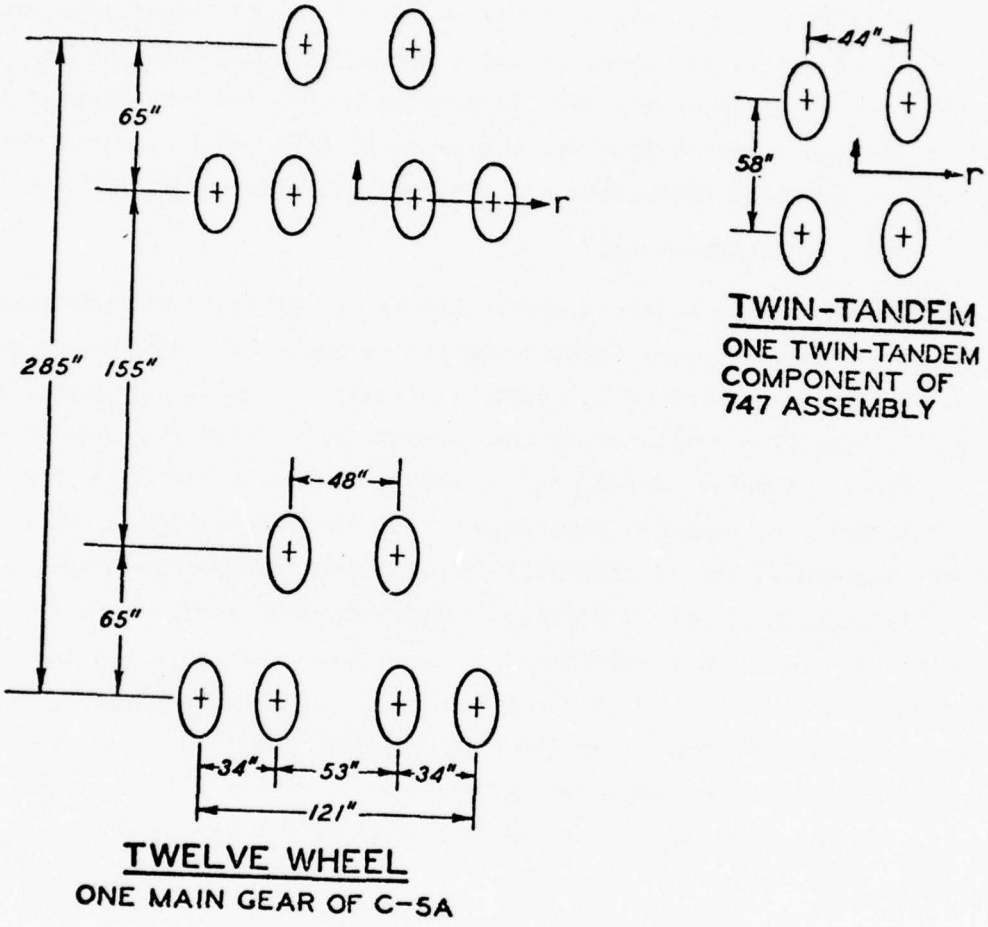

Figure 21. Wheel arrangements for twelve-wheel and twin-tandem assemblies

resilient modulus of the granular layers, as evaluated from laboratory tests. Studies conducted at WES have found that these modulus ratios are very reasonable for Corps of Engineers and FAA type pavements; i.e., 3-in. AC surface, 6-in. crushed stone base, and a thick sand and gravel subbase. In the computations, Poisson's ratio of 0.45 was used. It will be seen later that the criterion developed using these ratios is very close to that developed by The Asphalt Institute (shown in Table 2).

SUBGRADE SOILS

The empirical relation $E = 1500\ CBR$ was used in the analysis to determine the moduli of subgrade soils.[49] A discussion of the adequacy of this relationship for characterizing subgrade soils can be found in the review of the state of the art in material characterization.[50] Poisson's ratio of 0.4 was used in the computations.

TEST PAVEMENTS

Table 8 gives test data for 11 selected test pavements under multiple-wheel heavy gear loads. The pavements were trafficked by prototype loadings of a 12-wheel assembly (one main gear of a C-5A) and a twin-tandem assembly (one twin-tandem component of a Boeing 747). All test pavements were constructed over a 4-CBR subgrade soil, except test pavements 2 and 6 in which an extra-weak layer (3 ft) of 2-CBR material was placed 21 in. below the surface of the 4-CBR subgrade. The purpose of this arrangement in the test program was to determine possible effects of a deep soft layer beneath very heavy multiple-wheel aircraft. The results of the multiple-wheel heavy gear load tests[51] revealed that the existence of a deep soft layer in the pavement has no significant effect on the overall performance. The failure coverage of each pavement shown in Table 8 was determined when either of the following two conditions occurred:

a. Surface upheaval of 1 in. or greater of the pavement adjacent to the traffic lane (pavement shear failure).

b. Severe surface cracking to significant depths.

Surface rutting was not considered in the failure criterion; however, this has a vital significance in the design considerations of rutting. It will be discussed further in this report.

Table 8

Multiple-Wheel Data

Test Pavement	Aircraft Type	Assembly Load kips	Tire Contact Area, in.^{2}	Thickness, in.			Subgrade CBR	Coverages at Failure
				Surface	Base	Subbase		
1	Boeing 747	240	290	3	6	24	3.8	40
2*	Boeing 747	240	290	3	6	24	4	40
3	Boeing 747	240	290	3	6	32	4	280
4	C-5A	360	285	3	6	6	3.7	8
5	C-5A	360	285	3	6	24	3.8	1500
6*	C-5A	360	285	3	6	24	4	1500
7	C-5A	360	285	3	12**	0	4	98
8	C-5A	360	285	15	0	0	4	425
9	C-5A	360	285	3	6	15	4	104
10	C-5A	360	285	9	0	15	4	734
11	C-5A	360	285	9	15**	0	4	2198

Note: 1 kip = 4.44822 kN; 1 in.^{2} = 6.451600 cm.^{2}

* A 3-ft-thick layer of 2-CBR soil was placed 21 in. below the subgrade surface.

** Asphalt-stabilized.

In the use of laboratory repeated load test data (as shown in Figures 13-16) to compute the permanent deformations occurring in the pavement induced by the traffic loads, 1 coverage in the field is assumed to be equal to 1 strain repetition in the laboratory. Concerning the lateral distribution characteristics of aircraft or runways, this assumption is not correct. However, as will be seen later, this assumption would not change the conclusions derived from this study.

RESULTS

AC Surfacing. Computations of permanent deformations were not made on the AC surfacing due to the following reason: The present state of knowledge on the prediction of permanent deformations of AC is still in its infancy. Controversial concepts and different results have been presented by different agencies.[7,8] In a recent paper, Brown[33] suggested an improved approach to overcome some of the inherent disadvantages of the laboratory triaxial test. However, Brown admitted that for lower temperatures and thin layers, the approach still has inadequacies. It was thus decided to concentrate the effort to the study of permanent deformations only in untreated granular materials and subgrade soils.

Untreated Granular Materials. Difficulty was encountered in the computations of permanent deformations in granular materials due to the fact that the stresses computed by the linear layered elastic program do not truly represent field conditions.

Thompson[52] in utilizing layered elastic theory for computing stresses in granular materials under highway pavements encountered the same difficulty and made the following statement:

> According to these calculations a small amount of tension develops in the base. However, it has been stated previously that this particular base material cannot take tension and yet the unsoaked pavements did not deteriorate significantly. Therefore, it is suggested that the particles of the base move, and the stresses are redistributed so that no tension exists.

Also, Morgan and Scala,[53] in a review of flexible pavement behavior and application of elastic theory to pavement analysis, came to the following conclusion:

> The general failure of two- and three-layer systems to satisfy the Burmister prediction appears to be due to lower-than-expected modulus for the stiffer layers resulting from their inability to withstand tension, or their dependence on confining stress which may not be sufficient.

Even when nonlinear finite element analysis is applied to airport pavement analysis, stresses are computed which violate accepted failure laws. In such an analysis, Barker[54] makes the following statement:

> Tensile stresses were generated in the granular material to such an extent that the pavement response (referring to computed response) was dictated more by limiting minimum moduli than by true material properties. The field data indicated much better performance of the granular material under the high loads than was indicated by the finite element analysis. The most plausible explanation is that a marked increase in Poisson's ratio probably occurred as the granular material approached failure. The increase of Poisson's ratio in the crushed stone would be greater than the increase in the sandy gravel and could explain the better comparative performance of this material than was indicated in the analysis. It is felt that at near failure Poisson's ratio for both materials go above 0.5 and thus generate additional complications in the analysis of heavily loaded pavement systems.

Prior to further discussion, it will be beneficial to present the experience gained from this study.

a. When the layered elastic computer programs were used to obtain information on the stress states in the pavement structures, tensile radial stresses were generally computed at the bottom layers of the granular materials. This posed a serious problem in the use of laboratory repeated load test data.

b. In conducting laboratory repeated load tests on untreated granular materials, confining pressures were required during the test to prevent the specimen from collapsing under the load applications. The magnitude of the required confining pressure σ_3 depended upon the magnitude of the applied vertical pressure σ_1. In general, the ratio of σ_1/σ_3 could not exceed a value of 5. In other words, if the applied vertical stress σ_1 was 20 psi, the confining stress σ_3 must be kept at 4 psi or greater.

When the stress states in the granular layers were computed and expressed by the relation $(\sigma_1 - \sigma_3)/\sigma_3$ (as shown in Figures 14 and 15), the expression becomes negative when tensile radial stresses σ_3 were computed. Consequently, the laboratory repeated load test data could not be used to estimate the permanent strains because the tests were

conducted with compressive confining pressures; i.e., σ_3 was always positive. To circumvent the situation, the ratios of octahedral shear stress to octahedral normal stress τ_{oct}/σ_{oct} were used. The advantage of this expression is that the stress ratio was always positive even though the value of σ_3 was negative. This can be readily seen in Equations 8 and 9. In using Equations 8 and 9, the intermediate stress σ_2 was equal to the minor principal stress σ_3.

Although the octahedral stress ratios eliminated the problem caused by the negative confining stress σ_3, difficulties still existed. Figure 22 shows the relationships between permanent strain and octahedral stress ratio plotted for 5000 strain repetitions. It can be seen that the octahedral stress ratios for specimens tested in the laboratory have magnitudes less than one, and the rate of increase of permanent strain with stress ratio is very rapid. However, the stress ratios computed using linear layered elastic computer programs have values greater than three in most cases. Extrapolations have to be used to estimate the permanent strains at high stress ratios. It can be seen in Figure 22 that the extrapolation to a stress ratio of two is beyond the acceptable confidence level.

The problem of estimating permanent deformations in granular layers using a mechanistic approach, such as the one used in this study, lies in the difficulty of computing the stress states. It is believed that when heavy wheel loads are applied on the pavement surface, radial tensile stresses tend to develop at the lower part of the granular base layer and slip of the material becomes incipient. The granular material can sustain a certain amount of tensile stresses which are resisted by frictional stresses developed between the granular particles caused by the vertical compressive stresses that exist in the base. Once the material starts to slip, passive pressure due to overburden will be mobilized and the confining pressure will be increased. Consequently, the moduli of the granular materials will increase. Since granular particles will separate under tensile stress and since granular layers in a well-constructed pavement do not fail under a few passes of traffic loads, the author believes that the large radial tensile stresses in

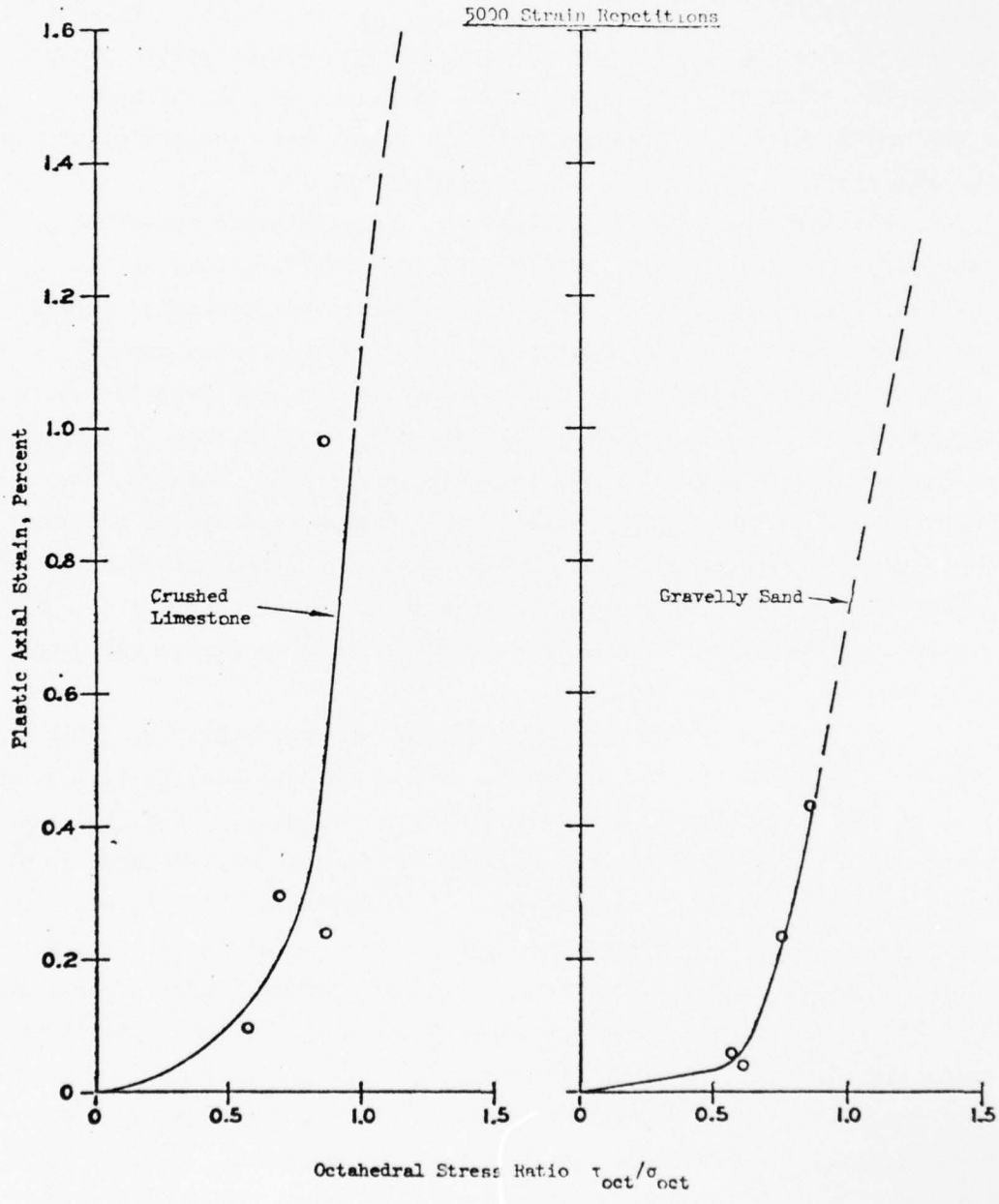

Figure 22. Relationships between plastic axial strain and octahedral stress ratio for untreated granular materials

granular layers computed by the linear layered elastic program do not truly represent realistic field conditions. The author also believes that eventually the granular particles start to move, and since energy is dissipated during the movement, the stress intensities may be substantially changed as compared to those during the stress buildup stage. Since the magnitude of vertical compressive stress under a wheel load depends upon the magnitude of confining pressure in granular materials, the magnitude of vertical compressive stress σ_1 in a pavement structure may not be a constant but rather will vary during the loading process. Also, since aircraft loadings are not always applied at one point but vary laterally with respect to the center line of the runway, it is likely that material in a pavement may move in directions other than the vertical when the load is not directly over the point where the material is located. It can be concluded that (a) the states of stress existing in the granular layers under aircraft loadings are extremely complicated, which cannot be simply described by constant values of vertical compressive stress σ_1 and horizontal stress σ_3, which are computed by the layered elastic program; and (b) the response of the granular materials to the repeated applications of aircraft loads cannot be simulated by the laboratory repeated load triaxial tests.

A nonlinear finite element program which incorporates the stress-dependent moduli of granular materials was also used to compute the stress states in the granular layer. Compressive radial stresses were computed in many cases, but the magnitudes were very small; i.e., 1/2 to 1 psi. The octahedral stress ratios computed at the bottom of the granular layer were generally two. However, extrapolations beyond the confidence level still had to be used to estimate the permanent strains (see Figure 22).

It should be pointed out that although layered elastic program predicts radial stresses incorrectly, the presence of radial tensile stresses in granular layers does not seem to affect the predictions of vertical stresses and deflections appreciably. Reference 55 presents the results of comparisons of computed and measured stresses and deflections. A nonlinear finite element program was used to compute stresses and

deflections in a prototype test section constructed at WES and the computed values were compared with instrumentation values. The comparisons were favorable.

It can be concluded that the response of granular materials to repeated applications of aircraft loads in an actual runway are extremely complicated and are not fully understood. The stress states in the granular layers cannot be accurately predicted using existing computer programs. For design purposes to minimize the potential of permanent deformation in untreated granular materials, it may be the best, at least at the present time, to specify strict compaction requirements and select materials with higher modulus values.

Fine-Grained Subgrade Soil. Since vertical subgrade strains have been used in rational pavement design as a means to insure that permanent deformation in the subgrade does not lead to excessive rutting at the pavement surface, relationships between the computed vertical strains at subgrade surface and coverage levels for all the pavements analyzed were included in the figures which show permanent subgrade deformations (Figures 23, 26, and 27).

Stress Factor. The concept of a stress factor was explored in this study to estimate the potential of permanent deformation in subgrade soils. As shown in Equation 10, permanent strain in the subgrade soil is proportional to the applied stress state. (It is the deviator stress in this case.) When the deviator stresses in the subgrade along the vertical depth are increased or decreased, it is anticipated that the permanent deformation will also be increased or decreased accordingly. Therefore, the computed deviator stresses along the vertical depth of the subgrade soil of a pavement may be used as an indirect measurement of the potential permanent deformations in the subgrade. The term stress factor is defined in this report as the summation of deviator stresses along the vertical depth of the subgrade, which can be computed as the sum of the products of the deviator stress computed at various points in the subgrade and the thickness of the corresponding sublayer. The stress factor is expressed in units of pounds per inch.

It will be seen later that the stress factor is very useful in discussing the differences in stress conditions in pavements under single- and multiple-wheel loads.

The following example illustrates the computation of a stress factor in the subgrade of a pavement. The procedure is shown in Table 9 and the stress factor computed is 1580.9 lb/in. It should be pointed out that for a given pavement under a given wheel load the stress factor is always a constant, but the accumulated permanent deformation in the subgrade always increases as the number of load repetitions increase.

Multiple-Wheel Heavy Gear Load (MWHGL) Tests. The relationships between the computed values of vertical strains, permanent deformations, and stress factors in the subgrade and the coverages at failure of the 11 MWHGL test pavements are shown in Figures 23a-23c, respectively. Information on the 11 pavements is shown in Table 8. Because of the special subgrade condition in pavements 2 and 6, the computed values of these two pavements deviated from pavements 1 and 5, respectively. Straight lines shown in Figures 23a-23c were drawn through data points without considering pavements 2 and 6. The significances of the computed values of these two pavements are discussed separately.

Figure 23a indicates that good correlation exists between the subgrade vertical strains and the coverage levels, indicating that subgrade strain is a good parameter to correlate pavement performance. Of special interest is the fact that strain values shown in Figure 23a are very close to those developed by The Asphalt Institute and shown in Table 2. Figure 23b shows permanent deformations computed at the failure coverage for the 11 test pavements. Figure 23b also shows that the computed subgrade deformations for the test pavements are independent of the coverages by a given type of wheel configuration and load; however, the deformations are different for the two types of wheel configuration and load. For the C-5A loading, a subgrade permanent deformation of approximately 0.2 in. (computed) failed the pavement. In Figure 23b, the measured magnitudes of upheavals, maximum permanent surface deformations, and pavement thicknesses for each test pavement

Table 9

Computation of a Stress Factor

Depth* in.	Thickness of Layer, in.	Deviator Stress** $\sigma_1 - \sigma_3$, psi	Deviator Stress × Thickness
5	10	23.68	236.8
15	10	17.91	179.1
25	10	13.96	139.6
40	20	10.06	201.2
60	20	6.95	139.0
80	20	5.91	118.2
115	50	3.63	181.5
165	50	2.09	104.5
240	100	1.11	111.0
340	100	0.64	64.0
440	100	0.46	46.0
590	200	0.30	60.0
			Sum = 1580.9 lb/in.

* The depth is measured from the subgrade surface.
** The stress is computed at the midpoint of the layers.

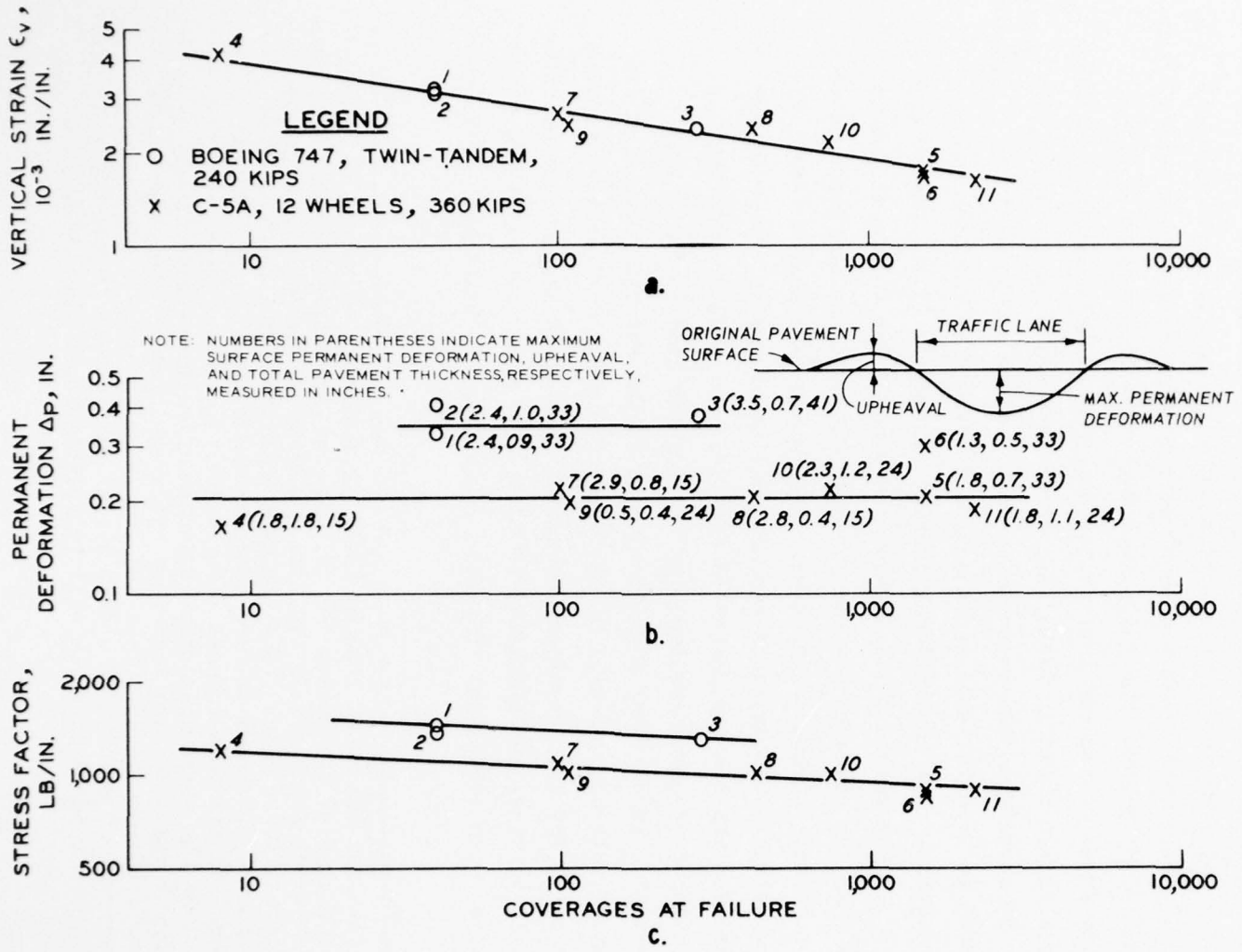

Figure 23. Relationship between vertical strain at subgrade surface, permanent deformation in the subgrade, and stress factor in the subgrade and performance of pavement under single-wheel loads

are given in parentheses by the pavement numbers. It can be seen that for all pavements the measured surface deformations or ruttings were much greater than computed subgrade ruttings. It is interesting to note that surface ruttings for pavements with thick AC layers (pavements 7, 8, 10, and 11*) were much greater than those for the corresponding conventional flexible pavements. The large ruts must have been caused by the hot temperatures during the traffic period. The asphalt contents of these pavements are shown in Table 10. Since pavement 4 was failed by less than 10 coverages, the measured surface rutting and upheaval were considered to be unreliable and are thus discarded in the subsequent discussions. For conventional flexible pavements (i.e., pavements 1 and 3 for the Boeing 747 and pavements 9 and 5 for C-5A), it can be seen that the measured surface ruts are not constant but increase as the pavement thickness increases. At a given performance level, say 280 coverages, the measured surface rutting of the thicker pavement needed for the heavier load** (Boeing 747) was greater than that of the thinner pavement required for the lighter load (C-5A). This observation is of vital significance in design for the prevention of pavement rutting, and will be discussed further. Similar results were also noted for test sections containing stabilized layers; the measured surface ruttings are tabulated in Table 11. Each test section was constructed with sufficient width to conduct traffic tests with different

---

* Although the total load of the C-5A assembly (360 kips) is heavier than that of the Boeing 747 twin-tandem assembly (240 kips), the load per wheel for the C-5A (30 kips) is much lighter than that of the Boeing 747 (60 kips), and the gear configurations (Figure 21) are such that the load is more concentrated for the Boeing 747 than for the C-5A and thus induces more rutting in the pavement.

** Since the measured permanent deformation in pavement 11 (24-in. AC layer) was much less than that measured in other deep asphalt pavements (pavements 7, 8, and 10), it leads to the belief that the majority of rutting in a deep AC pavement occurs in the upper portion and the subgrade soil is well protected from rutting under the thick AC layer.

Table 10

Asphalt Contents in the Full-Depth AC Pavements

Pavement No.*	Top 3 in.	Other Layers	
8	AC surface course (4.5 percent asphalt)	3 to 15 in.	Bituminous stabilized base course gravelly sand with 6.5 percent cement filler (2.9 percent asphalt)
7		3 to 9 in.	Surface mix (5.0 percent asphalt) base course
		9 to 15 in.	Surface mix (2.9 percent asphalt) base course
11		3 to 9 in.	Surface mix (5.0 percent asphalt) base course
		9 to 24 in.	Bituminous stabilized gravelly sand subbase (2.9 percent asphalt)
10		3 to 9 in.	Surface mix (5.0 percent asphalt) base course
		9 to 24 in.	Unstabilized gravelly sand subbase

* Numbers refer to pavement number in Table 8.

Table 11

Measured Surface Ruttings in Pavements with Stabilized Layers

Pavement No.	Aircraft Type	Assembly Load kips	Thickness of Surface Course, in.	Pavement Description						Subgrade CBR	Measured Maximum Deformation at Failure, in.	Degree of Pavement Cracking	Coverages to Failure
				Thickness in.	Material	Stabilizing Agent	Thickness in.	Material	Stabilizing Agent				
1a	Boeing 747	200	3	6	Crushed Stone	--	24	Lean clay	3 percent lime 2 percent portland cement 10 percent fly ash	5.6	1.2	Severe	3,660
1b	Boeing 747	240	3	Same as 1a						4.4	3.2	Severe	600
2a	Boeing 747	200	3	--	--	--	25	Lean clay	5 percent portland cement	5.4	1.1	Severe	3,660
2b	Boeing 747	240	3	Same as 2a						4.0	1.4	Severe	340
3a	Boeing 747	200	3	25	Gravelly Sand	5 percent portland cement	--	--	--	3.8	1.5	Severe	7,820
3b	Boeing 747	240	3	Same as 3a						3.2	2.5	Slight	620
4a	Boeing 747	200	3	25	Clayey Sand	5 percent portland cement	--	--	--	4.9	0.7	Severe	1,280
4b	Boeing 747	240	3	Same as 4a						5.2	1.7	Severe	120
5a	C-5A 12 Wheels	360	3	6	Crushed Stone	--	15	Lean clay	3.5 percent lime	5.0	0.96	Severe	138
5b	Boeing 747	160	3	Same as 5a						5.0	0.96	Severe	140
5c	Single	50	3	Same as 5a						5.0	0.6	Severe	40
6a	C-5A 12 Wheels	360	3	6	Crushed Stone	--	15	Lean clay	10 percent portland cement	4.3	1.08	Severe	1,200
6b	Boeing 747	160	3	Same as 6a						4.3	1.8	Severe	1,000
6c	Single	50	3	Same as 6a						4.3	1.0	Severe	90
7a	C-5A 12 Wheels	360	3	21	Clayey Gravelly Sand	6 percent portland cement	--	--	--	4.3	0.84	Slight	No Failure at 10,000
7b	Boeing 747	160	3	Same as 7a						4.2	1.32	Severe	1,610
7c	Single	75	3	Same as 7a						4.2	0.8	Severe	120

gear assemblies. It can be seen that for the same pavements, which the sections trafficked by heavier load failed earlier, the measured surface ruts were greater than those failed by lighter loads. Table 11 also shows that under a given load assembly, the measured surface ruts increase with increasing coverages. The relationships are plotted in Figure 24. In other words, two different pavements failed by a given assembly load at different coverage levels can experience different degrees of surface rutting, with greater rutting measured in stronger pavements.

Permanent deformations computed for pavements 2 and 6 were substantially greater than those for pavements 1 and 5, respectively. This is because of the existence of the extra-weak layer in pavements 2 and 6. It should be reiterated that the existence of a deep soft layer in the pavement was observed to have no significant effect on overall performance.

Figure 23c shows the computed stress factors for the 11 test pavements. The stress factor decreases with increasing coverages (or increasing thickness of the pavement). However, different aircraft loads result in different relationships between the stress factor and the number of coverages, while the relationships shown by the straight lines are parallel to each other. The reason for the larger stress factors in pavements subjected to the Boeing 747 load is the closer spacing of the wheels and the heavier load for each wheel (consequently, the stresses in the subgrade were more concentrated). The stress factors computed for pavements 2 and 6 were slightly smaller than those for pavements 1 and 5 because of the existence of the extra-weak layer in the pavements.

The computed permanent deformations shown in Figure 23b are maximum values under the assembly loads. Since pavement performance also depends on deformations at offset points, attempts were made to compare the deformation basins of several pavements designed for Boeing 747 and C-5A loadings at the same coverage levels. The thicknesses of these conventional flexible pavements were determined by the subgrade vertical strain criterion shown in Figure 23a. A trial-and-error procedure was used to determine the correct thicknesses of pavements constructed on

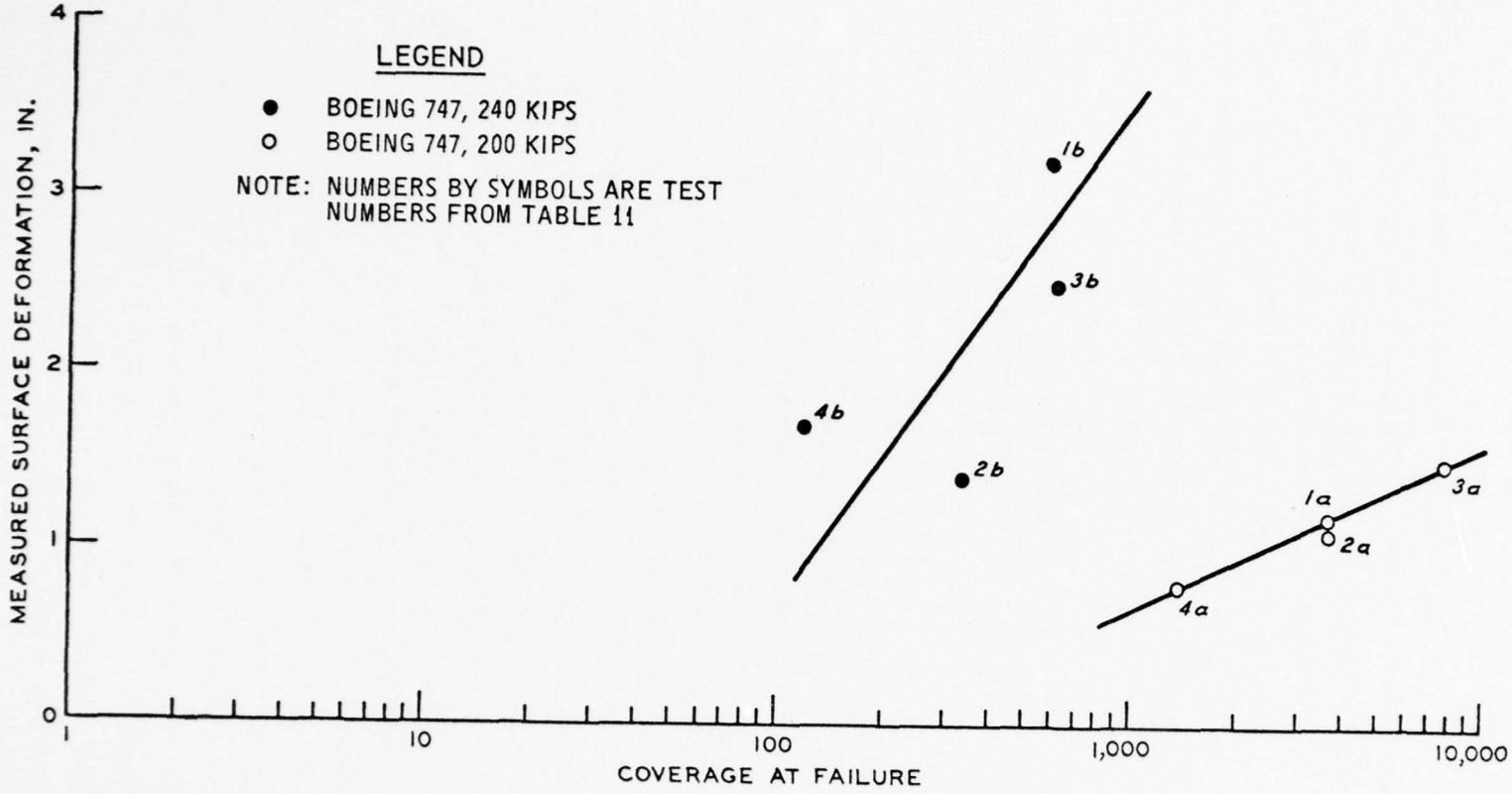

Figure 24. Measured surface permanent deformations of test pavements at time of failure, pavements with stabilized layers

4-CBR subgrade soil in which the computed vertical strains at the subgrade surface were 2.7×10^{-3} and 1.9×10^{-3} in./in. for pavements designed at coverage levels of 100 and 1000, respectively. Permanent deformations at offset points of these pavements were computed and the deformation basins are presented in Figure 25. While the maximum deformations are nearly the same, the deformation basins for thicker pavements are flatter than those of the thinner ones. The flatter basin naturally would cause less shearing deformation in the overlying pavement layers and contribute to better performance. On the other hand, the sharper deformation basin in the subgrade soil of thinner pavements causes more severe shearing deformation in the pavement layers and contributes to surface layer cracking and earlier failure of the pavement. Explaining it in another manner, the better performance of thicker pavements, besides many other reasons, is due to not only its greater structural capacity, but also the flatter deformation basin in the supporting subgrade soil.

Attempts were made to compare the deformation basins of the Boeing 747 and C-5A gear assemblies. It was difficult to select basins which were comparable since the wheel configurations are very different. However, it can be readily seen that under the C-5A load the maximum deformation is smaller and the basin is flatter and broader because the assembly has more wheels and they are spaced much farther apart. Consequently, pavements designed for C-5A loadings at the same coverage levels as for Boeing 747 loadings require much less thickness. For instance, for pavements designed for 1000 coverages, a 48.5-in.-thick pavement is required for the Boeing 747 but only a 29.6-in.-thick pavement is required for the C-5A.

The subgrade permanent deformations presented in Figure 23b are computed values. Measured deformations from open trench tests were available for several test pavements. Comparisons between measured and computed deformations are presented in Figure 26. If the computed values are the same as the measured ones, the points should be plotted on the 1:1 line. Although the measured values from open trench tests are not very accurate, the results presented in Figure 26 indicate that the computed values are much smaller than the measured ones. Although the

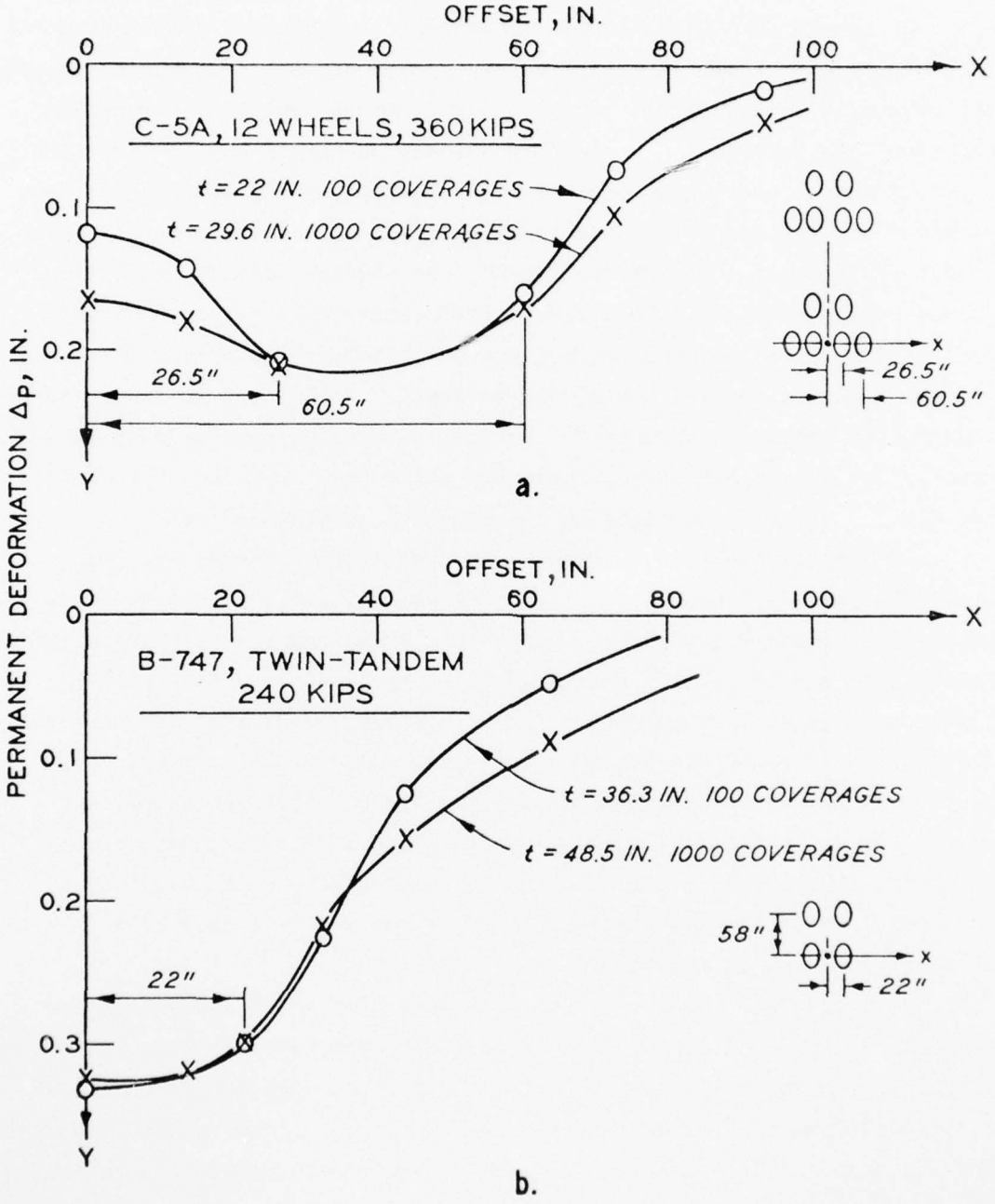

Figure 25. Subgrade permanent deformation basins in pavements

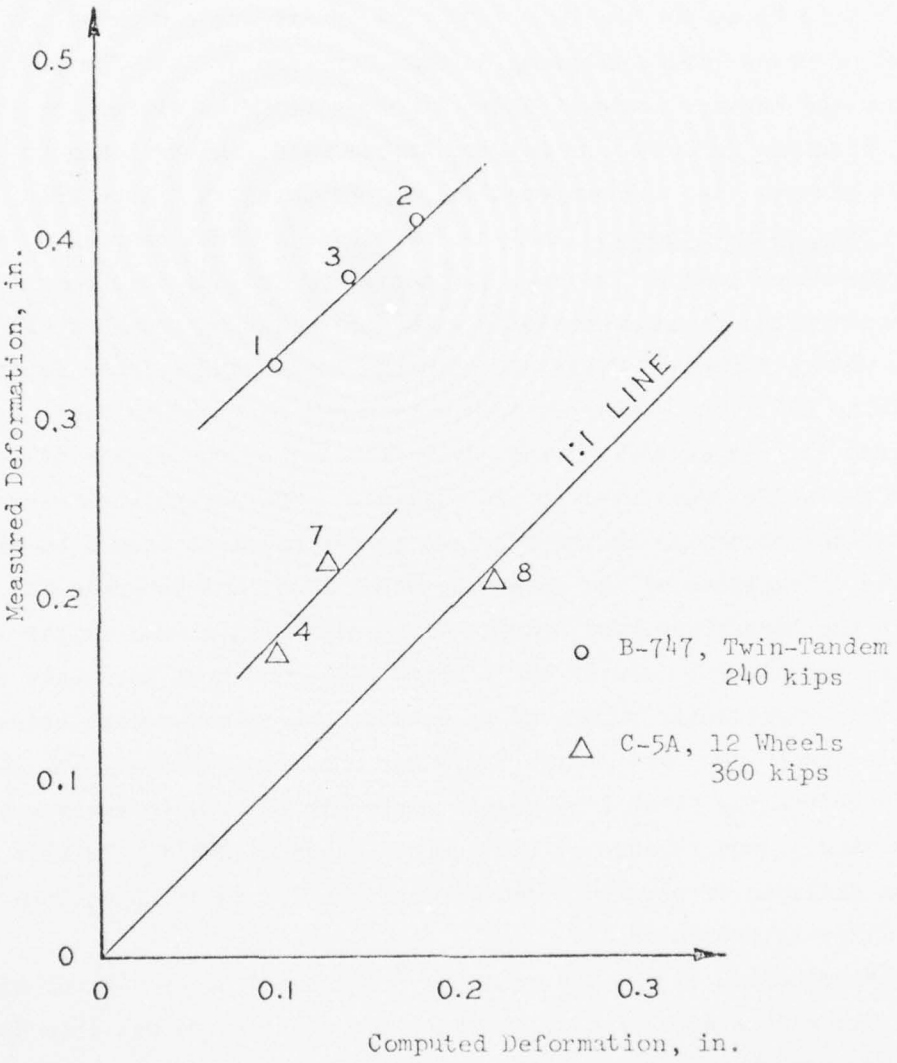

Figure 26. Comparisons of measured and computed subgrade permanent deformations

measured values are greater than those computed, the conclusions derived from those in Figure 23 still hold. For instance, Figure 23b shows that the computed subgrade deformations for the Boeing 747 (240 kips) are greater than those for the C-5A (360 kips).* It was concluded that, at a given coverage level, subgrade deformations are greater for pavements designed for heavier loads. Figure 26 shows that the difference in the actual subgrade deformations between heavier and lighter loads could even be greater than the computed values presented in Figure 23b.

Single-Wheel Loads. Analyses were made on test pavements failed by single-wheel loads. The test pavements had various thicknesses and were constructed on subgrade soils with CBR's ranging from 4 to 18. The pavements failed at different coverage levels under loads ranging from 10 to 200 kips. Pavement information can be found in Table 1 of Reference 51. Repeated load test data from the second series of tests (Figures 17a-17e) were used in the analysis. The accumulated permanent deformations occurring in the subgrade of the pavement seemed to vary with the thicknesses of the pavement, wheel load, and subgrade CBR. Because the laboratory test data were inconsistent, as was explained earlier, and also because of the limited number of test pavements and the relatively significant number of variables, the relationships between the variables cannot be used as the basis for a meaningful analysis. Laboratory data from the first test series could not be used to analyze the single-wheel loads because of the limited range of CBR's. In this report, only an analysis of pavements designed by the CBR equation at lower subgrade CBR's is presented.

Formulation of the CBR equation[56] was based on results of numerous full-scale accelerated traffic tests, which represented reliable data and extensive observations of the Corps of Engineers. A pavement designed by the CBR equation has a thickness sufficient to prevent shear failure in the subgrade soil. The equation has the form

---

* The Boeing 747 (240 kips) is considered to be heavier than the C-5A (360 kips). The explanation can be found in the footnote on page 86.

AD-A044 269 ARMY ENGINEER WATERWAYS EXPERIMENT STATION VICKSBURG MISS F/G 1/5
ANALYSIS OF PERMANENT DEFORMATIONS OF FLEXIBLE AIRPORT PAVEMENT--ETC(U)
FEB 77 Y T CHOU DOT-FA73WAI-377
UNCLASSIFIED WES-TR-S-77-8 FAA-RD-77-6 NL

2 OF 2
ADA044269

END
DATE FILMED
10-77
DDC

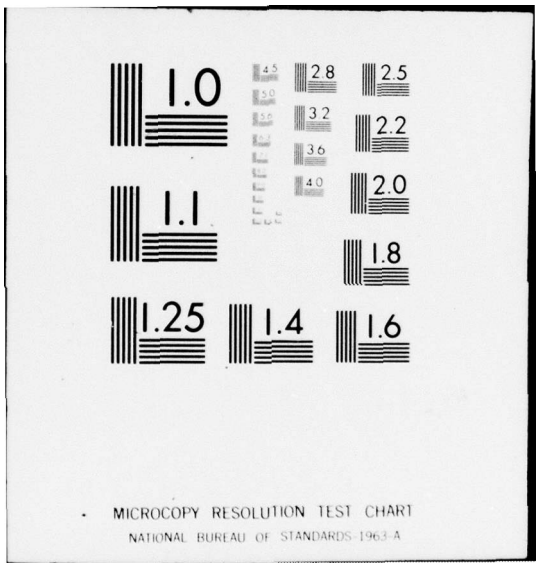
1.0
1.1
1.25
1.4
1.6
1.8
2.0
2.2
2.5
2.8
3.2
3.6
4.0
4.5
5.0
5.6
MICROCOPY RESOLUTION TEST CHART
NATIONAL BUREAU OF STANDARDS-1963-A

$$t = \alpha\sqrt{\frac{P}{8.1\ CBR} - \frac{A}{\pi}} \qquad (12)$$

in which P is the wheel load in pounds, A is the tire contact area in square inches, α is a factor depending upon the selected coverage level, and t is the total thickness in inches, including the AC and granular base layers. The thicknesses of AC and base layers were determined by Corps of Engineers standard flexible pavement design procedure.

Many pavements were designed by the CBR equation for 5000 coverages and for various loads and subgrade strengths. Elastic vertical strains and deviator stresses were computed by the elastic layered program,[46] and permanent deformations at the subgrade surface were computed by Equation 11. The results are presented in Figure 27. It can be seen that for pavements designed for same coverage level, the elastic vertical strain at the subgrade surface (Figure 27a) increases slightly with an increase in the subgrade CBR. At a given subgrade CBR, the subgrade strain also varies slightly with the load, with larger strains induced by greater loads. For subgrade CBR ranging from 2.4 to 6.3, the average strain increase was from 1.5×10^{-3} to 1.8×10^{-3} in./in. For practical design purposes, it can be assumed that subgrade strain is independent of the load. This becomes clear when these strain values are used to determine coverage values from the relationship between strain and coverage at failure shown in Figure 23a.

The computed deviator stresses at the subgrade surface of these pavements are presented in Figure 27b. It can be seen that for pavements designed for the same coverage level, the deviator stress at the subgrade surface increases nearly linearly with an increase in the subgrade CBR, but is nearly independent of the magnitude of the wheel load. The lack of dependence of the deviator stress on the magnitude of the wheel load is reasonable because these pavements were designed by the CBR equation and therefore an adequate thickness of pavement was provided to protect the subgrade from shear failure. For pavements constructed over a subgrade having the same CBR, the stresses of the subgrade surface should be the same for any design wheel load.

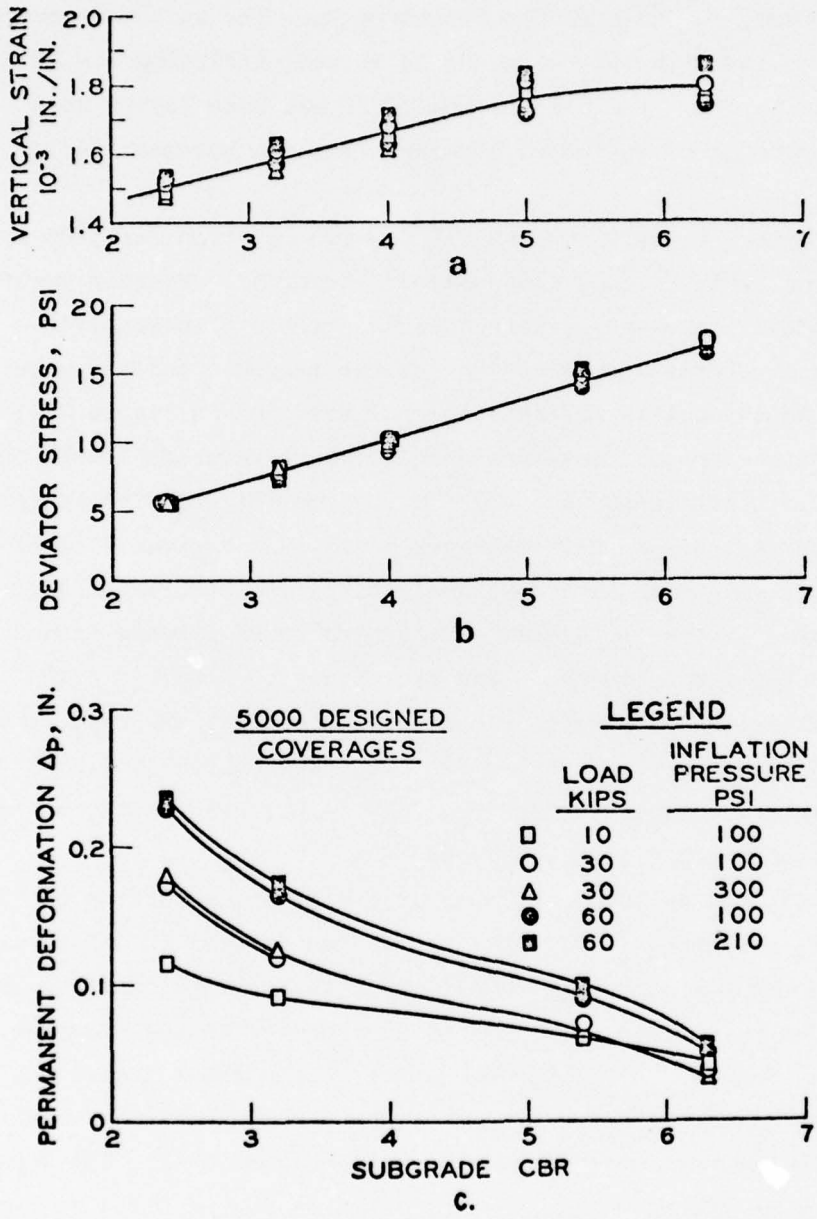

Figure 27. Relationships between elastic vertical strain and deviator stress at subgrade surface and permanent deformation in the subgrade for pavements designed at 5000 coverages for many single-wheel loads

Figure 27c indicates that, for pavements designed for the same coverage level, the subgrade permanent deformation decreases with increasing subgrade CBR and with decreasing wheel load. This effect may be explained as follows. Laboratory repeated load test results shown in Figure 18 indicate that at the same load repetition level the permanent strains of subgrade soils with higher CBR's are much smaller than those with lower CBR's. Although the stress intensity in subgrades with higher CBR's is larger, which tends to increase the permanent deformation (Figure 27c), the decrease in permanent deformation because of the stronger soil exceeds the increase due to the higher stress intensity. Consequently, the permanent deformation decreases with an increase in the subgrade CBR. At a given subgrade CBR, larger wheel loads induce larger stress intensities in the subgrade and thus cause larger permanent deformations. It should be noted that the deviator stresses shown in Figure 27b are stresses on the subgrade surface; however, it is the stresses along the vertical depth in the subgrade (i.e., the stress factor) which govern the total permanent deformation in the subgrade.

The analysis presented in Figure 27 is for pavements designed at 5000 coverage levels. Analyses were also made on pavements designed at different coverage levels. The relationships between the computed values of vertical subgrade strains, permanent deformations, and stress factors in the subgrade and the designed coverage levels of three pavements are shown in Figure 28a-28c, respectively. It can be seen that good correlations exist between the three parameters and the design coverage levels. It should be noted, however, that permanent deformation occurring in the subgrade decreases with increasing designed coverage levels, which is a different response from that under multiple-wheel loads (Figure 23b) in which the permanent deformations under one given type of aircraft load were nearly the same for all the coverage levels within the test range. The difference may lie in the differences in stress intensities occurring in the subgrade soils between single and multiple wheels. The difference may be explained by the stress factors.

Figure 29 shows a comparison of relationship between the stress factors and coverages at failure for single- and multiple-wheel loads

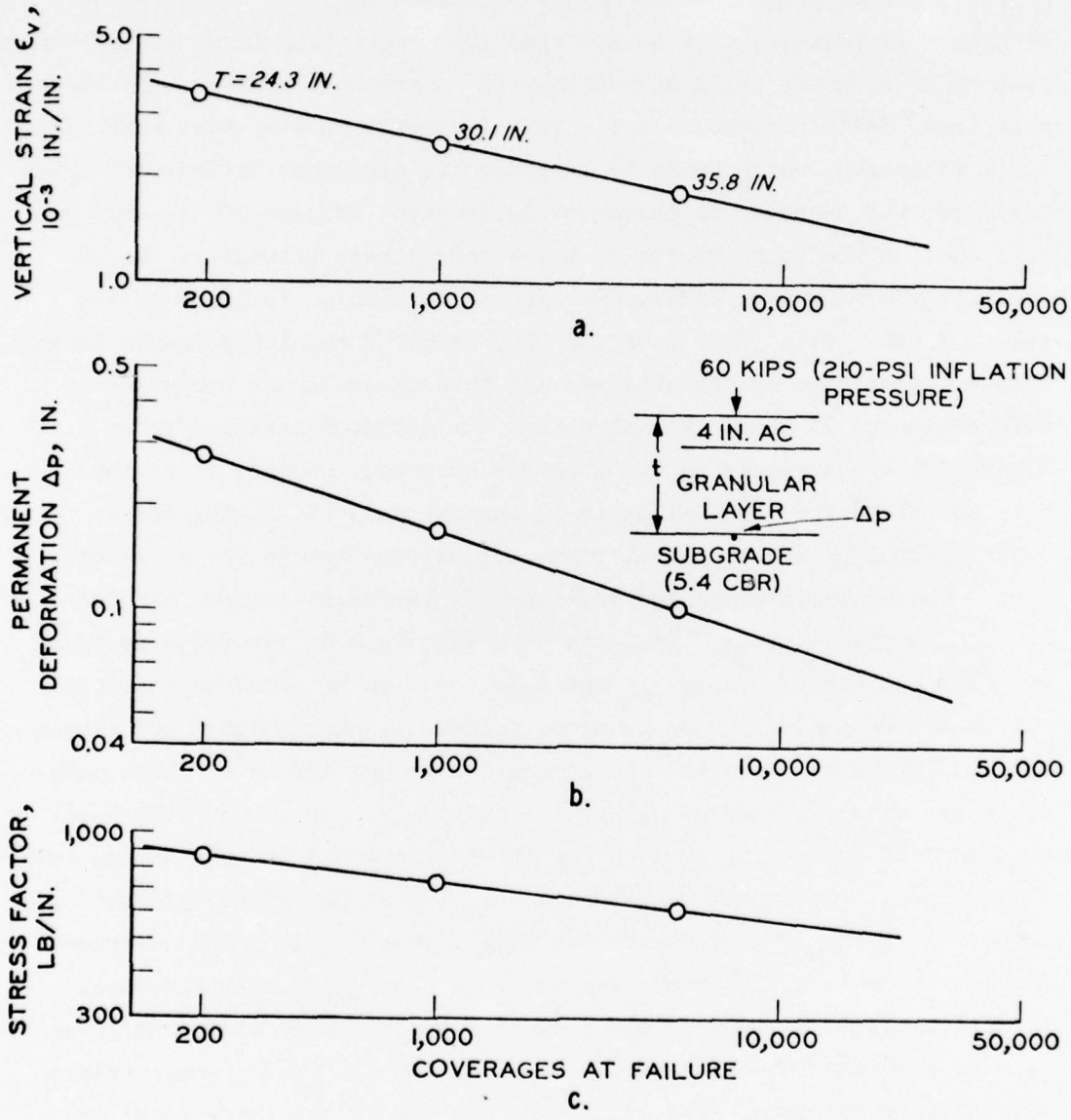

Figure 28. Relationships between vertical strain at the subgrade surface, permanent deformation in the subgrade, and stress factor in the subgrade and performance of a pavement under single-wheel loads

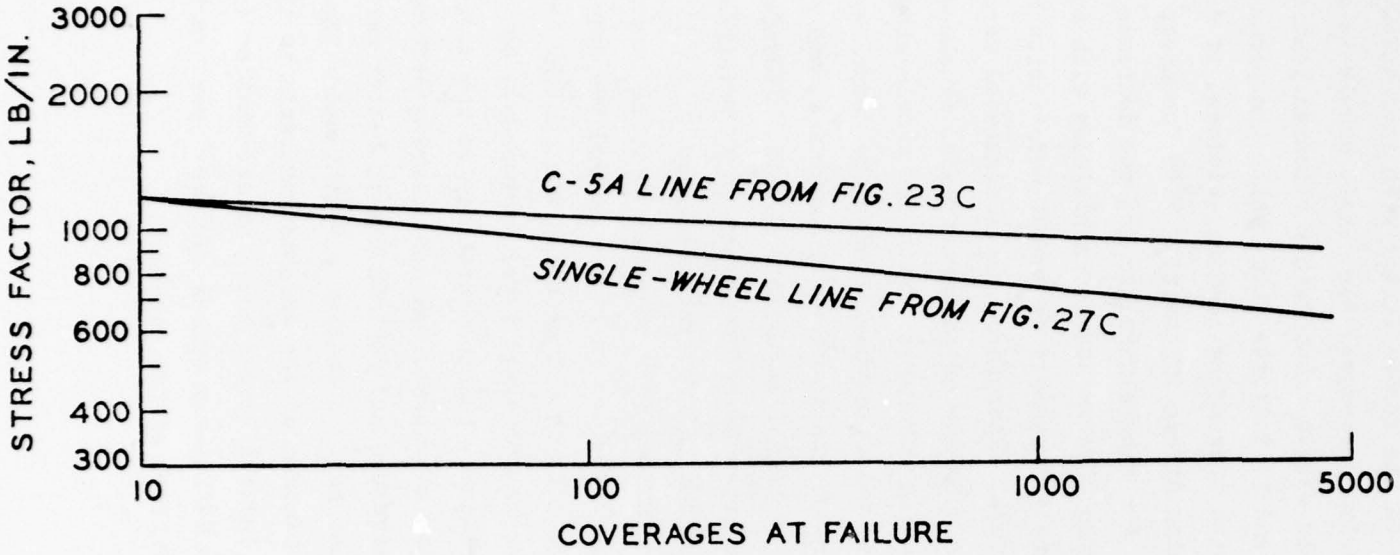

Figure 29. Comparison of stress factors for single- and multiple-wheel loads

(the curves were taken from Figures 23c and 28c). It can be seen that the rate of decrease in the stress factor with increasing pavement thickness (or increasing coverages) for single wheels is much greater than that for multiple wheels. Laboratory repeated load test results shown in Figures 16 and 17 indicate that, while the permanent strain increases slightly with increasing load repetitions, it decreases rapidly with decreasing stress intensity. With the steep slope of this curve (in Figure 28) for single-wheel loads, the decrease in permanent deformation due to reduction in stress intensities with increase in thickness exceeded the increase in permanent deformation because of higher repetition levels. Therefore, the accumulated permanent deformation occurring in the subgrade of pavements under single-wheel loads decreases with increasing coverages. With the gentle slope of the line shown in Figure 29 for multiple-wheel loads, the decrease of pavement deformation, due to reduction in stress intensities, may equally offset the increase because of higher repetition levels. Therefore, the accumulated permanent subgrade deformations under multiple-wheel loads become nearly the same for all coverage levels.

Permanent deformations were computed at offset points for the three pavement thicknesses shown in Figure 28 and the deformation basins are shown in Figure 30. It should be noted that as the thickness of the pavement increases (or the coverage level increases), not only is the maximum deformation reduced, but the curvature of the deformation basin is also reduced. This, of course, reduces shearing deformations in the overlying pavement structure and contributes to better performance of the pavement. On the other hand, a thinner pavement under the same wheel load has a sharper curvature of the deformation basin in the subgrade than the surface and induces larger shearing deformation in the overlying pavement layer. This definitely causes surface layer cracking and contributes to earlier failure of the pavement.

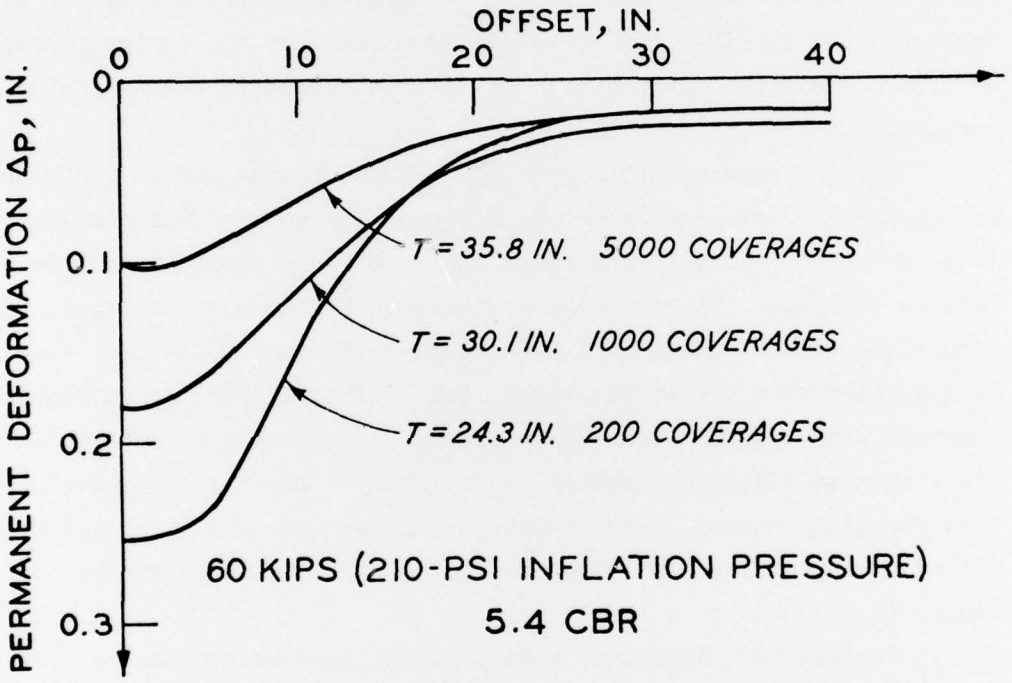

Figure 30. Permanent deformation basins in pavements designed at various coverage levels under single-wheel loads

DESIGN IMPLICATIONS OF COMPUTED RESULTS

Because computations of permanent deformation in AC and untreated granular materials could not be made in this study, discussion on their design implications has been omitted in this section. Computations of permanent deformations were only made for fine-grained subgrade soils in pavement systems. Although the deformation characteristics of subgrade soil alone cannot fully describe the overall deformation behavior of the pavement, the findings can certainly shed light on the design concept of flexible airport pavements. They are discussed in the following paragraphs.

The difference in the rate of decrease in the stress factor with an increase in pavement thickness between single- and multiple-wheel loads shown in Figure 28 indicates that, as the design pavement service life is increased, the need for an increase in pavement thickness to reduce the stress intensity in the subgrade for multiple-wheel loads is less than that for single-wheel loads. This difference in requirements conforms with present Corps of Engineers and FAA design criteria in which the thickness adjustment factor α is smaller for multiple-wheel loads than for single-wheel loads. (Details of the development of the design criteria can be found in Reference 51, Volume I, with reference to Figure 69.)

The analysis indicates that pavement performance can be predicted much easier by the resilient vertical strain at the subgrade surface than by accumulated subgrade permanent deformation. Unlike the resilient vertical strain, the accumulated permanent deformation in the subgrade was found to be dependent on many factors: load, gear configuration, pavement thickness, subgrade strength, subgrade condition, and coverage level. They are discussed separately as follows:

a. Load. Figure 23b indicates that the computed accumulated permanent deformations of the Boeing 747 240-kip assembly load were much greater than those of the C-5A 360-kip assembly load. The analysis of single-wheel loads shown in Figure 27c also shows that, for pavements designed for the same performance level, the permanent subgrade deformation increases with an increase in wheel load, with the increase being more pronounced for pavements on weaker subgrades.

b. Gear configuration. The main differences in the gear configurations of the C-5A 12-wheel assembly and the Boeing 747 twin-tandem assembly are that C-5A has more wheels and the wheels are much farther apart. Pavements 1 and 5 had identical thicknesses and subgrade strengths, but the failure coverage levels of these two pavements subjected to C-5A and Boeing 747 assembly loads were 1500 and 40, respectively. A comparison of the deformation basins of the C-5A (Figure 26a) and the Boeing 747 (Figure 26b) indicates that, for pavements designed for the same performance level, the maximum deformations in the subgrade of pavements designed for C-5A are not only much smaller, but the basins are much flatter and broader.

c. Pavement thickness. In Figure 23b, the accumulated subgrade deformations computed for the Boeing 747 were much greater than those computed for the C-5A. It should be noted that for the same performance level, the Boeing 747 requires a much thicker pavement than the C-5A. It can be stated that for pavements designed for the same performance level, heavier loads* require thicker pavements and thicker pavements can withstand larger subgrade deformations. This fact is well illustrated by the deformation basins plotted in Figure 25. As shown, for the two pavements designed for the 1000 coverage level, the required pavement thickness is 29.6 in. for the C-5A, but is 48.5 in. for the Boeing 747. The deformations in the pavement under the heavier load (Boeing 747) were not only much greater but the deformation basin was also much sharper than that under the lighter load (C-5A).

d. Subgrade strength. Figure 27c shows that the permanent subgrade deformation decreases with increasing subgrade CBR for all the single-wheel loads. The pavements were designed using the CBR equation for a coverage level of 5000. For multiple-wheel loads, although an analysis was not performed on pavements with subgrade CBR's higher than 4, it is believed that permanent subgrade deformation would also decrease with increasing subgrade CBR. This behavior occurs because a stronger subgrade requires a thinner pavement and a thinner pavement is followed by lower subgrade permanent deformation as was discussed in the previous paragraphs.

e. Subgrade condition. The difference between pavements 1 and 2 and pavements 5 and 6 is that an extra-weak layer (3 ft) was placed deep in the subgrade of pavements 2 and 6. Figure 23b shows that the permanent subgrade deformations in pavements 2 and 6 were much larger than those in pavements 1 and 5, respectively, while the overall performance of pavements 1 and 2

---

* Heavier load refers to load per wheel and closer gear spacings. More information can be found in the footnote on page 86.

and pavements 5 and 6 were the same. Apparently, the soft layer deep in the subgrade deformed nearly uniformly under the action of the multiple-wheel loads. Consequently, the pavement structure above the soft layer moved downward nearly uniformly following the movement of the soft layer without experiencing any significant additional bending stresses as compared with those in pavements 1 and 5 in which the soft layer did not exist.

f. Coverage level. An analysis made on pavements designed using the CBR equation for single-wheel loads (Figure 28b) revealed that the accumulated permanent subgrade deformation decreased as the performance level of the pavement increased. In other words, the permanent subgrade deformation of a pavement designed for a higher coverage level is less than that of a pavement designed for a lower coverage level. However, an analysis of pavements failed under multiple-wheel loads revealed that under a given aircraft load pavements of different thicknesses failed under different coverage levels but experienced nearly the same amount of computed permanent subgrade deformation (Figure 23b). This is due possibly to the differences between single- and multiple-wheel stress distributions in the subgrade. These results are reasonable because the laboratory repeated load test results shown in Figure 19 indicate that for a given value of elastic strain the permanent strain in the subgrade increases with decreasing CBR values. This relationship also explains why, for pavements designed using the CBR equation for 5000 coverages, permanent strain increased with decreasing subgrade CBR's (shown in Figure 27c), while the subgrade elastic strains were nearly the same (Figure 27a).

Prior to further discussion, the current concept and practice in considering pavement rutting in flexible pavements should be reviewed, and the measurements of surface deformations obtained from field test pavements should be investigated. The conclusions can thus be compared with the results of this study.

As was stated in the beginning of this report, one of the current approaches to consider pavement rutting under repeated traffic loading is to limit the vertical compressive strain at the subgrade surface to some tolerable amount associated with a specific number of load repetitions (e.g., limiting subgrade strains in Table 2). By controlling the characteristics of the materials in the pavement section through materials design and proper construction procedures (unit weight or relative compaction requirements) and by insuring that materials of adequate stiffness

and sufficient thickness are used so that the strain level is not exceeded, permanent deformation can be limited to a value equal to or less than the prescribed amount. It should be reiterated that in the Corps of Engineers failure criteria, from which failure coverages of field test pavements were determined, surface rutting is not considered to be a critical factor in judging pavement failure. The criteria were described on page 75 of the report. Consequently, surface rutting measured at failure in the field test pavements constructed and tested at WES was not constant but varied with pavement thickness and gear loads. It was found that at a given performance level, the measured surface rutting increased with increasing pavement thickness. The need for thicker pavements may be due to either heavier loads or softer subgrade soils (see Figure 23b). Since the limiting subgrade strain criteria developed by The Asphalt Institute (shown in Table 2) were based in part on an analysis of Corps of Engineers test data,[50] it is evident that the criterion of surface rut depth is not included in the developed performance models. Although the criteria developed by Shell[20] (Table 2) were developed using elastic analysis of pavements designed according to the CBR procedure and performance results of the AASHO Road Test, the criteria are thought to be associated with ultimate rut depths on the order of 3/4 in. Limiting surface rutting is a concept that has been advocated in recent years; however, it has not yet been implemented in any existing design procedure.

The discussions presented in this report are in direct contrast with the generally accepted concept which assumes that if the material and thickness of a pavement are properly selected and proper compaction is applied so that the elastic subgrade strain is limited, subgrade rutting will be controlled and surface rutting equal to or less than some prescribed amount can be assured. This concept is based on the assumption that when two pavements are designed for the same performance level (same coverage at failure), not only are the subgrade elastic strains the same but also the subgrade rutting is very nearly the same. This assumption is not strictly correct based on the results of the analysis in this study.

It is the author's belief that the surface rut depth measured at the time when the pavement is judged to be failed increases as the thickness of the pavement is increased, even though the material in each layer of the pavement may be properly selected and compacted. Since surface rut depth is not limited in the failure criteria, when two pavements are designed for the same performance level, the surface rut depth and subgrade rutting will be greater for the thicker pavement (greater thickness due to either heavier applied loads or weaker subgrade support), while the elastic vertical strain at the surface of the subgrade will be nearly the same for the two pavements.

If it is desirable that pavements designed for the same performance level have the same degree of rutting in the subgrade, the elastic vertical strains at the subgrade surface induced by the load will have to be varied, with smaller elastic strains allowed for weaker subgrades and greater elastic strains allowed for stronger subgrades in accordance with the relationships between the elastic and permanent strains shown in Figure 19. This is, of course, in contrast with the current limiting subgrade strain criteria concept in which pavements designed for the same performance level have the same elastic vertical strains at the subgrade surface. The limiting subgrade strains for both highway and airport pavements adopted by a number of agencies are shown in Table 2.

CONCLUSIONS AND RECOMMENDATIONS

CONCLUSIONS

Based on the material from the literature survey and results of analysis of full-scale test pavements and pavements designed using the CBR equation, the following conclusions were drawn. A linear layered elastic computer program was used to compute the permanent deformations in granular layers and in the subgrade soils, with the material characterizations described in the section LABORATORY REPEATED LOAD TESTS. Therefore, the computed results are subjected to the criticism of the computer program as well as the material characterization.

a. AC surfacing. There is no general consensus on the method with which the permanent deformation of an AC layer in a pavement system can be computed. Laboratory tests to determine the rutting properties of AC are expensive and time-consuming.

b. Untreated granular layers. A serious problem exists in the prediction of permanent deformations in untreated granular layers in a pavement system. The stress states in the granular layers under the aircraft loadings cannot be computed correctly using Burmister layered elastic solution and the nonlinear finite element program in its present form. Also, the stress states under aircraft loadings cannot be correctly simulated by laboratory tests.

c. An analysis made on the computed permanent deformations occurring in the subgrade soil of many full-scale test pavements and pavements designed using the CBR equation indicates that the current concept of controlling subgrade rutting through limiting subgrade strains in flexible pavements is not strictly correct. When subgrade strains are limited, not only the subgrade rutting may not be limited, but also the control of surface rutting may not be assured. If surface rut depth is limited in design procedures, however, the limiting subgrade strain criteria proposed and adopted by many agencies (Table 2) will have to be modified to vary according to subgrade strength.

d. The approach used in this study was not successful in providing a prediction model to estimate the amount of permanent deformation in flexible pavements subjected to aircraft loadings.

RECOMMENDATIONS

Based on the results of analysis of this study, it is recommended that (a) continuing efforts be made to investigate the basic deformation characteristics of AC and untreated granular soils in a pavement system subjected to aircraft loadings which move in a longitudinal direction and also wander from the center line of a runway; (b) a development program be initiated in prediction models to estimate permanent deformations in each component layer of a pavement system when the information described in (a) becomes available; and (c) efforts be concentrated on selecting proper component materials and specifying construction techniques to minimize the potential of deformation, before a complete prediction model is developed.

LIST OF NOMENCLATURE

The following symbols are used in this report:

A = tire contact area;

c = cohesion;

CBR = California Bearing Ratio;

D = equivalent particle size of filler (0.000004 in.);

E = modulus of elasticity;

FB = filler-bitumen factor;

LL = liquid limit;

P = wheel load;

PI = plasticity index;

q = effective deviator stress;

q_{ult} = bearing capacity;

S_{bit} = stiffness of the bitumen;

S_{mix} = stiffness of the asphaltic concrete mixture;

t = thickness of the pavement;

V = void factor;

γ = shear strain;

δ_p = permanent deformation;

ΔZ = thickness of the sublayer;

ε_p = permanent strain;

ε_{vs} = maximum compressive subgrade strain;

$d\varepsilon/dt$ = rate of application of axial strain;

η_{mass} = viscosity of mass;

σ = normal stress;

σ_{ij} = stress state;

σ_{oct} = octahedral normal stress;

σ_1, σ_2, σ_3 = major, intermediate, and minor principal stresses, respectively;

τ = shear strength;

τ_e = initial cohesion when $\frac{d\varepsilon_1}{dt} = 0$;

τ_{oct} = octahedral shear stress; and

ϕ = angle of internal friction.

REFERENCES

1. Monismith, C. L., "Rutting Prediction in Asphalt Concrete Pavements; A State-of-the-Art," prepared for the Symposium on Predicting Rutting in Asphalt Concrete Pavements, 1976 Annual Meeting of the Transportation Research Board, Jan 1976.

2. Dorman, G. M. and Metcalf, C. T., "Design Curves for Flexible Pavements Based on Layered Systems Theory," ER Record 71, 1965.

3. Yoder, E. J. and Witczak, M. W., Principles of Pavement Design, 2d ed., Wiley, 1975, Tables 8 and 9.

4. Barker, W. R. and Brabston, W. N., "Development of a Structural Design Procedure for Flexible Airport Pavements," Report No. FAA-RD-74-199 (WES TR S-75-17), Sep 1975, Federal Aviation Administration, Washington, D. C.

5. Hofstra, A. and Klomp, A. J. G., "Permanent Deformation of Flexible Pavements Under Simulated Road Traffic Conditions," Proceedings, Third International Conference on the Structural Design of Asphalt Pavements, London, 1972, pp 613-621.

6. Heukelom, W. and Klomp, A. J. G., "Consideration of Calculated Strains at Various Depths in Connection with the Stability of Asphalt Pavements," Proceedings, Second International Conference on the Structural Design of Asphalt Pavements, University of Michigan, 1967.

7. McLean, D. B., The Measurement of Deformation Properties of Asphaltic Materials Under Triaxial Repeated Load Tests, Ph. D. Thesis (in preparation), 1973.

8. Morris, J., "The Prediction of Permanent Deformation in Asphalt Concrete Pavements," A technical report based on the author's Ph. D. Thesis, Sep 1973.

9. Monismith, C. L., "A Design Framework for Asphalt Concrete Pavements Using Available Theory," A paper used in the Institute on Flexible Pavement Design and Performance, Pennsylvania State University, Nov 1973.

10. U. S. Army Corps of Engineers, "Flexible Airfield Pavements," TM 5-824-2, 1958, U. S. Government Printing Office, Washington, D. C.

11. California Division of Highways, "Test Method No. 304; Materials Manual, 1, 1963.

12. Nijboer, L. W., Plasticity as a Factor in the Design of Dense Bituminous Carpets, N. Y. Elsevier Publishing Co., 1948.

13. Smith, W. R., "Triaxial Stability Methods for Flexible Pavement Design," Proceedings, Association of Asphalt Paving Technologists, 1949, pp 63-94.

14. McLeod, N. W., "A Rational Approach to the Design of Bituminous Paving Mixtures," Proceedings, Association of Asphalt Paving Technologists, 1950, pp 82-224.

15. Saal, R. N. J., "Mechanics of Technical Applications of Asphalt," Preprint of Proceedings, Symposium of Fundamental Nature of Asphalt, 1960.

16. Nijboer, L. W., "Mechanical Properties of Asphalt Materials and Structural Design of Asphalt Roads," Proceedings, Highway Research Board, 1954, pp 185-200.

17. Valkering, C. P., "Effects of Multiple Wheel Systems and Horizontal Surface Loads on Pavement Structures," Proceedings, Third International Conference on the Structural Design of Asphalt Pavements, London, 1972, pp 542-549.

18. Marais, C. P., "Tentative Mix Design Criteria for Gap-Graded Bituminous Surfacings," Jan 1974, Highway Research Board Meeting, Washington, D. C.

19. Heukelom, W. and Klomp, A. J. G., "Consideration of Calculated Strains at Various Depths in Connection with the Stability of Asphalt Pavements," Proceedings, Second International Conference on the Structural Design of Asphalt Pavements, 1967, pp 155-168.

20. Elloitt, J. F. and Moavenzadeh, F., "Moving Load on Viscoelastic Layered System - Phase II," Report No. R69-64, Sep 1969, Department of Civil Engineering, Materials Division, Massachusetts Institute of Technology, Cambridge, Mass.

21. Elliott, J. F., Moavenzadeh, F., and Findakly, H., "Moving Load on Viscoelastic Layered Systems, Phase II - Addendum," Research Report R70-20, Apr 1970, Department of Civil Engineering, Massachusetts Institute of Technology to U. S. Department of Transportation, Federal Highway Administration, Bureau of Public Roads Under Contract No. FH-11-6916.

22. Moavenzadeh, F. and Elliott, J. F., "A Stochastic Approach to Analysis and Design of Highway Pavements," Proceedings, Third International Conference on the Structural Design of Asphalt Pavements, London, 1972, pp 490-505.

23. Barksdale, R. D., "Laboratory Evaluation of Rutting in Base Course Materials," Proceedings, Third International Conference on Structural Design of Asphalt Pavements, London, 1972, pp 161-174.

24. Romain, J. E., "Rut Depth Prediction in Asphalt Pavements," Proceedings, Third International Conference on Structural Design of Asphalt Pavements, London, 1972, pp 705-710.

25. Hills, J. F., "The Creep of Asphalt Mixes," Journal, Institute of Petroleum, Nov 1973.

26. Hills, J. F., Brien, D., and Van de Loo, P. J., "The Correlation of Rutting and Creep Tests on Asphalt Mixes," Journal, Institute of Petroleum, Paper IP 74-001, Jan 1974.

27. Van de Loo, P. J., "Creep Testing, A Simple Tool to Judge Asphalt Mix Stability," Paper presented to the 49th Annual Meeting of the Association of Asphalt Paving Technologists, Feb 1974.

28. Snaith, M. S., Permanent Deformation Characteristics of a Dense Bitumen Macadam, Ph. D. Thesis, University of Nottingham, 1973.

29. McElvaney, J., Brown, S. F., and Pell, P. S., "Permanent Deformation of Bituminous Materials," Internal Report No. JMcE/1, May 1974, University of Nottingham.

30. Morris, J. et al., "Permanent Deformation in Asphalt Pavements Can Be Predicted," Paper presented to the 49th Annual Meeting of the Association of Asphalt Paving Technologists, Feb 1974.

31. Chompton, G. and Valayer, P. J., "Applied Rheology of Asphalt Mixes - Practical Application," Proceedings, Third International Conference on the Structural Design of Asphalt Pavements, London, 1972, pp 214-225.

32. Brown, S. F., Pell, C. A., and Brodrick, B. V., "Permanent Deformation of Flexible Pavements," Contract No. DAJA 73-74-1306, Nov 1974, University of Nottingham, England.

33. Brown, S. F., "An Improved Framework for the Prediction of Permanent Deformation in Asphaltic Layers," A paper presented at the 50th Annual Meeting of the Transportation Research Board, 1975.

34. Van der Poel, C., "A General System Describing the Viscoelastic Properties of Bitumen and Its Relation to Routine Test Data," Journal of Applied Chemistry, Vol 4, 1954, pp 221-236.

35. Van Draat, W. E. F. and Sommer, P., "Ein Gerät zur bestimmung der dynamischen elastizität modulu von Asphalt," Strasse Autobahn 6, 1965, pp 206-211.

36. Allen, J. J., The Effects of Nonconstant Lateral Pressures on the Resilient Response of Granular Materials, Ph. D. Thesis, University of Illinois at Urbana-Champaign, May 1973.

37. Kalcheff, I. V., "Characteristics of Graded Aggregates as Related to Their Behavior Under Varying Loads and Environments," Presented at Conference of Graded Aggregate Base Materials in Flexible Pavements, Oak Brook, Ill., 25-26 Mar 1976.

38. Brown, S. F., "Repeated Load Testing of a Granular Material," Journal of the Geotechnical Engineering Division, American Society of Civil Engineers, Vol 100, No. GT7, Proceeding Paper 10684, Jul 1974, pp 825-841.

39. Barrett, J. R., "Modeling Permanent Strain Behavior of Unbound Base Course Materials - A Review," Technical Paper No. 26, 1976, Division of Applied Geomechanics, Commonwealth Scientific and Industrial Research Organization, Australia.

40. Finn, W. D. L., "Applications of Limit Plasticity in Soil Mechanics," Proceedings, American Society of Civil Engineers, SM-5, Part I, 1967, pp 101-120.

41. Hyde, A. F. L., Repeated Load Triaxial Testing of Soils, Ph. D. Thesis, University of Nottingham, 1974.

42. Monismith, C. L., Ogawa, N., and Freeme, C. R., "Permanent Deformation Characteristics of Subgrade Soils Due to Repeated Loading," Transportation Research Record No. 537, 1975.

43. Barker, W. R., "The Relationship Between Resilient and Permanent Strain in the Design of Airport Pavements," A paper prepared for the Symposium on Rutting in Asphaltic Concrete Pavements at the 55th Annual Meeting of the Transportation Research Board, Washington, D. C., Jan 1976.

44. Chisolm, E. E. and Townsend, F. C., "Behavioral Characteristics of Gravelly Sand and Crushed Limestone for Pavement Design, FAA-RD-75-177 (TR S-76-17), Sep 1976, U. S. Army Engineer Waterways Experiment Station, CE, Vicksburg, Miss.

45. Townsend, F. C. and Chisolm, E. E., "Plastic and Resilient Properties of Heavy Clay Under Repetitive Loadings," FAA-RD-76-107 (TR S-76-16), Nov 1976, U. S. Army Engineer Waterways Experiment Station, CE, Vicksburg, Miss.

46. Chou, Y. T., "An Iterative Layered Elastic Computer Program for Rational Pavement Design," FAA-RD-75-226 (TR S-76-3), Feb 1976, U. S. Army Engineer Waterways Experiment Station, CE, Vicksburg, Miss.

47. Kingham, R. I. and Kallas, B. F., "Laboratory Fatigue and Its Relationship to Pavement Performance," Proceedings, Third International Conference on the Structural Design of Asphalt Pavements, 1972, Figures 6 and 7.

48. Witczak, M., "Design of Full-Depth Asphalt Airfield Pavements," Proceedings, Third International Conference on the Structural Design of Asphalt Pavements, University of Michigan, 1972.

49. Heukelom, W. and Foster, C. R., "Dynamic Testing of Pavements," Journal Soil Mechanics and Foundations Divisions, American Society of Civil Engineers, 1960.

50. Chou, Y. T., "Engineering Behavior of Pavement Materials: State-of-the-Art," FAA-RD-77-37 (TR S-77-__), Chapter 6, Feb 1977 (in preparation), U. S. Army Engineer Waterways Experiment Station, CE, Vicksburg, Miss.

51. Ahlvin, R. G. et al., "Multiple-Wheel Heavy Gear Load Pavement Tests," U. S. Army Engineer Waterways Experiment Station, CE, Vicksburg, Miss., Technical Report S-71-17, Vol 1-4, Nov 1971.

52. Thompson, O. O., Evaluation of Flexible Pavement Behavior with Emphasis on the Behavior of Granular Layers, 1969, Ph. D. Dissertation, University of Illinois, Urbana, Ill.

53. Morgan, J. R. and Scala, A. J., "Flexible Pavement Behavior and Application of Elastic Theory--A Review," Proceedings, Australian Road Research Board, Vol 4, Part 2, 1968, pp 1201-2143.

54. Barker, W. R., "Nonlinear Finite Element Analysis of Heavily Loaded Airfield Pavement Systems," Proceedings, Symposium on Applications of the Finite Element Method in Geotechnical Engineering, Vicksburg, Miss., May 1972.

55. Chou, Y. T., "Evaluation of Nonlinear Resilient Moduli of Unbound Granular Materials from Accelerated Traffic Test Data," FAA-RD-76-65 (TR S-76-12), Aug 1976, U. S. Army Engineer Waterways Experiment Station, CE, Vicksburg, Miss.

56. Turnbull, W. J. and Ahlvin, R. G., "Mathematical Expressions of the CBR (California Bearing Ratio) Relations," Proceedings, Fourth International Conference on Soil Mechanics and Foundation Engineering, 1957.

* U.S. GOVERNMENT PRINTING OFFICE : 1977 O-729-321/1379